

Theory of two-dimensional quantum Heisenberg antiferromagnets with a nearly-critical ground-state

Andrey V. Chubukov^{1,2}, Subir Sachdev¹, and Jinwu Ye¹
¹*Departments of Physics and Applied Physics, P.O. Box 208120,
Yale University, New Haven, CT 06520-8120,*
and ²*P.L. Kapitza Institute for Physical Problems, Moscow, Russia*
(April 16, 1993; revised July 21, 1993)

Abstract

We present the general theory of clean, two-dimensional, quantum Heisenberg antiferromagnets which are close to the zero-temperature quantum transition between ground states with and without long-range Néel order. While some of our discussion is more general, the bulk of our theory will be restricted to antiferromagnets in which the Néel order is described by a 3-vector order parameter. For Néel-ordered states, ‘nearly-critical’ means that the ground state spin-stiffness, ρ_s , satisfies $\rho_s \ll J$, where J is the nearest-neighbor exchange constant, while ‘nearly-critical’ quantum-disordered ground states have a energy-gap, Δ , towards excitations with spin-1, which satisfies $\Delta \ll J$. The allowed temperatures, T , are also smaller than J , but *no* restrictions are placed on the values of $k_B T/\rho_s$ or $k_B T/\Delta$. Under these circumstances, we show that the wavevector/frequency-dependent uniform and staggered spin susceptibilities, and the specific heat, are completely universal functions of just three thermodynamic parameters. On the ordered side, these three parameters are ρ_s , the $T = 0$ spin-wave velocity c , and the ground state staggered moment N_0 ; previous works have noted the universal dependence of the susceptibilities on these three parameters only in the more restricted regime of $k_B T \ll \rho_s$. On the disordered side the three thermodynamic parameters are Δ , c , and the spin-1 quasiparticle residue \mathcal{A} . Explicit results for the universal scaling functions are obtained by a $1/N$ expansion on the $O(N)$ quantum non-linear sigma model, and by Monte Carlo simulations. These calculations lead to a variety of testable predictions for neutron scattering, NMR, and magnetization measurements. Our results are in good agreement with a number of numerical simulations and experiments on undoped and lightly-doped $La_{2-\delta}Sr_\delta CuO_4$.

Typeset using REVTeX

I. INTRODUCTION

The subject of two-dimensional quantum antiferromagnetism has witnessed a remarkable revival in recent years¹⁻³. This is largely due to the intense interest in understanding the properties of the CuO_2 layers in the high temperature superconductors. However, the experimental motivation is not limited to these cuprate compounds; recent investigations⁴⁻⁸ have refocused interest on a number of other layered insulating compounds which are rather well described as Heisenberg antiferromagnets at low temperatures⁹.

The bulk of the existing theoretical work on two dimensional antiferromagnets can be divided into two broad classes:

First, there are the studies of the low temperature properties of antiferromagnets with well-established long-range Néel order in their ground state^{1,2,10,11}. Definitive results have been obtained for these systems by Chakravarty *et.al.*^{12,13}. They showed that the long-wavelength, low energy properties were well described by a mapping to a *classical* two-dimensional Heisenberg magnet. All effects of quantum fluctuations could be absorbed into almost innocuous renormalizations of the coupling constants. Good agreement with neutron scattering experiments on La_2CuO_4 was obtained.

Second, there have been numerous investigations on spin-fluid, or quantum disordered, ground states¹⁴⁻¹⁹. These are states in which quantum-fluctuations have removed all vestiges of the Néel order. An entirely new physical picture is necessary for visualizing the ground states: it is phrased most often in terms of resonating singlet valence-bonds between pairs of quantum spins²⁰. Many interesting questions on the presence of alternative symmetry breaking in the ground state have been addressed. The nature of the excitations above the ground state is also of some interest. The two experimentally distinguishable possibilities are (*i*) the low-lying states correspond to those associated with weakly-interacting spin-1/2 quanta ('spinons'), or (*ii*) the spinons are confined in pairs, leading to integer-spin excitations with infinite lifetimes. The reader is referred to a recent review³ where many of these questions are addressed in greater detail.

In this paper, we present a detailed theory of quantum antiferromagnets which fall *in between* the above two classes. These nearly-critical antiferromagnets are neither strongly Néel ordered nor fully quantum disordered in the ground state. The ordered Néel moment, if it exists, is much smaller than the ordering moment of the corresponding classical antiferromagnet. If the ordering moment is absent, the resulting quantum-disordered ground state has an energy-gap towards excitations with non-zero spin which is much smaller than all microscopic energy scales in the problem. Such nearly critical antiferromagnets were considered briefly by Chakravarty *et. al.*¹²; they identified three different regimes of behavior (See Fig. 1) which we now outline. At short length and energy scales the spin correlations in these antiferromagnets are essentially critical. The spins fluctuate strongly between ordered and non-ordered configurations. At very low temperatures, the quantum-fluctuating system only makes up its mind at a fairly large scale, and crosses over to behavior characteristic of either a Néel-ordered ground state (this is the 'renormalized-classical' region of Fig. 1) or a quantum-disordered ground state (the 'quantum-disordered' region of Fig. 1; see also Fig. 2). At larger T there is another, very interesting possibility: the critical quantum fluctuations may be quenched by thermal effects *before* the system has had a chance to undergo the above crossover to one of its two ground states (the 'quantum-critical' region of Figs. 1 and 2). The

system then does not display the properties of either Néel-order or quantum-disorder at *any length scale*; instead it crosses over from critical spin fluctuations to a thermally-induced, quantum-relaxational regime which will be described for the first time in this paper.

The above three crossover occur at a large length-scale in nearly-critical antiferromagnets, suggesting that their properties should be universal. The bulk of this paper is devoted to making this statement more precise. We will indeed find that the long-wavelength, low-energy uniform and staggered spin susceptibilities are completely characterized by universal scaling functions. The contribution of the spins to the specific heat will also be found to be similarly universal. The only required inputs are three thermodynamic parameters, which will be described more precisely below. Some of the results reported here have been discussed briefly in recent reports^{21,22}. Some other recent work has also discussed quantum criticality near related magnetic phase transitions^{23,24}.

Our motivation in examining nearly-critical antiferromagnets comes primarily from numerous recent experiments on undoped and weakly doped $La_{2-\delta}Sr_{\delta}CuO_4$.

We consider first undoped La_2CuO_4 . It is by now well established that La_2CuO_4 is described extremely well as a spin-1/2 square lattice Heisenberg antiferromagnet with nearest-neighbor interactions¹. Almost all theoretical studies^{12,25,26} of this system have focussed primarily on its properties at very low temperatures, where a description in terms of classical fluctuations of the Néel order parameter is appropriate; this range of temperatures was referred to as the ‘renormalized-classical’ region¹². There is good accord between theory^{1,12,27} and experiments^{28–30} at these low temperatures (T): the correlation length $\xi(T)$ increases exponentially with falling T , the equal-time structure factor, $S(k)$, at zero momentum behaves as $S(0) \propto T^2\xi^2$, and the ^{63}Cu spin-lattice relaxation rate $1/T_1$ decreases rapidly with the increasing T , all of which is in good agreement with the renormalized classical theory. However, recent experiments³⁰ have shown that at intermediate temperatures ($T \geq 0.4J$ where J is the nearest-neighbor exchange constant), $1/T_1$ becomes nearly independent of T . The crossover to this behavior occurs at a T which is small compared to J , so one can hope that a low-energy theory of the expected crossover to the quantum-critical region might still be appropriate; the possibility of such a crossover was already noted earlier²⁷. We will show in this paper that this new behavior is well described quantitatively by a theory of the quantum-critical spin fluctuations. The correlation length $\xi(T)$ is also expected to display a crossover at these temperatures¹²; unfortunately, there are no experimental data for ξ for $T \geq 0.4J$. However, strong support for our interpretation comes from the experimental³¹ and numerical^{32–34} measurements of the uniform static spin susceptibility $\chi_u^{st}(T)$. We will show that its temperature-dependent slope above $T \sim 0.35J$ is in excellent accord with the predictions of the quantum-critical theory, and in clear disagreement (by a factor of three) with the result deduced from a renormalized-classical theory. Taken together, we will argue that the above results imply the following: the square lattice spin-1/2 Heisenberg antiferromagnet with nearest-neighbor exchange has long-range Néel order in its ground state, and is well described by a renormalized classical theory at low temperatures; however it is apparently close enough to a quantum phase transition to a quantum disordered phase to display quantum-critical spin fluctuations over an appreciable range of intermediate temperatures.

Consider next weakly doped $La_{2-\delta}Sr_{\delta}CuO_4$. Nonzero doping ($\delta \geq 0$) has two important consequences: (i) the bare value of the spin-stiffness ρ_s takes a smaller value, pushing the antiferromagnet closer to the quantum phase transition, and (ii) the antiferromagnet is per-

turbed by the random potential of the dopant ions. Randomness is a relevant perturbation at the $T = 0$ quantum phase transition²¹ and must be included in any theory of the low T properties. Dynamic neutron scattering measurements^{35,36} near $\delta = 0.04$ show that the spin spectrum can be collapsed in a scaling plot in which the measurement frequency ω is scaled by T ; a related dependence of the susceptibility on ω and T was also discussed in the phenomenological theory of the marginal Fermi liquid³⁷. We have argued that this ω/T scaling is in fact a rather general property of quantum-critical spin fluctuations, *even in the presence of randomness and doping*²¹. Furthermore, the pre-factor of the scaling function at low ω and T shows clear evidence of the importance of randomness²¹. However many other experiments^{30,36} on doped $La_{2-\delta}Sr_{\delta}CuO_4$ have been performed at relatively large temperatures. For these T we assume that the antiferromagnet is insensitive to the weak randomness and is still in the vicinity of the pure fixed point. The primary effect of non-zero doping will then be to reduce the value of ρ_s - an immediate consequence is that the NMR relaxation $1/T_1$ should be nearly T independent (the quantum-critical behavior) over a T range which increases with doping. This is indeed what is observed. We will discuss this and other comparisons with experiments on the doped cuprates in more detail later in Section VII. With a single adjustable parameter (the doping dependent ρ_s) we will find good agreement between our theory and the experiments.

We turn now to a more complete description of our results. Consider the antiferromagnet described by the following Hamiltonian

$$\mathcal{H} = \sum_{i<j} J_{ij} \mathbf{S}_i \cdot \mathbf{S}_j, \quad (1.1)$$

where i, j extend over the sites of two-dimensional lattice, \mathbf{S}_i are on-site spin operators acting on states with spin S on the site i , and the J_{ij} are exchange constants which fall off rapidly with the separation between i and j . The J_{ij} are assumed to be invariant under the translation symmetry of the underlying lattice. The energy scale J will be used to denote the largest of the J_{ij} . The J_{ij} are predominantly antiferromagnetic, so that the classical ground state has no average uniform magnetization. We will be interested primarily in antiferromagnets which undergo a zero-temperature quantum phase transition from a Néel-ordered to a quantum disordered state as the ratios of the J_{ij} are varied, and the strength of the quantum fluctuation increases. Let us represent this strength by an all-purpose coupling constant g ; the system is assumed to be Néel-ordered for g smaller than a critical coupling g_c and quantum-disordered for $g > g_c$. We will assume further that the critical ground state at $g = g_c$ is described by a continuum field theory of excitations which propagate with a non-singular spin-wave velocity c - a number of explicit mean-field solutions of such transitions have this property^{15,16}, although other possibilities have also been discussed^{17,38,39}. It should be possible to extend our results to antiferromagnets which have different velocities for different spin-wave polarizations^{11,40}, but we will not consider this complication here. In Section VII we will argue that the following scaling results also apply unchanged to the corresponding quantum phase transitions in lightly-doped antiferromagnets.

The nature of the classical ordering helps us identify the proper continuum fields necessary for a hydrodynamic theory of the quantum phase transition. The first of these is of course the Néel order parameter. We will restrict the analysis in this paper to antiferromagnets with an ordinary vector order parameter. This type of order parameter is associated

with ground states with collinear spin-ordering *i.e.* the on-site spin condensates are either parallel or anti-parallel to each other. More complicated order parameters can arise in systems with stronger frustration *e.g.* the triangular and kagomé lattices which have co-planar spins and matrix order parameters^{41–44}; we will not discuss these complications here. Returning to the vector order-parameter case, we assume that the condensate is oriented in the $\pm z$ direction, and define a continuum quantum field $\mathbf{n}(\mathbf{r})$, which will be used as the hydrodynamic order-parameter variable, as: $\mathbf{n}(\mathbf{r}_i) = \mathbf{S}_i$ on sites where the condensate points up, and $n^z(\mathbf{r}_i) = -S_i^z$; $n^\pm(\mathbf{r}_i) = S_i^\mp$ on sites where the condensate points down. The staggered magnetization N_0 is then

$$N_0 = \langle n_z(\mathbf{r}) \rangle_{T=0}. \quad (1.2)$$

Upon approaching the critical point at $T = 0$, this staggered magnetization will vanish as^{12,45}

$$N_0 \sim (g_c - g)^\beta, \quad (1.3)$$

where β is a universal critical exponent. We have $N_0 = 0$ for $g > g_c$. Furthermore, $\langle n_z(\mathbf{r}) \rangle = 0$ at all finite T because it is not possible to break a continuous non-abelian symmetry in a two-dimensional system. At the critical point, $g = g_c$, equal-time $\mathbf{n}(\mathbf{r})$ correlations will decay with an anomalous power law⁴⁵

$$\langle \mathbf{n}(\mathbf{r}) \cdot \mathbf{n}(0) \rangle \sim \frac{1}{r^{D-2+\eta}}, \quad (1.4)$$

where $D = 3$ is the dimension of space-time.

The second important hydrodynamic variable is the magnetization density quantum field $\mathbf{M}(\mathbf{r})$

$$\mathbf{M}(\mathbf{r}_i) = \frac{g\mu_B}{a^2} \mathbf{S}_i, \quad (1.5)$$

where a^2 is the volume per spin, and $g\mu_B$ is the gyromagnetic ratio of each spin. Although the ordering has no net magnetization, magnetization fluctuations decay slowly due to the conservation law on the total magnetization.

Finally, the Hamiltonian \mathcal{H} is itself associated with a conserved total energy. The contribution of the spins to the specific heat per unit volume, C_V , is the appropriate experimental observable, sensitive to this hydrodynamic quantity.

The hydrodynamic properties of the order parameter and magnetization fluctuations can be determined from the following two retarded response functions:

$$\begin{aligned} \chi_s(k, \omega) \delta_{\ell, m} &= -\frac{i}{\hbar} \int d^2r \int_0^\infty dt \\ &\quad \langle [n_\ell(\mathbf{r}, t), n_m(0, 0)] \rangle e^{-i(\mathbf{k}\cdot\mathbf{r} - \omega t)}, \\ \chi_u(k, \omega) \delta_{\ell, m} &= -\frac{i}{\hbar} \int d^2r \int_0^\infty dt \\ &\quad \langle [M_\ell(\mathbf{r}, t), M_m(0, 0)] \rangle e^{-i(\mathbf{k}\cdot\mathbf{r} - \omega t)}, \end{aligned} \quad (1.6)$$

where all fields have now acquired a Heisenberg-picture time (t) dependence, the indices ℓ, m extend over the three spin directions x, y, z , and the average is with respect to a thermal Gibbs ensemble at a temperature T . These correlation functions are the dynamic staggered and uniform spin-susceptibilities respectively; their values predict the result of essentially all the experiments that have been performed on antiferromagnets. An important exception is the Raman-scattering cross-section⁴⁶ - we will not discuss its properties here.

We now present the scaling forms satisfied by χ_s , χ_u , and C_V in the vicinity of the quantum phase transition at $g = g_c$. The temperature, T , is taken to be non-zero, but must satisfy

$$k_B T \ll J. \quad (1.7)$$

A non-zero T implies the absence of a spin-condensate, and the response functions are therefore rotationally invariant. It is useful to describe separately the scaling properties of magnets with and without Néel order in their ground state. This will be followed by a discussion of the relationship between the two cases.

A. Néel ordered ground state:

The scaling properties should clearly depend upon a variable which measures the distance of the ground state from criticality. The most convenient choice is the ground state spin-stiffness⁴⁷ ρ_s . Its value can be easily determined by experiments and by various numerical analyses on model Hamiltonians, with no arbitrary overall scale factors. In two-dimensions, ρ_s has the dimensions of energy, and the requirement that the magnet is not too far from criticality is

$$\rho_s \ll J. \quad (1.8)$$

Upon approaching g_c , ρ_s obeys Josephson scaling⁴⁸

$$\rho_s \sim (g_c - g)^{(D-2)\nu}, \quad (1.9)$$

where ν is the usual correlation length exponent. We can now state one of the central results of this paper: For $g \leq g_c$, and under the conditions on T and ρ_s noted above, the values of χ_s , χ_u and C_V satisfy the following scaling forms

$$\chi_s(k, \omega) = \frac{N_0^2}{\rho_s} \left(\frac{\hbar c}{k_B T} \right)^2 \left(\frac{N k_B T}{2\pi \rho_s} \right)^\eta \Phi_{1s} \left(\frac{\hbar c k}{k_B T}, \frac{\hbar \omega}{k_B T}, \frac{N k_B T}{2\pi \rho_s} \right), \quad (1.10a)$$

$$\chi_u(k, \omega) = \left(\frac{g \mu_B}{\hbar c} \right)^2 k_B T \Phi_{1u} \left(\frac{\hbar c k}{k_B T}, \frac{\hbar \omega}{k_B T}, \frac{N k_B T}{2\pi \rho_s} \right), \quad (1.10b)$$

$$C_V = \frac{3\zeta(3)}{\pi} k_B \left(\frac{k_B T}{\hbar c} \right)^2 \Psi_1 \left(\frac{N k_B T}{2\pi \rho_s} \right), \quad (1.10c)$$

where N is the number of components of the order-parameter, ζ is the Reimann zeta function, and Φ_{1s} , Φ_{1u} and Ψ_1 are completely universal, dimensionless, functions (Φ_{1u} and Φ_{1s} are

complex while Ψ_1 is real) defined such that they remain finite as $T/\rho_s \rightarrow \infty$; this will also be true for other scaling functions introduced below. For simplicity, we have explicitly specialized to antiferromagnets with spacetime dimension $D = 2 + 1$, although analogous results for general D are not difficult to write down. Particularly striking is the absence of any non-universal scale factors (in either the arguments or the prefactors of the scaling functions) in all scaling forms. Everything is fully determined by the values of ρ_s , c and N_0 and there is no further dependence on lattice scale physics. The universal dependence of the spin susceptibilities on ρ_s , N_0 and c was implicit in the analysis of Chakravarty *et.al.*¹² (see also the recent work of Hasenfratz and Niedermayer²⁵) for the low T regime $T \ll \rho_s$; our results are however valid for *all* values of T/ρ_s . Also Castro Neto and Fradkin⁴⁹ have recently discussed closely related scaling forms for C_V near general quantum phase transitions in $2+1$ dimensions. The coefficient of Ψ_1 in (1.10c) has been chosen to be the specific heat of a single gapless bose degree of freedom with dispersion $\omega = ck$ in 2 dimensions. The number $\Psi_1(T \rightarrow 0)$ is thus a measure of the effective number of such modes in the ground state. This number is given by $\Psi_1(0)$ for the ordered Néel phase, and by $\Psi_1(\infty)$ for the quantum critical state at $g = g_c$.

We note further that all scaling forms continue to be valid even at $g = g_c$: the prefactor of Φ_{1s} in (1.10a) remains non-singular at $g = g_c$ because of the results (1.3), (1.9) and the exponent identity⁴⁵

$$2\beta = (D - 2 + \eta)\nu. \quad (1.11)$$

The arguments of the scaling functions will occur frequently in this paper. We therefore introduce the dimensionless variables

$$\bar{k} = \frac{\hbar ck}{k_B T} \quad ; \quad \bar{\omega} = \frac{\hbar \omega}{k_B T}, \quad (1.12)$$

which represent momentum and frequency measured in units of a scale set by the absolute temperature T . The third argument

$$x_1 = \frac{N k_B T}{2\pi \rho_s}, \quad (1.13)$$

determines whether the antiferromagnet is better described at the longest distances as a quantum-critical or a renormalized-classical model (see Fig. 1). The factor of N in the definition of x_1 is to facilitate the large N limit in which $\rho_s \sim N$; the variable x_1 will therefore remain of order unity. The factor of $1/(2\pi)$ is purely for future notational convenience. For large x_1 , the energy scale $k_B T$ is the largest energy which first cuts-off the critical spin fluctuations, and the system never fully realize that its coupling g is in fact different from g_c and that the ground state is ordered: the spin-fluctuations are quantum-critical at the shortest scales, and are eventually quenched in a universal way by the temperature. For small x_1 the antiferromagnet is in the renormalized-classical region. There is a large intermediate scale over which the antiferromagnet behaves as if it has long-range Néel order; eventually, strong two-dimensional classical thermal fluctuations of the order-parameter destroy the Néel order.

B. Quantum-disordered ground state:

We now consider the case $g \geq g_c$. We will assume that the quantum-disordered state has a gap towards all excitations. This has certainly been satisfied by all explicit large N constructions of such states in frustrated antiferromagnets in the vicinity of the transition to long-range Néel order^{15,16}. We will assume further that there are no deconfined spin-1/2 excitations above the ground state: this is expected to be true in systems with a collinear Néel order parameter¹⁶. Antiferromagnets on the triangular or kagome lattices with coplanar spin correlations are expected to possess deconfined spin-1/2 spinon excitations^{16,44} - their critical properties will therefore not be described by the present theory. For the case of confined spinons which is under consideration here, the lowest excitation with non-zero spin will carry spin 1. Further, at $T = 0$, this excitation should have an infinite lifetime at small enough k . The distance from criticality is conveniently specified by the gap, Δ , to this spin 1 excitation. The equal-time order parameter correlation function will decay exponentially on a scale ξ which is inversely proportional to Δ . Therefore Δ will vanish as

$$\Delta \sim (g - g_c)^\nu \quad (1.14)$$

upon approaching criticality. One is not too far from criticality provided

$$\Delta \ll J. \quad (1.15)$$

Further, we need an observable which sets the scale for order-parameter fluctuations. On the ordered side this was done by N_0 . A convenient choice on the disordered side is to use an amplitude of the local, on-site, dynamic susceptibility, χ_L . This susceptibility is defined by

$$\begin{aligned} \chi_L(\omega)\delta_{\ell m} &= -\frac{i}{\hbar} \int_0^\infty dt \langle [S_{i\ell}(t), S_{im}(0)] \rangle \\ &\approx \delta_{\ell m} \int \frac{d^2k}{4\pi^2} \chi_s(k, \omega). \end{aligned} \quad (1.16)$$

In principle, χ_u also contributes to χ_L , but when (1.15) is satisfied its contribution is subdominant to that from χ_s , and can therefore be neglected. For $g > g_c$, it can be shown that at $T = 0$, χ_L has the following imaginary part for small ω close enough to the threshold Δ :

$$\text{Im}\chi_L(\omega)|_{T=0} = \frac{\mathcal{A}}{4} \text{sgn}(\omega)\theta(\hbar|\omega| - \Delta), \quad (1.17)$$

where θ is the unit step function, and $\mathcal{A}/4$ is an amplitude with the dimensions of inverse-energy. We will show later that the discontinuity $i\mathcal{A}/4$ in the local dynamic susceptibility is precisely a quarter of the quasiparticle residue \mathcal{A} of the low-lying spin-1 excitation. As g approaches g_c , \mathcal{A} vanishes as

$$\mathcal{A} \sim (g - g_c)^{\eta\nu}. \quad (1.18)$$

We have now assembled all the variables necessary for obtaining the scaling forms for χ_s and χ_u for $g \geq g_c$. The relations analogous to (1.10a), (1.10b) and (1.10c) are

$$\chi_s(k, \omega) = \mathcal{A} \left(\frac{\hbar c}{k_B T} \right)^2 \left(\frac{k_B T}{\Delta} \right)^\eta \Phi_{2s} \left(\frac{\hbar c k}{k_B T}, \frac{\hbar \omega}{k_B T}, \frac{k_B T}{\Delta} \right), \quad (1.19a)$$

$$\chi_u(k, \omega) = \left(\frac{g \mu_B}{\hbar c} \right)^2 k_B T \Phi_{2u} \left(\frac{\hbar c k}{k_B T}, \frac{\hbar \omega}{k_B T}, \frac{k_B T}{\Delta} \right), \quad (1.19b)$$

$$C_V = \frac{3\zeta(3)}{\pi} k_B \left(\frac{k_B T}{\hbar c} \right)^2 \Psi_2 \left(\frac{k_B T}{\Delta} \right), \quad (1.19c)$$

where Φ_{2s} , Φ_{2u} , and Ψ_2 are completely universal functions, which are finite in the limit $T/\Delta \rightarrow \infty$. The physical response functions are again completely determined by three thermodynamic parameters: Δ , c , and \mathcal{A} , with no further sensitivity to lattice scale physics. As in Sec IA, all scaling forms continue to be valid even at $g = g_c$: the prefactor of Φ_{2s} in (1.19a) remains non-singular at $g = g_c$ because of the scaling results (1.14), (1.18).

We also introduce, for future convenience, the variable

$$x_2 = \frac{k_B T}{\Delta}, \quad (1.20)$$

which determines whether the antiferromagnet is in the quantum-critical or quantum disordered regions (see Fig 1). For large x_2 , the temperature T predominates the small zero-temperature gap, Δ , and the system may as well be at $g = g_c$. For small x_2 , the ground-state gap Δ quenches the spin fluctuations, putting the system in the quantum-disordered region. The thermodynamics is well described in terms of a dilute gas of activated excitations.

C. Critical point:

We have obtained above two separate universal scaling forms at the critical coupling $g = g_c$, but T finite, by taking the limits $g \nearrow g_c$ and $g \searrow g_c$. It follows therefore that the two results must be simply related:

$$\begin{aligned} \Phi_{2s}(\bar{k}, \bar{\omega}, x_1 = \infty) &= Z_Q \Phi_{1s}(\bar{k}, \bar{\omega}, x_2 = \infty), \\ \Phi_{2u}(\bar{k}, \bar{\omega}, x_1 = \infty) &= \Phi_{1u}(\bar{k}, \bar{\omega}, x_2 = \infty), \\ \Psi_2(\infty) &= \Psi_1(\infty), \end{aligned} \quad (1.21)$$

where Z_Q is a universal number. Recall that the universal functions have been chosen to have a finite limit as $x_{1,2} \rightarrow \infty$.

Note that there is no rescaling factor for the uniform susceptibility and the specific heat. This is because their overall scale is universal and was not set by some thermodynamic observable, as was the case for the staggered susceptibility. This universality in scale is related to the fact that \mathbf{M} and the energy are conserved quantities: this will be discussed further in Sec II. For the staggered susceptibility, we have performed a $1/N$ expansion of the scale factor on antiferromagnets with an N -component order-parameter and found

$$Z_Q = 1 - \frac{0.229191243}{N}. \quad (1.22)$$

Actually it is not just the values, but the entire asymptotic expansions of the universal functions which have matching conditions at $x_{1,2} = \infty$. As the antiferromagnet has no phase transition at finite temperature, all its measurable properties should be smooth functions of the bare coupling constant $g - g_c$ provided $T \neq 0$. This fact, combined with $x_1 \sim (g_c - g)^{-\nu}$, $x_2 \sim (g - g_c)^{-\nu}$, can be used to easily deduce the constraints on the asymptotic expansions of Φ_{1s} , Φ_{1u} , Ψ_1 , Φ_{2s} , Φ_{2u} , Ψ_2 about $x_{1,2} = \infty$.

D. Experimental Observables

The main purpose of the rest of the paper is to describe the universal functions Φ_{1s} , Φ_{1u} , Ψ_1 , Φ_{2s} , Φ_{2u} , and Ψ_2 as completely as possible. An large amount of information is contained in them; in particular, as we shall see later, in a suitable limit they contain the complete static and dynamic scaling functions of Chakravarty *et. al.*¹² and Tyc *et. al.*¹³. A large number of experimentally testable quantities can be obtained from these functions; now we highlight some of the most important by endowing them with their own scaling functions.

We begin with the measurements related to χ_u .

1. Static, uniform spin susceptibility and spin diffusivity

The conservation of \mathbf{M} makes the small k and ω dependence of χ_u rather simple. In the hydrodynamic limit, $\omega\tau_\ell \ll 1$, where τ_ℓ is a typical lifetime of excitations, the magnetization fluctuations must obey a diffusion equation; we find for $g \leq g_c$ that

$$\Phi_{1u}(\bar{k}, \bar{\omega}, x_1) = \Omega_1(x_1) \frac{D_1(x_1) \bar{k}^2}{-i\bar{\omega} + D_1(x_1) \bar{k}^2}; \quad \bar{k}, \bar{\omega} \ll 1, \quad (1.23)$$

and an analogous expression for $g \geq g_c$ with $1 \rightarrow 2$. The functions $\Omega_1(x_1)$, $\Omega_2(x_2)$, $D_1(x_1)$, $D_2(x_2)$ are all universal. From (1.10b), (1.12), (1.19b) we see that they are related to the static, uniform spin susceptibility χ_u^{st} , and spin diffusion constant D_S . We have for $g \leq g_c$

$$\begin{aligned} \chi_u^{\text{st}}(T) &= \left(\frac{g\mu_B}{\hbar c} \right)^2 k_B T \Omega_1(x_1), \\ D_S(T) &= \frac{\hbar c^2}{k_B T} D_1(x_1), \end{aligned} \quad (1.24)$$

and analogous expressions for $g \geq g_c$ with $1 \rightarrow 2$.

2. Wilson Ratio

The Wilson ratio is defined by

$$W = \frac{k_B^2 T \chi_u^{\text{st}}(T)}{(g\mu_B)^2 C_V(T)}. \quad (1.25)$$

Its properties are therefore easily obtainable from our scaling results for χ_u^{st} and C_V . It follows from (1.10c), (1.19c) and (1.24) that W is a completely universal function of x_1 (x_2) for $g \leq g_c$ ($g \geq g_c$). We have for $g \leq g_c$

$$W = \frac{\pi}{3\zeta(3)} \frac{\Omega_1(x_1)}{\Psi_1(x_1)}. \quad (1.26)$$

and analogous expression for $g \geq g_c$ with $1 \rightarrow 2$.

We turn next to experiments sensitive to χ_s .

3. Structure factor

The equal-time spin structure factor, $S(k)$, is related to $\chi_s(k, \omega)$ by

$$\begin{aligned} S(k)\delta_{\ell m} &= \int d^2r \langle n_\ell(\mathbf{r}, 0)n_m(0, 0) \rangle e^{-i\mathbf{k}\cdot\mathbf{r}} \\ &= \hbar \int_{-\infty}^{\infty} \frac{d\omega}{\pi} \frac{\delta_{\ell m}}{1 - e^{-\hbar\omega/(k_B T)}} \text{Im}\chi_s(k, \omega). \end{aligned} \quad (1.27)$$

From (1.10a), we deduce that for $g \leq g_c$ it satisfies the scaling form

$$S(k) = \frac{N_0^2 (\hbar c)^2}{\rho_s k_B T} x_1^\eta \Xi_1(\bar{k}, x_1), \quad (1.28)$$

where the universal function Ξ_1 is given by

$$\Xi_1(\bar{k}, x_1) = \int_{-\infty}^{\infty} \frac{d\bar{\omega}}{\pi} \frac{1}{1 - e^{-\bar{\omega}}} \text{Im}\Phi_{1s}(\bar{k}, \bar{\omega}, x_1). \quad (1.29)$$

Similarly for $g \geq g_c$, we can relate $S(k)$ to a universal function $\Xi_2(\bar{k}, x_2)$ with the prefactor N_0^2/ρ_s replaced by \mathcal{A} and the subscript $1 \rightarrow 2$.

4. Antiferromagnetic correlation length

We define the correlation length ξ from the long-distance, $e^{-r/\xi}$, decay of the equal time $\mathbf{n} - \mathbf{n}$ correlation function. This correlation function will have such an exponential decay for all g provided $T \neq 0$ (the actual asymptotic form also has powers of r as a prefactor). Equivalently, one can define ξ as κ^{-1} , where $i\kappa$ is the location of the pole of $S(k)$ closest to the real k axis. The scaling function for ξ for $g \leq g_c$ is

$$\xi^{-1} = \frac{k_B T}{\hbar c} X_1(x_1). \quad (1.30)$$

For $g \geq g_c$ we have an identical form with $1 \rightarrow 2$. Since the correlation lengths must match at $g = g_c$, we clearly have $X_1(\infty) = X_2(\infty)$. The universal linear T dependence of ξ^{-1} at $g = g_c$ ($x_1 = \infty$) was noted by Chakravarty *et. al.*¹².

5. Local susceptibility

From its definition (1.16), and the scaling form (1.10a), we can deduce the following for $g \leq g_c$:

$$\text{Im}\chi_L(\omega) = \frac{N_0^2}{\rho_s} x_1^\eta |\bar{\omega}|^\eta F_1(\bar{\omega}, x_1), \quad (1.31)$$

where the universal function F_1 is

$$F_1(\bar{\omega}, x_1) = \frac{1}{\bar{\omega}^\eta} \int \frac{d^2\bar{k}}{4\pi^2} \text{Im}\Phi_{1s}(\bar{k}, \bar{\omega}, x_1). \quad (1.32)$$

On general grounds we expect $\text{Im}\chi_L(\omega) \sim \omega$ for small ω and T non-zero; this implies that

$$F_1 \sim \text{sgn}(\bar{\omega}) |\bar{\omega}|^{1-\eta} \quad \text{for small } \bar{\omega}. \quad (1.33)$$

In principle, the real part of χ_L also has a singular piece which satisfies a scaling form analogous to (1.31); however the momentum integral in (1.32) is divergent at the upper cutoff (provided $\eta > 0$). Thus $\text{Re}\chi_L$ has a leading contribution which is non-universal and dominated by lattice scale physics. There is no such problem for $\text{Im}\chi_L$ however - in this case the momentum integral sums over intermediate states which are on-shell and only long-wavelengths contribute. Finally we note that a similar scaling form for $\text{Im}\chi_L$ for $g \geq g_c$ can be obtained by replacing N_0^2/ρ_s by \mathcal{A} and the substitution $1 \rightarrow 2$.

6. NMR relaxation rate

We consider the relaxation of nuclear spins coupled to electronic spins of the antiferromagnet (*e.g.* Cu spins in La_2CuO_4). We assume that the relaxation is dominated by contributions near the antiferromagnetic ordering wavevector. After suitably accounting for lattice-scale form factors and integrating out high-energy lattice excitations, a coupling A_π between the nuclear spins and the antiferromagnetic order parameter \mathbf{n} can be obtained. The typical frequencies in NMR experiments are much smaller than the temperature and the relaxation rate, $1/T_1$ of the nuclear spins is given by

$$\frac{1}{T_1} = \lim_{\omega \rightarrow 0} 2A_\pi^2 \frac{k_B T}{\hbar^2 \omega} \int \frac{d^2k}{4\pi^2} \text{Im}\chi_s(k, \omega). \quad (1.34)$$

From (1.31) we deduce the following result for $1/T_1$ for $g \leq g_c$

$$\frac{1}{T_1} = \frac{2A_\pi^2 N_0^2}{\hbar \rho_s} x_1^\eta R_1(x_1), \quad (1.35)$$

where $R_1(x_1)$ is a universal function given by

$$R_1(x_1) = \lim_{\bar{\omega} \searrow 0} \frac{F_1(\bar{\omega}, x_1)}{\bar{\omega}^{1-\eta}}. \quad (1.36)$$

As before, the scaling form for $1/T_1$ for $g \geq g_c$ involves replacing N_0^2/ρ_s by \mathcal{A} and replacing $1 \rightarrow 2$ on the right-hand-side.

We will discuss the general form of our results for the scaling functions for the different regions of the phase diagram in turn (Fig. 1). We will consider first the quantum-critical region ($x_1 \gg 1, x_2 \gg 1$), followed by the renormalized-classical ($x_1 \ll 1$) and the quantum-disordered ($x_2 \ll 1$) regions. Precise numerical results will not be presented here: the reader is referred to Sections III-VI for precise results obtained in the $1/N$ expansion of the $O(N)$ non-linear sigma model.

E. Quantum-critical region ($x_1 \gg 1$ or $x_2 \gg 1$)

At short length/time scales the spin fluctuations in any nearly-critical antiferromagnet should be indistinguishable from those at the critical point. The special property of the quantum-critical region is that the deviations from criticality at longer length/time scales arise primarily from the presence of a finite T . The fact that the ground state of the system is not exactly at the critical point is never terribly important, and the system does not display behavior characteristic of either ground state at any length/energy scale. The critical spin fluctuations are instead quenched in a universal way by thermal relaxational effects.

It should therefore be evident that there are two distinct types of spin fluctuations in wavevector/frequency space (Fig. 2). With either $\hbar ck$ or $\hbar\omega$ significantly larger than $k_B T$, the spin-dynamics is that of the critical 2+1 dimensional field theory of the critical point $g = g_c$. Otherwise, damping from thermally-excited, critical spin-waves produces a regime of quantum-relaxational dynamics.

The crossover from the 2+1 critical to quantum-relaxational behavior is clearly evident in the dynamic staggered susceptibility (See Fig. 3). In the 2+1 dimensional critical region ($\bar{k} \gg 1$ or $\bar{\omega} \gg 1$) we have

$$\Phi_{1s}(\bar{k}, \bar{\omega}, \infty) = \frac{A_Q}{(\bar{k}^2 - \bar{\omega}^2)^{1-\eta/2}} ; \quad \bar{k} \gg 1 \text{ or } \bar{\omega} \gg 1, \quad (1.37)$$

where A_Q is a universal number, and the exponent $\eta = 8/(3\pi^2 N)$ at order $1/N$ but is known⁵⁰ to order $1/N^3$. For $N = 3$, precision Monte Carlo simulations⁵¹ place the value of η around $\eta \approx 0.028$; this extremely small, but positive, value of η will have important consequences for experiments. Note that in this regime $\text{Im}\Phi_{1s}$ is non-zero only for $\bar{\omega} > \bar{k}$ where one obtains a broadband spectrum of critical spin-waves. The small value of η implies however that the damping is small and the spectrum is almost a delta-function. In the quantum-relaxational regime ($\bar{k} \ll 1$ and $\bar{\omega} \ll 1$), there is strong damping due to thermally-excited, critical spin-waves and excitations are not well-defined. However the spectrum of overdamped spin-waves remains universal and is shown in Fig. 3

The same crossover is also present in the structure factor. Its universal scaling function $\Xi_1(\bar{k}, \infty) = Z_Q^{-1}\Xi_2(\bar{k}, \infty)$ has the 2+1 critical form $\Xi_1(\bar{k}, \infty) \sim \bar{k}^{-1+\eta}$ at large \bar{k} , and a Lorentzian form at small \bar{k} .

The various static observables have a value set by the absolute temperature in a universal way. Their T dependence can be deduced easily from the scaling forms with the knowledge

that all scaling functions were chosen to have a finite limit as $x_{1,2} \rightarrow \infty$. The first corrections away from $x_{1,2} = \infty$ are given by⁵²

$$U(x_{1,2}) = U_\infty + U_{1,2}/x_{1,2}^{1/\nu} + \dots \quad x_{1,2} \gg 1 \quad (1.38)$$

where U represents any of the scaling functions X , Ω , Ψ for the correlation length, uniform static susceptibility, and specific heat respectively. The form of the subleading term above follows from the requirement that the physics at finite temperature is a smooth function of the bare coupling $g - g_c$. Chakravarty *et. al.*¹² have noted the $x_1 = \infty$ result for the case of the correlation length.

F. Renormalized classical region ($x_1 \ll 1$)

We now describe our results at low temperatures on the ordered side, $g < g_c$, $x_1 \ll 1$. Extensive results on a closely related regime have been obtained by Chakravarty *et.al.*¹² and Tyc *et.al.*¹³. The relationship between our and their results is discussed below. We will find that, in the appropriate limit, our scaling functions reduce exactly to theirs.

We begin with a qualitative discussion of the nature of the spin correlations in the renormalized-classical region. The spin-fluctuations now fall naturally into *three* different regimes in wavevector-frequency space (see Fig. 2). At the largest $\bar{k}, \bar{\omega}$ we have 2+1 dimensional critical spin fluctuations which are essentially identical to those in the quantum critical region and are therefore described by a staggered spin susceptibility Φ_{1s} similar to that in (1.37). Upon moving to longer distances/times, the first crossover occurs at length (time) scales of order ξ_J (ξ_J/c) to a ‘Goldstone’ regime where the spin dynamics is well described by rotationally averaged spin-wave fluctuations about a Néel ordered ground state. The scale ξ_J , controlling the critical to Goldstone crossover, is the Josephson correlation length⁴⁸, and determines the vicinity of the ground state of the antiferromagnet to the quantum phase transition. Near g_c , ξ_J diverges as

$$\xi_J \sim (g_c - g)^{-\nu}. \quad (1.39)$$

The second crossover in the renormalized classical region (Fig. 2) occurs at the length scale ξ , which is the actual correlation length. At this scale, strong, classical, two-dimensional, thermal fluctuations of locally Néel ordered regions destroy the long range Néel order, so that at scales larger than ξ , the antiferromagnet again appears disordered, with all equal-time spin correlations decaying exponentially in space. The scale ξ is roughly given by

$$\xi \sim \xi_J \exp\left(\frac{N}{(N-2)x_1}\right), \quad (1.40)$$

where we have omitted pre-exponential power-law factors of x_1 . For small x_1 , ξ is clearly much larger than ξ_J ; the three regimes in Fig. 2 are therefore well separated.

Our explicit results for the scaling functions will be restricted to the vicinity of the second crossover described above: thus they are valid when $x_1 \ll 1$, $k\xi_J \ll 1$, and $\omega\xi_J/c \ll 1$. In this regime, all of our scaling functions, which in general depend upon three arguments $\bar{k}, \bar{\omega}$,

and x_1 , collapse into reduced scaling function depending only on two arguments measuring momentum and frequency, $k\xi$ and $\omega\xi/c$. Further, the reduced scaling functions turn out to be exactly those obtained by Chakravarty *et. al.*¹² Tyc *et. al.*¹³ and Hasenfratz *et. al.*^{25,26}. At first sight this result may seem a bit surprising. Our results were obtained for antiferromagnets with a small stiffness, *i.e.* $\rho_s \ll J$, while in other work^{12,13,25,26}, no restrictions was placed on the value of ρ_s . The equivalence to order $1/N$ between the two theories is a consequence of the fact that the low T results in the renormalized classical region contain *no corrections of order ρ_s/J to order $1/N$* . In a recent analysis Hasenfratz *et. al.*^{25,26} have suggested that such corrections are in fact absent at low T at all orders in $1/N$.

We show the nature of the collapse in the scaling functions explicitly for the structure factor. Chakravarty *et. al.*¹² proposed the scaling form

$$S(k) = S(0) f(k\xi), \quad (1.41)$$

where f is a universal function. We find that f is related to the scaling function Ξ_1 by

$$f(y) = \lambda_f \left(\frac{N}{N-2} \right)^{1/(N-2)} \lim_{x_1 \rightarrow 0} \left\{ (x_1)^{\eta-1/(N-2)} X_1^2(x_1) \right. \\ \left. \times \Xi_1[yX_1(x_1), x_1] \right\}, \quad (1.42)$$

where the universal number λ_f was found to be $\lambda_f = 1 - 0.188/N + \mathcal{O}(1/N^2)$.

In Section V we will present the details of our computations of the reduced scaling functions of the renormalized-classical regime in a $1/N$ expansion. Our results agree with those of Chakravarty *et. al.*¹²; however we are also able to obtain a number of universal amplitudes which were previously only determined by numerical simulations.

Another of our new results here is the low T dependence ($x_1 \ll 1$) of the scaling functions for the uniform susceptibility and specific heat:

$$\Omega_1(x_1) = \frac{1}{\pi x_1} + \frac{N-2}{N\pi} \\ \Psi_1(x_1) = N-1 \quad (1.43)$$

These results have also been obtained independently by Hasenfratz *et. al.*²⁵ The first of these results will be important to us later in the comparison with experiments. The second result simply implies that the number of low energy degrees of freedom are the $N-1$ spin waves. The two results together also imply that the Wilson ration $W \sim 1/T$ at low temperatures provided $g < g_c$.

G. Quantum disordered region ($x_2 \ll 1$)

At $T = 0$ ($x_2 = 0$), the ground state of the antiferromagnet has a gap towards all excitations in this region. Unlike both previous regions, therefore, finite T is almost always a weak perturbation on the $T = 0$ results; all finite temperature corrections are accompanied by factors of $\exp(-\Delta/(k_B T)) = \exp(-1/x_2) \ll 1$. Furthermore, the ground state is rather well described by the $N = \infty$ theory. We will therefore refrain, here, from giving complete

expressions for all the observables; we refer the reader to Section III A 2 for the exact results at $N = \infty$.

However, thermal effects and $1/N$ corrections are important at measurement frequencies smaller than Δ ; in this region the dynamics is controlled by a dilute concentration of thermally excited quasiparticles. The dissipative effects of such quasiparticles will be discussed in Section IV.

We now discuss the plan of the remainder of the paper. In Section II we present a phenomenological derivation of the scaling forms used above. Section III introduces the quantum $O(N)$ non-linear sigma model and presents the complete solution for all the scaling functions at $N = \infty$. The formal structure of the model at order $1/N$ is also discussed. The remainder of the paper contains the details of the calculations. The calculations are discussed for the quantum-critical, renormalized-classical, and quantum-disordered regions in turn in Sections IV, V, VI. Finally in Section VII the comparison with experimental results is presented. The appendixes contain a discussion of the effects of disorder and Berry phases, results of a Monte-Carlo simulation, and some technical details.

II. PHENOMENOLOGICAL DERIVATION OF SCALING FORMS

In this section we will present a phenomenological derivation of the scaling forms (1.10a), (1.19a) for the order-parameter dynamic susceptibility, the scaling forms (1.10b), (1.19b) for the uniform spin susceptibility, and the scaling forms (1.10c), (1.19c) for the specific heat. These are valid in the vicinity of a quantum phase transition in a two-dimensional quantum Heisenberg antiferromagnet from a state with long-range Néel order to a spin-fluid state. We will only consider the case in which the Néel order parameter is a 3-vector. The following discussion does not explicitly refer to the quantum non-linear sigma model. It should instead be regarded more generally as a study of the consequences of the scaling hypothesis on a quantum phase transition in a Heisenberg antiferromagnet. The non-linear sigma model provides a realization and verification of these hypothesis for a particular field theory.

Let us first present the precise ingredients from which our results follow.

1. The spin-wave velocity, c , should be non-singular at the $T = 0$, quantum fixed-point separating the two phases. We will also assume, for simplicity, that there is no spatial anisotropy; this assumption is not crucial and our results can be easily extended to include quantum transitions in anisotropic systems like spin chains coupled in a plane. These systems will of course have two spin-wave velocities, whose effects can be absorbed into a rescaling of lengths. In the presence of spatial isotropy, and for the case of the vector order-parameter, the non-singularity of the spin-wave velocity implies that the critical field-theory has the Lorentz invariance of 2+1 dimensions.
2. The antiferromagnet in the vicinity of the critical point satisfies ‘hyperscaling’⁴⁵ hypothesis. For a quantum transition in $D = 2 + 1$ dimensions, this hypothesis implies that the singular part of the free energy density (\mathcal{F}_s) at $T = 0$ has the form

$$\mathcal{F}_s = \hbar c \tilde{\Upsilon} \xi^{-D} \tag{2.1}$$

where ξ is the correlation length which diverges at the transition (of course, on the ordered side $\xi = \xi_J$). The number $\tilde{\Upsilon}$ is dimensionless, and like all such numbers at the critical point, it is expected to be universal. The statement of the universality of $\tilde{\Upsilon}$ is known in the literature as the hypothesis of ‘two-scale factor’ universality^{53,54}.

3. Turning on a finite temperature places the critical field theory in a slab geometry which is infinite in the two spatial directions, but of finite length,

$$L_\tau = \frac{\hbar c}{k_B T}, \quad (2.2)$$

in the imaginary time (τ) direction. The consequences of a finite T can therefore be deduced by the principles of finite-size scaling⁵⁶.

In the following we measure temperature, time, and length in units which make k_B , \hbar , and c equal to unity.

A. Staggered susceptibility, $g < g_c$

Consider first the application of the scaling hypothesis to the staggered spin susceptibility for $g < g_c$. A straightforward application of finite-size scaling yields

$$\begin{aligned} \chi_s(k, \omega) &= AL_\tau^{2-\eta} \tilde{\Phi} \left(kL_\tau, \omega L_\tau, \frac{\xi_J}{L_\tau} \right) \\ &= \frac{A}{T^{2-\eta}} \tilde{\Phi} \left(\bar{k}, \bar{\omega}, \frac{\xi_J}{L_\tau} \right), \end{aligned} \quad (2.3)$$

where A is a non-universal amplitude, and the scaling function $\tilde{\Phi}$ is universal upto an overall pre-factor. In particular there are no non-universal metric factors⁵⁷ in any of the three arguments of $\tilde{\Phi}$. We now wish to eliminate the dependence of this result on ξ_J . It has been argued recently^{55,47} that the result (2.1) can be extended to deduce a simple, universal relationship between ρ_s and ξ_J , valid in the limit $\xi_J \rightarrow \infty$:

$$\rho_s = \frac{\hbar c \Upsilon}{\xi_J} \quad (2.4)$$

where Υ is another universal number. Now, from (1.13), (2.4) and (2.2) we see that that the third argument

$$\frac{\xi_J}{L_\tau} = \frac{\Upsilon T}{\rho_s} = \frac{N\Upsilon}{2\pi} x_1. \quad (2.5)$$

We therefore define a new universal function Φ_{1s}

$$\Phi_{1s}(\bar{k}, \bar{\omega}, x_1) \equiv \tilde{\Phi} \left(\bar{k}, \bar{\omega}, \frac{N\Upsilon}{2\pi} x_1 \right). \quad (2.6)$$

We shall soon see that Φ_{1s} is the same function as in (1.10a).

To make Φ_{1s} completely universal, we have to fix its overall scale, which we now do. First, we notice that in the renormalized classical region ($x_1 \ll 1$), there is a Goldstone regime ($k\xi_J \ll 1$, $k\xi \gg 1$, see Fig. 2 and Section IF) of non-interacting spin-waves. In this regime, the hydrodynamics predicts that the static staggered susceptibility has a simple form:

$$\chi_s(k, \omega = 0) = \left(1 - \frac{1}{N}\right) \frac{N_0^2}{\rho_s k^2};$$

$$x_1 \ll 1, \quad k\xi_J \ll 1, \quad k\xi \gg 1. \quad (2.7)$$

The scale of the susceptibility has been set by the magnitude of $T = 0$ staggered moment. The factor of $(1 - 1/N)$ arises from the fact that only $N - 1$ transverse modes contribute the Goldstone singularity, while the longitudinal mode is massive; after rotationally averaging this induces a factor of $(N - 1)/N$. We now demand that in the appropriate limit, the scaling-form (2.3) obey this Goldstone form. The key constraint is that (2.7) is T independent. It is easy to show that this can be satisfied by (2.3) only if

$$\Phi_{1s}(\bar{k}, \bar{\omega} = 0, x_1) = \frac{b}{\bar{k}^2 x_1^\eta};$$

$$x_1 \ll 1, \quad \bar{k}x_1 \ll 1, \quad \bar{k}e^{N/((N-2)x_1)} \gg 1, \quad (2.8)$$

for some constant b . In the last restriction on \bar{k} we have used (1.40), valid for the $O(N)$ sigma model and neglected pre-exponential factors of x_1 . The prefactor in (2.8) is of course arbitrary. We now make the specific choice, $b = 1 - 1/N$ and thus specify the overall scale of Φ_{1s} . Comparing (2.3), (2.6), (2.7), and (2.8), we can now fix the value of the prefactor A

$$A = \frac{N_0^2}{\rho_s} \left(\frac{N}{2\pi\rho_s}\right)^\eta. \quad (2.9)$$

Inserting this value of A into (2.3), we obtain (1.10a) as desired.

B. Staggered susceptibility, $g > g_c$

A similar analysis can be carried out in the spin-fluid phase for the staggered susceptibility and its scaling function Φ_{2s} as in (1.19a). We remind the reader that our theory is valid only for antiferromagnets with a 3-vector order parameter, in which case the quantum disordered phase is expected to have only integer spin excitations^{3,15,16}; in particular if spin-1/2 spinons are present at intermediate scales, they are always confined at the longest distances.

At $T = 0$ the equal-time order parameter correlation function will decay in space with a correlation length ξ . As the theory has a Lorentz invariance, this implies that the gap towards spin-1 excitations, Δ , is

$$\Delta = \frac{\hbar c}{\xi}, \quad (2.10)$$

where we have momentarily reinserted explicit factors of \hbar and c . An application of finite-size scaling, very similar to that for the ordered side, now yields immediately the scaling function (we now return to units in which $k_B = \hbar = c = 1$)

$$\chi_s(k, \omega) = \frac{\tilde{A}}{T^{2-\eta}} \Phi_{2s} \left(\frac{\bar{k}}{T}, \frac{\bar{\omega}}{T}, \frac{T}{\Delta} \right). \quad (2.11)$$

The only non-universal components on the right-hand-side are the amplitude \tilde{A} and the related overall scale of the function Φ_{2s} . As before, we will fix this scale by matching with an experimental observable at $T = 0$. Let us therefore think about the nature of the spectrum in the spin-fluid phase at $T = 0$. As all excitations have a gap, the spin 1 quasiparticle should have an infinite lifetime for energies close enough to the threshold Δ (this quasiparticle appears as the bound state of two spinons in large M theories of $SU(M)$ and $Sp(M)$ antiferromagnets^{15,16}). Further, the Lorentz invariance of the theory implies that the dispersion spectrum, ω_k of this spin-1 quasiparticle is given by

$$\omega_k = \sqrt{k^2 + \Delta^2} \quad (2.12)$$

for small enough k . These facts combine to imply the following form for χ_s at $T = 0$

$$\chi_s(k, \omega) = \frac{\mathcal{A}}{k^2 - (\omega + i\varepsilon)^2 + \Delta^2}; \quad T = 0, \quad k \ll \Delta, \quad |\omega - \Delta| \ll \Delta, \quad (2.13)$$

where ε is a positive infinitesimal and \mathcal{A} is the spin-1 quasiparticle residue. This residue can be experimentally measured by examining the imaginary part of the local susceptibility, $\text{Im}\chi_L$. Using (1.16) and (2.13) we find

$$\text{Im}\chi_L(\omega) = \frac{\mathcal{A}}{4} \theta(\omega - \Delta); \quad T = 0, \quad |\omega - \Delta| \ll \Delta. \quad (2.14)$$

The discontinuity in the local dynamic susceptibility is therefore precisely a quarter of the spin-1 quasiparticle amplitude. We now demand that the scaling form (2.11) satisfy (2.13) as $T \rightarrow 0$. A little experimentation shows that this is only possible if

$$\Phi_{2s}(\bar{k}, \bar{\omega}, x_2) = \frac{x_2^{2-\eta}}{(\bar{k}x_2)^2 - (\bar{\omega}x_2 + i\varepsilon)^2 + 1}; \quad x_2 \ll 1, \quad \bar{k}x_2 \ll 1, \quad |\bar{\omega}x_2 - 1| \ll 1. \quad (2.15)$$

Here we have arbitrarily set the overall scale of Φ_{2s} ; this function is now completely universal. Finally, the derivation of (1.19a) is completed by obtaining the amplitude \tilde{A} in (2.11):

$$\tilde{A} = \frac{\mathcal{A}}{\Delta^\eta}. \quad (2.16)$$

The prefactor \tilde{A} is expected to be non-singular as $g \searrow g_c$; therefore the quasiparticle amplitude \mathcal{A} must vanish as

$$\mathcal{A} \sim (g - g_c)^{\eta\nu}. \quad (2.17)$$

This was noted earlier in (1.18).

C. Uniform susceptibility

The key ingredient in the determination of the scaling form for χ_u is the realization that χ_u is simply a stiffness related to twists in boundary conditions on the system along the imaginary time (τ) direction⁵⁸. A uniform magnetic field on the antiferromagnet causes a precession of all the spins at the same rate. The relative angle between any two spins remains unchanged. Therefore by transforming to a rotating reference frame almost all vestiges of the magnetic field can be removed. However the partition function in the laboratory frame had periodic boundary conditions along the τ direction, implying that the system in the rotating frame has a twist in its boundary condition. The susceptibility is the response to such a twist, which is precisely the spin stiffness.

The Lorentz invariance of the theory now implies that the scaling properties of χ_u should be the same as those of ρ_s , which is the stiffness for twists about the *spatial* boundary conditions. In other words, the scaling dimension of χ_u is exactly $D - 2$, and at $T = 0$ the combination $\xi_J \chi_u$ approaches a universal number as $g \nearrow g_c$. The scaling laws (1.10b), (1.19b) are now a completely straightforward consequence of the principles of finite-size scaling. Unlike χ_s , there is no need for any normalization condition to set the overall scale of the scaling function. It is already fixed to a universal value by the hypothesis of two-scale factor universality^{53–55}.

D. Specific heat

Consider the $D = 2 + 1$ dimensional Lorentz invariant theory in a slab geometry in the vicinity of $g = g_c$. An early paper by Fisher and de Gennes⁵⁹ argued by extending (2.1) to finite sizes, that the free energy density \mathcal{F} must have the following dependence on the size, L_τ of the finite dimension

$$\mathcal{F} = \mathcal{F}_0 + \frac{1}{L_\tau^D} \varphi \left(\frac{\xi_J}{L_\tau} \right), \quad (2.18)$$

where \mathcal{F}_0 is the bulk free energy density and we have assumed that $g \leq g_c$. The function φ is universal at all x ; there are no non-universal metric factors in either the argument or the scale of φ ⁵⁷. The scaling function (1.10c) for C_V now follows immediately from the thermodynamic relationship between \mathcal{F} and C_V , the relationship (2.4) between ρ_s and ξ_J , and the relationship (2.2) between L_τ and T . An entirely analogous argument can be made for $g \geq g_c$.

We note that a related result has been discussed recently by Castro Neto and Fradkin⁴⁹ in the context of 2+1 dimensional quantum systems; they have also discussed an interesting connection to the Zamalodchikov's C-theorem⁶⁰. We have chosen a numerical prefactor of the scaling function Ψ_1 in (1.10c) which is the specific heat of a single gapless bose degree of freedom with dispersion $\omega = ck$ in 2 dimensions. The number $\Psi_1(T \rightarrow 0)$ is thus a measure of the effective number of such modes in the ground state. For $g < g_c$, this number should equal $N - 1$, the number of spin-wave modes in the ordered state. For $g = g_c$, the number $\Psi_1(\infty)$ is probably irrational and will be calculated later in this paper to order $1/N$. Finally,

in the quantum disordered phase, $g > g_c$, there are no gapless modes and we should have $\Psi_2(0) = 0$.

A very similar connection between the effective number of gapless modes and C_V was established some time ago for 1 + 1 dimensional spin chains⁶¹; in this case $C_V \sim T$ with C_V/T universal and related to the central charge of a conformal field theory, which in effect measures the number of gapless quasiparticle modes.

III. THE QUANTUM $O(N)$ NON-LINEAR SIGMA MODEL

In this section we will discuss the $O(N)$ quantum non-linear sigma model field theory. This theory may be viewed as the simplest model which displays a quantum phase transition in 2+1 dimensions. Moreover, a microscopic connection between weakly frustrated antiferromagnets with short-range Néel order and the $O(3)$ sigma model can also be established³.

There are several subtle and difficult questions relating to the consequences of Berry phase terms which are present in the antiferromagnet but are absent in the sigma model¹⁵. In this paper we will simply neglect the effects of the Berry phase terms. In Appendix B we will present some circumstantial evidence, in computations for $SU(M)$ antiferromagnets, which suggests that these Berry phases are irrelevant both in the Néel phase and at the quantum critical point, but do significantly modify the properties of the quantum disordered phase. In critical phenomena terminology this implies that the Berry phases are ‘dangerously-irrelevant’. As all of our scaling functions are properties of flows in the vicinity of the quantum-critical point, we do not expect any modifications of our results by Berry phase effects in this scenario. Berry phases will however modify the corrections to scaling.

In passing, we note that there is an alternative expansion which could have been used to obtain the scaling functions of this paper: this is the large M expansion about antiferromagnets with $SU(M)$ or $Sp(M)$ symmetry^{15,16,62}. However, the presence of a gapless gauge field in the perturbative $1/M$ corrections, makes this expansion somewhat more involved than the $O(N)$ expansion. For general M, N , both approaches predict that the lowest-lying non-zero spin excitation above the quantum-disordered ground state in an antiferromagnet with collinear order¹⁶ carries spin $S = 1$; the detailed structure of the spectrum at higher energies is however different in the two theories. The results of this paper show that the $O(N)$ expansion is numerically much more accurate at $N = 3$ than is the $Sp(M)$ or $SU(M)$ expansion at $M = 2$. This can be seen immediately by comparing the values of η in the two theories: the large M theory gives $\eta = 1 - \mathcal{O}(1/M)$ while the large N theory has $\eta = 0 + \mathcal{O}(1/N)$ - compare this with the known value⁵¹ in the $D = 3$ classical Heisenberg model $\eta \approx 0.028$. We shall see below that, at $N = 3$, the $1/N$ corrections in the $O(N)$ model to the universal scaling functions are almost always less than about 20% of the leading $N = \infty$ term.

We will begin this section by a definition of the quantum $O(N)$ non-linear sigma model. The first subsection will present its exact solution at $N = \infty$. This solution has also been discussed earlier by Rosenstein *et. al.*⁶³, although they did not emphasize the universal scaling properties of the solution. For clarity, we will repeat some of the step in Ref.⁶³ and will then explicitly compute all of the scaling functions introduced in Section I in the $N = \infty$ limit. The $N = \infty$ computations are also similar to earlier studies of finite-size scaling properties of the spherical model⁶⁴ - in our case the inverse temperature plays the

role of the finite-size along the time direction. The second subsection will present complete formal expressions for the staggered and uniform susceptibility which are correct to order $1/N$; to the best of our knowledge, these constitute the first computations of finite-size corrections to two-loop order in any system. Subsequent sections will manipulate these expressions into the appropriate scaling forms for the three regions of Fig. 1. The structure of the $1/N$ corrections is however rather involved and the casual reader may be satisfied by studying only the $N = \infty$ solution of Section III A. Even this limited solution is quite rich and instructive; its main shortcoming is the absence of spin-wave damping and anomalous dimensions which appear only at order $1/N$.

The $O(N)$ non-linear sigma model is defined by the functional integral

$$Z = \int \mathcal{D}n_\ell \delta(n_\ell^2 - 1) \exp \left(-\frac{\rho_s^0}{2\hbar} \int d^2\mathbf{r} \int_0^{\hbar/k_B T} d\tau \left[(\nabla_{\mathbf{r}} n_\ell)^2 + \frac{1}{c_0^2} (\partial_\tau n_\ell)^2 \right] \right), \quad (3.1)$$

where the index ℓ runs from 1 to N , ρ_s^0 is the bare spin stiffness, and c_0 is the bare spin-wave velocity. Both ρ_s^0 and c_0 differ from their renormalized values ρ_s and c ; however at $N = \infty$ we will find $c_0 = c$, although the renormalization of c_0 will be quite crucial in subsequent sections. Further analysis is simply expressed in terms of the coupling constant,

$$g = \frac{N\hbar c_0}{\rho_s^0}, \quad (3.2)$$

which has the units of inverse-length. We will find that the quantum transition occurs at a g of order unity. This implies that we have to choose $\rho_s^0 \sim N$ in the large N limit. In the remainder of this section we will use units such that $k_B = \hbar = c_0 = 1$. The large N analysis of Z begins with the introduction of the rescaled field,

$$\tilde{n}_\ell = \sqrt{N} n_\ell, \quad (3.3)$$

and the imposition of the constraint by a Lagrange multiplier λ . This transforms Z into

$$Z = \int \mathcal{D}\tilde{n}_\ell \mathcal{D}\lambda \exp \left(-\frac{1}{2g} \int d^2\mathbf{r} \int_0^\beta d\tau \left[(\nabla_{\mathbf{r}} \tilde{n}_\ell)^2 + (\partial_\tau \tilde{n}_\ell)^2 + i\lambda(\tilde{n}_\ell^2 - N) \right] \right). \quad (3.4)$$

This action is quadratic in the n_ℓ , which can therefore be integrated out. This induces an effective action for the λ field which has the useful feature of having all its N dependence in a prefactor. Therefore, for large N the λ functional integral can be evaluated by using its value at its saddle-point. Terms higher-order in $1/N$ can be obtained by a systematic expansion of the functional integral about this saddle-point. We parametrize the saddle-point value of λ by

$$i\langle\lambda\rangle = m^2, \quad (3.5)$$

where the ‘mass’ m is to be determined by solving the constraint equation $n_\ell^2 = 1$, order-by-order in $1/N$. This value of m can then be used to obtain a $1/N$ expansion of the n_ℓ - n_ℓ correlator and hence of all the observables related to the staggered susceptibility.

Determination of the uniform susceptibility requires introduction of a slowly-varying magnetic field \vec{B} into the non-linear sigma model. In the $O(3)$ model such a field causes

a precession of the local order parameter about the magnetic field axis. This precession is realized in the $O(3)$ sigma model by the substitution⁵⁸

$$\partial_\tau \vec{n} \rightarrow \partial_\tau \vec{n} - i \frac{g\mu_B}{\hbar} \vec{B} \times \vec{n} \quad (3.6)$$

in functional integral Z ; here $g\mu_B/\hbar$ is the Bohr magneton for a single spin; in the remainder of this section we will measure the field in units of $g\mu_B/\hbar$ and hence omit explicit factors of $g\mu_B/\hbar$. For the general $O(N)$, the analog of the magnetic field is a second-rank antisymmetric tensor $b_{\ell m}$ which causes a precession of the spin-components lying in the plane defined by the ℓ , m directions. For $N = 3$, $b_{\ell m}$ is related to \vec{B} by

$$b_{\ell m} = \epsilon_{\ell mp} B_p. \quad (3.7)$$

The full action in the presence of the b field is defined by (3.1) and the substitution

$$\partial_\tau n_\ell \rightarrow \partial_\tau n_\ell - i b_{\ell m} n_m. \quad (3.8)$$

The uniform susceptibility, χ_u is now obtained by evaluating $\ln Z$ in powers of b and picking out the coefficient of the quadratic term:

$$\chi_u = \frac{1}{2TV} \frac{\partial^2}{\partial b_{\ell m}^2} \log Z, \quad (3.9)$$

where V is the volume of the system.

A. Solution at $N = \infty$

The $O(N)$ sigma model can be solved exactly at $N = \infty$. Closed form expressions for all the scaling functions introduced in Section I can be easily obtained. We begin with the staggered spin susceptibility which is given by

$$\chi_s(k, \omega) = \frac{g\tilde{S}^2}{N} \frac{1}{k^2 - (\omega + i\varepsilon)^2 + m_0^2}. \quad (3.10)$$

We have introduced here the mass m_0 which is the value of m at $N = \infty$, and $\tilde{S} = Z_S S$ which is a rescaling factor between the actual susceptibility of a quantum spin- S antiferromagnet and the susceptibility of the unit n -field in the $O(3)$ sigma model. The renormalization factor Z_S accounts for the fluctuations at short scales, which have to be integrated out in the derivation of the sigma model from the original spin Hamiltonian. Expressions for all the experimental observables dependent upon χ_s can now be easily obtained; we will refrain from giving explicit expressions. One quantity we will need is the correlation length ξ , which we defined earlier from the long-distance decay $\sim e^{-r/\xi}$ of the equal-time n - n correlation function. Such a decay is present at all finite T for all values of g . At $N = \infty$ we find

$$\xi = \frac{1}{m_0}. \quad (3.11)$$

Now turn to the uniform spin susceptibility. There is no damping at $N = \infty$ and hence the spin-diffusion constant is infinite. We therefore consider only the value of the static susceptibility. Evaluating (3.9) at $N = \infty$ we find

$$\chi_u^{\text{st}} = 2T \sum_{\omega_n} \int \frac{d^2k}{4\pi^2} \frac{\epsilon_k^2 - \omega_n^2}{(\epsilon_k^2 + \omega_n^2)^2}, \quad (3.12)$$

where $\epsilon_k = k^2 + m_0^2$, and ω_n is the Matsubara frequency which takes the values $2\pi nT$ with n integer. The frequency summation and the subsequent momentum integration can be performed exactly. Moreover, the momentum integration is convergent in the ultraviolet, and final result depends only on m_0 and T :

$$\chi_u^{\text{st}} = \frac{T}{\pi} \left[\frac{m_0}{T} \frac{e^{m_0/T}}{e^{m_0/T} - 1} - \log(e^{m_0/T} - 1) \right]. \quad (3.13)$$

Note the absence of direct dependence on the coupling g .

Consider next the free energy density, \mathcal{F} , from which C_V can be obtained by taking two temperature derivatives. At $N = \infty$, \mathcal{F} can be directly obtained from the saddle-point value of the effective action. The result is^{63,65}

$$\begin{aligned} \mathcal{F} &= \frac{NT}{2} \sum_{\omega_n} \int \frac{d^2k}{4\pi^2} \log(k^2 + \omega_n^2 + m_0^2) - \frac{Nm_0^2}{2g} \\ &= NT \int \frac{d^2k}{4\pi^2} \log(1 - e^{-\epsilon_k/T}) \\ &\quad + \frac{N}{2} \int \frac{d^2k d\omega}{8\pi^3} \log(k^2 + \omega^2 + m_0^2) - \frac{Nm_0^2}{2g}, \end{aligned} \quad (3.14)$$

It now remains to determine the dependence of m_0 on g and T . The constraint $n_a^2 = 1$ takes the following form at $M = \infty$:

$$T \sum \int \frac{d^2k}{4\pi^2} \frac{g}{k^2 + \omega_n^2 + m_0^2} = 1. \quad (3.15)$$

It is easy to see that the momentum summation is divergent in the ultraviolet, and it is therefore necessary to introduce a cut-off. We use a relativistic Pauli-Villars cut-off at the momentum scale Λ , assumed to be much larger than the temperature. This transforms the constraint equation into

$$T \sum \int_0^\infty \frac{d^2k}{4\pi^2} \left(\frac{g}{k^2 + \omega_n^2 + m_0^2} - \frac{g}{k^2 + \omega_n^2 + \Lambda^2} \right) = 1. \quad (3.16)$$

The momentum integration is now convergent in the ultraviolet and can be performed exactly. The subsequent frequency summation is also tractable and yields

$$\frac{gT}{2\pi} \ln \left(\frac{\sinh(\Lambda/2T)}{\sinh(m_0/2T)} \right) = 1. \quad (3.17)$$

Finally, we can solve for the dependence of m_0 on T , g , and Λ

$$m_0 = \frac{1}{\xi} = 2T \operatorname{arcsinh} \left(\exp \left(-\frac{2\pi}{gT} \right) \sinh \left(\frac{\Lambda}{2T} \right) \right). \quad (3.18)$$

In the limit $T \ll \Lambda$, this equation can be rewritten as⁶³

$$m_0 = 2T \operatorname{arcsinh} \left[\frac{1}{2} \exp \left(-\frac{2\pi}{T} \left(\frac{1}{g} - \frac{1}{g_c} \right) \right) \right] \quad (3.19)$$

where

$$g_c = \frac{4\pi}{\Lambda}. \quad (3.20)$$

By examining the $T \rightarrow 0$ limit of this equation, it is immediately apparent that the behavior of ξ is quite different depending upon whether g is smaller, larger, or close to the critical value g_c . For $g > g_c$, ξ approaches a finite value as $T \rightarrow 0$, while for $g \leq g_c$, ξ diverges as $T \rightarrow 0$. The finite, $T = 0$ asymptote of ξ for $g > g_c$ itself diverges as g approaches g_c . We find

$$\xi(T = 0, g > g_c) \sim (g - g_c)^{-1}. \quad (3.21)$$

This identifies the $N = \infty$ value of the exponent ν to be

$$\nu = 1. \quad (3.22)$$

For $g < g_c$ this is a Josephson scale⁴⁸ ξ_J which diverges with the same exponent ν as g approaches g_c . However, this scale is not present in the $N = \infty$ theory: this is because the exponent $\eta = 0$ at $N = \infty$, making the critical and Goldstone fluctuations indistinguishable. At $g = g_c$, we have from (3.18)

$$m_0 = \Theta T, \quad (3.23)$$

where the number

$$\Theta = 2 \log \left(\frac{\sqrt{5} + 1}{2} \right) = 0.962424 \quad (3.24)$$

will occur frequently in our analysis. We see therefore that the correlation length scales with $1/T$ at the critical point.

We now examine the scaling limit of the above results. This limit is obtained when the temperature T , and the deviation from criticality $|g - g_c|/g_c^2$ are both much smaller than the upper cutoff Λ . We will consider the cases of g smaller or greater than g_c separately.

1. Scaling properties for $g \leq g_c$

From the discussions in Sections I A and II it is clear that the results become simple after they have been expressed in terms of the $T = 0$ ordered staggered moment N_0 and the fully

renormalized, $T = 0$ spin-stiffness ρ_s . In Appendix D we have performed a $1/N$ expansion of these $T = 0$ variables. At $N = \infty$ their exact values are

$$\begin{aligned}\rho_s &= N \left(\frac{1}{g} - \frac{1}{g_c} \right), \\ N_0^2 &= \tilde{S}^2 \left(1 - \frac{g}{g_c} \right).\end{aligned}\tag{3.25}$$

We now use these results with the expression (3.18) for ξ to study the limit $\rho_s/N, T \ll \Lambda$. It is not difficult to show then that ξ takes the scaling form (1.30) where the scaling function X_1 is

$$X_1(x_1) = 2 \operatorname{arcsinh} \left(\frac{e^{-1/x_1}}{2} \right).\tag{3.26}$$

Thus, in the renormalized classical region $x_1 \ll 1$, we have

$$X_1 = e^{-1/x_1}; \quad x_1 \ll 1,\tag{3.27}$$

implying a correlation length which is exponentially large, while in the quantum-critical region ($x_1 \gg 1$) we find

$$X_1 = 2 \log \left(\frac{\sqrt{5} + 1}{2} \right) - \frac{2}{\sqrt{5}x_1}; \quad x_1 \gg 1,\tag{3.28}$$

indicating that the correlation length, $\xi = 1/(TX_1)$ scales with $1/T$.

The scaling functions for all the other observables now follow in a straightforward manner. The scaling function Φ_{1s} for the staggered susceptibility in (1.10a) and the exponent η can be deduced from (3.10), (3.11), (3.25), and (1.30) to be

$$\begin{aligned}\eta &= 0, \\ \Phi_{1s}(\bar{k}, \bar{\omega}, x_1) &= \frac{1}{\bar{k}^2 - (\bar{\omega} + i\varepsilon)^2 + X_1^2(x_1)}.\end{aligned}\tag{3.29}$$

The scaling functions for the observables dependent upon χ_s now follow immediately. For the structure factor $S(k)$ we have the scaling function Ξ_1 in (1.28) which is

$$\Xi_1(\bar{k}, x_1) = \frac{1}{2[\bar{k}^2 + X_1^2(x_1)]^{1/2}} \coth \frac{[\bar{k}^2 + X_1^2(x_1)]^{1/2}}{2}.\tag{3.30}$$

The local susceptibility $\operatorname{Im}\chi_L(\omega)$ obeys (1.31) with the scaling function F_1 given by

$$F_1(\bar{\omega}, x_1) = \frac{1}{4} [\theta(\bar{\omega} - X_1(x_1)) - \theta(-\bar{\omega} - X_1(x_1))],\tag{3.31}$$

where $\theta(x)$ is the unit step function. The presence of a gap in F_1 at finite T is an artifact of the $N = \infty$ theory and will be cured upon including $1/N$ corrections. A consequence of

this gap is that there is no relaxation of nuclear spins at $N = \infty$ and the scaling function for $1/T_1$ in (1.35) is

$$R_1(x_1) = 0. \quad (3.32)$$

The result for the uniform susceptibility, χ_u^{st} , (3.13) can also be collapsed into the scaling form (1.24). We use (3.13), the expression (3.18) for m_0 , and (3.25) to obtain

$$\Omega_1(x_1) = \frac{1}{\pi x_1} + \frac{\sqrt{4 + e^{-2/x_1}}}{\pi e^{-1/x_1}} \operatorname{arcsinh} \left(\frac{e^{-1/x_1}}{2} \right). \quad (3.33)$$

In the renormalized classical limit $x_1 \ll 1$ this function has the limiting behavior

$$\Omega_1(x_1) = \frac{1}{\pi x_1} + \frac{1}{\pi}; \quad x_1 \ll 1, \quad (3.34)$$

while in the quantum-critical region ($x_1 \gg 1$) it obeys

$$\Omega_1(x_1) = \frac{\sqrt{5}}{\pi} \log \left(\frac{\sqrt{5} + 1}{2} \right) \left[1 + \frac{4}{5x_1} \right]; \quad x_1 \gg 1. \quad (3.35)$$

We turn now to the free-energy density, \mathcal{F} and the specific heat C_V . We will evaluate $\mathcal{F}(T) - \mathcal{F}(T = 0)$ at a fixed value of g . The calculations are performed most easily if we use relativistic cutoff and write the value of g_c in the following form

$$\frac{1}{g_c} = \int \frac{d^3P}{8\pi^3} \frac{1}{P^2}, \quad (3.36)$$

where $P = (\mathbf{k}, \omega)$ is the relativistic 3-momentum and the integral is suitably regulated in the ultraviolet. We now apply (3.25) and the result $m_0(T = 0) = 0$ to (3.14) to obtain

$$\begin{aligned} \mathcal{F}(T) - \mathcal{F}(0) &= NT \int \frac{d^2k}{4\pi^2} \log(1 - e^{-\epsilon_k/T}) \\ &+ \frac{N}{2} \int \frac{d^3P}{8\pi^3} \left[\log \left(\frac{P^2 + m_0^2}{P^2} \right) - \frac{m_0^2}{P^2} \right] - \frac{m_0^2 \rho_s}{2}. \end{aligned} \quad (3.37)$$

Using $m_0 = TX_1(x_1)$, and simplifying the above integrals, we get

$$\begin{aligned} \mathcal{F}(T) - \mathcal{F}(0) &= NT^3 \left[\int_{X_1(x_1)}^{\infty} \frac{\epsilon d\epsilon}{2\pi} \log(1 - e^{-\epsilon}) \right. \\ &\quad \left. - \frac{X_1^3(x_1)}{12\pi} - \frac{X_1^2(x_1)}{4\pi x_1} \right]. \end{aligned} \quad (3.38)$$

Finally we use the thermodynamic relation $C_V = -T\partial^2\mathcal{F}/\partial T^2$ to obtain the scaling function $\Psi_1(x_1)$ for the specific heat as defined in (1.10c)

$$\begin{aligned} \Psi_1(x_1) &= -\frac{N\pi}{3\zeta(3)x_1} \frac{d^2}{dx_1^2} \left[x_1^3 \left(\int_{X_1(x_1)}^{\infty} \frac{\epsilon d\epsilon}{2\pi} \log(1 - e^{-\epsilon}) \right) \right. \\ &\quad \left. - \frac{X_1^3(x_1)}{12\pi} - \frac{X_1^2(x_1)}{4\pi x_1} \right). \end{aligned} \quad (3.39)$$

We recall that the function $X_1(x_1)$ is given in (3.26). It is clearly that the universal crossover function $\Psi_1(x_1)$ is quite non-trivial even at $N = \infty$. In the renormalized classical limit, $x_1 \rightarrow 0$ it has the value

$$\Psi_1(0) = N, \quad (3.40)$$

which is the number of gapless spin wave modes (upto relative order $1/N$). The normalization in (1.10c) was chosen to make this result simple. In the quantum-critical limit, $x_1 \rightarrow \infty$, the integrals cannot be analytically evaluated. However, one of us has recently shown⁶⁶ that application of some unusual identities of polylogarithmic functions can be used to prove that the integrals reduce a surprisingly simple result

$$\Psi_1(\infty) = \frac{4N}{5}. \quad (3.41)$$

We have no physical understanding of why this number is rational.

The reduced scaling functions of the renormalized classical region, describing the crossover from Goldstone to classical, thermal disorder (Fig. 2) can also be easily obtained. From (1.41), (1.42), and (3.30) we find the scaling function $f(y)$ for the structure factor $S(k)$

$$f(y) = \frac{1}{y^2 + 1}. \quad (3.42)$$

2. Scaling properties for $g \geq g_c$

The first step is to obtain the value of the $T = 0$ gap. From (3.19) we have the exact $N = \infty$ result

$$\Delta = 4\pi \left(\frac{1}{g_c} - \frac{1}{g} \right). \quad (3.43)$$

Second, we also need the spin-1 quasiparticle amplitude \mathcal{A} . From (3.10) we obtain immediately at $N = \infty$

$$\mathcal{A} = \frac{g\tilde{S}^2}{N}. \quad (3.44)$$

From (3.18) we can now deduce the scaling function X_2 as defined in (1.30) for the correlation length

$$X_2(x_2) = 2 \operatorname{arcsinh} \left(\frac{e^{1/(2x_2)}}{2} \right). \quad (3.45)$$

(Recall that $x_2 = T/\Delta$.) This function has the following asymptotic limits in the quantum disordered and quantum-critical regions respectively

$$X_2(x_2) = \begin{cases} \frac{1}{x_2} + 2e^{-1/x_2}; & x_2 \ll 1, \\ 2 \log\left(\frac{\sqrt{5}+1}{2}\right) + \frac{1}{\sqrt{5}x_2}; & x_2 \gg 1. \end{cases} \quad (3.46)$$

These results imply a correlation length which is of order Δ^{-1} and T^{-1} respectively.

The scaling function $\Omega_2(x_2)$ for the uniform static susceptibility in (1.24) can be obtained from (3.13) combined with (3.18) and (3.43). We find

$$\Omega_2(x_2) = -\frac{1}{2\pi x_2} + \frac{\sqrt{4 + e^{1/x_2}}}{\pi e^{1/(2x_2)}} \operatorname{arcsinh}\left(\frac{e^{1/(2x_2)}}{2}\right). \quad (3.47)$$

In the quantum-disordered region ($x_2 \ll 1$), this function is exponentially small

$$\Omega_2(x_2) = \frac{e^{-1/x_2}}{\pi x_2}; \quad x_2 \ll 1, \quad (3.48)$$

while in the quantum-critical region it implies a χ_u^{st} of order the temperature

$$\Omega_2(x_2) = \frac{\sqrt{5}}{\pi} \log\left(\frac{\sqrt{5}+1}{2}\right) \left[1 - \frac{2}{5x_2}\right]; \quad x_2 \gg 1. \quad (3.49)$$

Next we consider the free-energy density, \mathcal{F} and the specific heat C_V . The following relation between the $T = 0$ gap, Δ , and the coupling g will be useful

$$\frac{1}{g} = \int \frac{d^3 P}{8\pi^3} \frac{1}{P^2 + \Delta^2}, \quad (3.50)$$

where $P = (\mathbf{k}, \omega)$ is the relativistic 3-momentum. Note that we again use relativistic cutoff for the value of g_c . Applying this result to (3.14), we obtain

$$\begin{aligned} \mathcal{F}(T) - \mathcal{F}(0) &= NT \int \frac{d^2 k}{4\pi^2} \log(1 - e^{-\epsilon_k/T}) \\ &+ \frac{N}{2} \int \frac{d^3 P}{8\pi^3} \left[\log\left(\frac{P^2 + m_0^2}{P^2 + \Delta^2}\right) - \frac{m_0^2 - \Delta^2}{P^2 + \Delta^2} \right]. \end{aligned} \quad (3.51)$$

Using $m_0 = TX_2(x_2)$, and simplifying the above integrals, we get

$$\begin{aligned} \mathcal{F}(T) - \mathcal{F}(0) &= NT^3 \left[\int_{X_2(x_2)}^{\infty} \frac{\epsilon d\epsilon}{2\pi} \log(1 - e^{-\epsilon}) \right. \\ &\quad \left. - \frac{X_2^3(x_2)}{12\pi} + \frac{3x_2^2 X_2^2(x_2) - 1}{24\pi x_2^3} \right]. \end{aligned} \quad (3.52)$$

Finally we use the thermodynamic relation $C_V = -T\partial^2 \mathcal{F}/\partial T^2$ to obtain the scaling function $\Psi_2(x_2)$ for the specific heat as defined in (1.19c)

$$\begin{aligned} \Psi_2(x_2) &= -\frac{N\pi}{3\zeta(3)x_2} \frac{d^2}{dx_2^2} \left[x_2^3 \left(\int_{X_2(x_2)}^{\infty} \frac{\epsilon d\epsilon}{2\pi} \log(1 - e^{-\epsilon}) \right. \right. \\ &\quad \left. \left. - \frac{X_2^3(x_2)}{12\pi} + \frac{3x_2^2 X_2^2(x_2) - 1}{24\pi x_2^3} \right) \right]. \end{aligned} \quad (3.53)$$

where the function $X_2(x_2)$ is given in (3.45). In the quantum disordered limit, $x_2 \rightarrow 0$, we have $\Psi_2(0) = 0$ corresponding to the absence of any gapless degrees of freedom. Recall also that $\Psi_2(\infty) = \Psi_1(\infty)$.

The scaling functions for the remaining observables are identical to those obtained above for $g \leq g_c$ after the substitution $X_1(x_1) \rightarrow X_2(x_2)$. Thus *e.g.* the scaling function Φ_{2s} for χ_s in (1.19a) differs from the function Φ_{1s} in (3.29) only by this substitution.

B. $1/N$ corrections

We now present formal expressions for the modifications to the uniform and staggered spin susceptibilities at order $1/N$. These expressions will be used in the following sections to determine the scaling properties of the quantum-critical, renormalized-classical and quantum-disordered regions.

The formal structure of the $1/N$ expansion has been reviewed in the book by Polyakov⁶⁷ (see also ^{68,69}). The leading corrections arise from considering the fluctuations of the λ field about its saddle point. The contribution to the staggered susceptibility, or equivalently the propagator of the n_ℓ field, is given by the Feynman graph in Fig. 6 This leads immediately to

$$\chi_s(k, i\omega_n) = \frac{g\tilde{S}^2}{N} \frac{1}{k^2 + \omega_n^2 + m^2 + \Sigma(k, i\omega_n)}, \quad (3.54)$$

where Σ is the self-energy arising from the λ fluctuations. It is convenient to absorb the value of $\Sigma(0, 0)$ into the mass m^2 ; all our expressions for Σ will therefore always include a subtraction which makes $\Sigma(0, 0) = 0$. The leading contribution to Σ is

$$\begin{aligned} \Sigma(k, i\omega_n) = \\ \frac{2}{N} T \sum_{\epsilon_n} \int \frac{d^2q}{4\pi^2} \frac{G_0(\mathbf{k} + \mathbf{q}, i\omega_n + i\epsilon_n) - G_0(q, i\epsilon_n)}{\Pi(q, i\epsilon_n)}, \end{aligned} \quad (3.55)$$

where $1/\Pi$ is the propagator of the λ field

$$\begin{aligned} \Pi(q, i\epsilon_n) = \\ T \sum_{\Omega_n} \int \frac{d^2q_1}{4\pi^2} G_0(\mathbf{q} + \mathbf{q}_1, i\epsilon_n + i\Omega_n) G_0(q_1, i\Omega_n), \end{aligned} \quad (3.56)$$

and G_0 is the propagator of the n_ℓ field at $N = \infty$

$$G_0(k, i\omega_n) = \frac{1}{k^2 + \omega_n^2 + m_0^2}. \quad (3.57)$$

It now remains to determine m^2 . The value of m^2 is set by solving the constraint equation $n_\ell^2 = 1$, or

$$T \sum_{\omega_n} \int \frac{d^2k}{4\pi^2} \chi_s(k, i\omega_n) = \frac{\tilde{S}^2}{N}, \quad (3.58)$$

order by order in $1/N$. At $N = \infty$, the dependence of m_0 on g and T is determined by solving the following equation exactly

$$gT \sum_{\omega_n} \int \frac{d^2k}{4\pi^2} G_0(k, i\omega_n) = 1. \quad (3.59)$$

This has of course already been done in the previous subsection. We represent the $1/N$ corrections to m^2 by δm^2 , where $m^2 = m_0^2 + \delta m^2$. Upon examining the $1/N$ corrections to (3.58) we find in a straightforward manner

$$\delta m^2 = -\frac{K_1(T, m_0)}{K_2(T, m_0)}, \quad (3.60)$$

where the constants K_1, K_2 are

$$\begin{aligned} K_1(T, m_0) &= T \sum_{\omega_n} \int \frac{d^2k}{4\pi^2} \Sigma(k, i\omega_n) G_0^2(k, i\omega_n), \\ K_2(T, m_0) &= T \sum_{\omega_n} \int \frac{d^2k}{4\pi^2} G_0^2(k, i\omega_n) \\ &= \frac{1}{8\pi m_0} \coth\left(\frac{m_0}{2T}\right). \end{aligned} \quad (3.61)$$

Note that K_1, K_2 depend only upon T and m_0 , and do not depend directly upon the value of the coupling g . Comparing (3.61) with (3.55), (3.56) and (3.57), the expression for K_1 can be manipulated into the following

$$\begin{aligned} K_1(T, m_0) &= -\frac{2}{N} T \sum_{\epsilon_n} \int \frac{d^2q}{4\pi^2} \frac{1}{\Pi(q, i\epsilon_n)} \\ &\quad \left(\frac{1}{4m_0} \frac{\partial \Pi(q, i\epsilon_n)}{\partial m_0} + G_0(q, i\epsilon_n) K_2(m_0, T) \right). \end{aligned} \quad (3.62)$$

These results for m^2, K_1 and K_2 will be quite useful in subsequent sections.

Expressions for observables that depend upon χ_s can now be obtained as before. In particular, the equal-time staggered structure factor $S(k)$ is given by

$$S(k) = T \sum_{\omega_n} \chi_s(k, i\omega_n). \quad (3.63)$$

Using (3.54) we see that to order $1/N$ this can be rewritten as

$$\frac{S(k)}{S_0(k)} = \left[1 + \frac{\sum_{\omega_n} (\delta m^2 + \Sigma(k, i\omega_n)) G_0^2(k, i\omega_n)}{S_0(k)} \right]^{-1}, \quad (3.64)$$

where $S_0(k)$ is the structure factor at $N = \infty$:

$$S_0(k) = \frac{g\tilde{S}^2}{N} T \sum_{\omega_n} G_0(k, i\omega_n). \quad (3.65)$$

The correlation length, ξ , is defined by the pole of $S(k)$ in the complex k plane which is closest to the real k axis; this pole is at $k = i/\xi$. From (3.63) it is clear that, at any finite T , the poles of $S(k)$ are simply the poles of $\chi_s(k, i\omega_n)$ for all ω_n . It is also clear that the pole closest to the real-axis is that associated with $\chi_s(k, i\omega_n = 0)$. The location of this pole can be simply determined from (3.54) in a $1/N$ expansion. We find

$$\xi^{-1} = m + \frac{1}{2m_0} \Sigma(k = im_0, i\omega_n = 0). \quad (3.66)$$

Finally, the residue of the pole in the structure factor, which sets the overall scale for exponentially decaying correlations, can be determined in a similar manner:

$$S(k) \approx \frac{g\tilde{S}^2}{N} T \left(1 - \frac{\partial \Sigma(k = im_0, i\omega_n = 0)}{\partial k^2} \right) \frac{1}{k^2 + \xi^{-2}}; \quad (3.67)$$

k close to $i\xi^{-1}$.

The results for ξ and $S(k)$ will be of great use to us in the subsequent sections.

Now we turn to a consideration of the $1/N$ corrections to the static uniform susceptibility, χ_u^{st} . This is a four-point function of the n_ℓ field and the Feynman graphs which contribute at order $1/N$ are shown in Fig. 6. The evaluation of these graphs is, in principle, quite straightforward, but rather tedious. After some fairly lengthy frequency summations, we obtained the following, surprisingly compact result:

$$\chi_u^{\text{st}} = \int \frac{d^2k}{4\pi^2} \left[-2n'_k - \frac{n''_k}{\epsilon_k} (m^2 - m_0^2) \right] - K_3(T, m_0), \quad (3.68)$$

where the energy $\epsilon_k = (k^2 + m_0^2)^{1/2}$ was introduced earlier, $n_k \equiv n(\epsilon_k)$ is the Bose function

$$n(\epsilon) = \frac{1}{e^{\epsilon/T} - 1}, \quad (3.69)$$

and $n'_k = dn(\epsilon_k)/d\epsilon_k$, etc. (note that the symbol n is used both for the Bose function and the non-linear sigma model field - the appropriate meaning should however be clear from the context). The very first term in (3.68) is identical to the $N = \infty$ result of (3.12), while the second term arises from effective mass renormalization of the the $N = \infty$ graphs. The remaining $1/N$ corrections are contained in the function $K_3(T, m_0)$ which is given by

$$K_3(T, m_0) = \frac{2}{N} T \sum_{\omega_n} \int \frac{d^2q}{4\pi^2} \frac{1}{\Pi(q, i\omega_n)} \int \frac{d^2k}{4\pi^2} \frac{n''_k}{\epsilon_k} \left[\frac{\epsilon_{k+q}^2 - \epsilon_k^2 + \omega_n^2}{(\epsilon_{k+q}^2 + \epsilon_k^2 + \omega_n^2)^2 - 4\epsilon_k^2 \epsilon_{k+q}^2} - \frac{1}{\epsilon_q^2 + \omega_n^2} \right]. \quad (3.70)$$

We will evaluate this expression in the later sections on the different critical regimes.

Lastly, the $1/N$ corrections to the free energy density, \mathcal{F} . The $1/N$ corrections to (3.14) arise from the functional determinant of the integration over the λ field. The propagator

of the λ field is Π as defined in (3.56) and the correction to the free energy is simply $(1/2)\text{Tr} \log \Pi$. We have therefore

$$\mathcal{F} = \frac{NT}{2} \sum_{\omega_n} \int \frac{d^2k}{4\pi^2} \left[\log(k^2 + \omega_n^2 + m_0^2) + \frac{1}{N} \log(\Pi(k, i\omega_n)) \right] - \frac{Nm_0^2}{2g}. \quad (3.71)$$

Note that we have not included the $1/N$ correction to the mass $i\langle\lambda\rangle = m$. This is because by construction $d\mathcal{F}/d\langle\lambda\rangle = 0$ at $N = \infty$. This immediately implies that the correction to $\langle\lambda\rangle$ at order $1/N$ will modify \mathcal{F} only at relative order $1/N^2$. Thus may as well use $i\langle\lambda\rangle = m_0$ to compute \mathcal{F} to order $1/N$.

IV. QUANTUM-CRITICAL REGION

This section will present expressions for the scaling functions in the quantum critical region to order $1/N$. We will restrict our discussion here to the critical point at $g = g_c$. This point will be accessed by taking the $x_1 \rightarrow \infty$ limit from the ordered side. We will thus present explicit results for the scaling functions $\Phi_{1s}(\bar{k}, \bar{\omega}, x_1 = \infty)$ and $\Phi_{1u}(\bar{k}, \bar{\omega}, x_1 = \infty)$. Those for Φ_{2s} and Φ_{2u} can be obtained immediately from (1.21).

An important issue that arises at the outset of any calculation of universal scaling functions is that of proper choice of an ultraviolet cutoff. In the preceding section, we chiefly used a Pauli-Villars cutoff to obtain the value of g_c . However, we will see that g_c does not explicitly show up in $1/N$ corrections and we are therefore free to choose the most convenient regularization scheme. All of the computations in this section were performed with two different cutoffs:

(a) Lattice-cutoff: The n_ℓ field was placed on a square lattice of spacing $1/\Lambda$, but no restriction was placed on the allowed values of the Matsubara frequencies ω_n . The scaling functions were obtained in the limit $\Lambda \rightarrow \infty$. By construction, in this cutoff scheme relativistic invariance is violated at short scales and is present only in the long-distance theory at $T = 0$. Consequently, the $T = 0$ spin-wave velocity will be renormalized from its bare value, and care will have to be taken to express the scaling functions in terms of the fully renormalized spin-wave velocity.

(b) Relativistic, hard cutoff: The momenta k , and frequencies ω_n carried by the n_ℓ field were restricted to satisfy

$$k^2 + \omega_n^2 < \Lambda^2. \quad (4.1)$$

Unlike the previous cutoff, this scheme has full relativistic invariance, and there will be no renormalization of the bare $T = 0$ spin-wave velocity.

All of the remaining discussion in this section will use the second, relativistic cutoff scheme; as a result we will not have to consider explicitly the renormalization of the spin-wave velocity. We emphasize however that all of our numerical computations have been carried out with both schemes. While many of the intermediate results of the two schemes were different, the final results for the universal scaling functions were found to be identical. This

agreement provides strong support for the complete universality of the scaling functions, and makes it virtually certain that there are no numerical errors in our computations in the quantum critical region.

The basic strategy for obtaining the scaling functions is straightforward. We evaluate χ_s and χ_u to order $1/N$ as outlined in Section III B, and then invert Eqns (1.10a,1.10b) to express $\Phi_{1s,u}$ in terms of $\chi_{s,u}$. We will also need in this procedure the $T = 0$ value of the ratio N_0^2/ρ_s . The structure of the $T = 0$ theory for $g < g_c$ is discussed in Appendix D where we found

$$\frac{N_0^2}{\rho_s} = \frac{g\tilde{S}^2}{N} \left[1 - \eta \log \left(\frac{N\Lambda}{16\rho_s} \right) \right], \quad (4.2)$$

where the number $\eta = 8/(3\pi^2 N)$ will become the critical exponent η defined in Section I.

We will begin by noting some of the significant issues that arose in the evaluation of the results of Sec III B in the quantum-critical region. We will then proceed to a statement of the results for the various scaling functions.

The first step was to develop a fast computer program for the rapid evaluation of $\Pi(q, i\epsilon_n)$, in (3.56) for $m_0 = \Theta T$. Simple power-counting shows that Π is convergent in the limit of the cutoff $\Lambda \rightarrow \infty$. However, it is not clear a-priori that it is valid to take the $\Lambda \rightarrow \infty$ limit at this early stage. The point is that subsequent integrals will involve values of $\Pi(q, i\epsilon_n)$ with q, ϵ_n itself of order Λ . However, we have shown by a detailed consideration of the relevant integrals, that these potentially dangerous contributions from Π cancel out in the final results for all universal quantities. Thus we will fearlessly evaluate Π in the limit of an infinite cutoff.

The evaluation of Π began with analytic determination of the integral over q_1 in (3.56). The summation over ω_n was then performed by a direct numerical evaluation. Terms upto some large value of ω_n were explicitly evaluated, and the remainder were summed by fitting to an inverse power series in $1/\omega_n^2$ upto order $1/\omega_n^6$. A very similar procedure was used to evaluate $\partial\Pi/\partial m_0$. Finally the results were checked against the following computed asymptotic expressions:

$$\begin{aligned} \Pi(q, i\epsilon_n) &= \frac{1}{8(q^2 + \epsilon_n^2)^{1/2}} \\ &\quad + \frac{(2\epsilon_n^2 - q^2)\Theta^3 T^3}{(q^2 + \epsilon_n^2)^3} \frac{1 - 6\gamma}{3\pi} + \mathcal{O}\left(\frac{T^5}{(q, \epsilon_n)^6}\right), \\ -\frac{1}{4m_0} \frac{\partial\Pi(q, i\epsilon_n)}{\partial m_0} &= \frac{\sqrt{5}}{8\pi\Theta T} \frac{q^2 + \epsilon_n^2}{(q^2 + \epsilon_n^2)^2 + 4\Theta^2 T^2 \epsilon_n^2} \\ &\quad + \mathcal{O}\left(\frac{T^3}{(q, \epsilon_n)^6}\right), \end{aligned} \quad (4.3)$$

where

$$\gamma = \frac{1}{\Theta^3} \int_{\Theta}^{\infty} dx \frac{x^2}{e^x - 1} = 2.32414354317. \quad (4.4)$$

Next, we evaluated the self-energy, Σ , and the constant K_3 defined in (3.70). It is not difficult to show from (4.3) that both these quantities are logarithmically divergent in the

limit $\Lambda \rightarrow \infty$. Further the coefficient of $\log(\Lambda)$ can be easily determined analytically. We numerically evaluated the integral over the momenta and the summation over the frequency for a fixed Λ and subtracted the known $\log(\Lambda)$ term. The remainder was found to be independent of Λ for large Λ , and was the required finite part of the result. These computations yielded the following catalog of useful results

$$\begin{aligned}
\frac{\partial \bar{\Sigma}(\bar{k} = 0, i\bar{\omega} = 0)}{\partial \bar{k}^2} &= \eta \log\left(\frac{\Lambda}{T}\right) - \frac{0.25266}{N} \\
\bar{\Sigma}(\bar{k} = i\Theta, i\bar{\omega}) &= -\Theta^2 \eta \log\left(\frac{\Lambda}{T}\right) + \frac{0.22616}{N}, \\
\frac{\partial \bar{\Sigma}(\bar{k} = i\Theta, i\bar{\omega} = 0)}{\partial \bar{k}^2} &= \eta \log\left(\frac{\Lambda}{T}\right) + \frac{0.69400}{N}, \\
\bar{\Sigma}(\bar{k}, \bar{\omega} \gg 1) &= (\bar{k}^2 + \bar{\omega}^2) \left[\eta \log\left(\frac{\Lambda}{T}\right) \right. \\
&\quad \left. - \frac{\eta}{2} \log(\bar{k}^2 + \bar{\omega}^2) + \frac{8}{9\pi^2 N} \right], \\
\frac{K_3(T, m_0 = \Theta T)}{T} &= -\frac{\eta \Theta^2}{2\pi} \log\left(\frac{\Lambda}{T}\right) + 0.17800.
\end{aligned} \tag{4.5}$$

where $\bar{\Sigma}(\bar{k}, i\bar{\omega}) = \Sigma(T\bar{k}, iT\bar{\omega})/T^2$.

A little care is required in inferring the $1/N$ correction to the mass m at $g = g_c$. The point is that the critical coupling g_c itself has $1/N$ corrections, and in addition to the correction δm^2 in (3.60), there is an additional T -independent shift to m_0 itself. Accounting for the $1/N$ correction to the value of g_c , we find the following result for m^2 at $g = g_c$

$$m^2 = m_0^2 - \frac{K_1(T, m_0) - K_1(0, 0)}{K_2(T, m_0)}, \tag{4.6}$$

where K_1, K_2 are to be evaluated using (3.60), (3.61), and (3.62) at $m_0 = \Theta T$. The above result for m^2 differs from that in Section III B by the T -independent correction $K_1(0, 0)$ which in fact ensures that $\delta m^2(T = 0) = 0$, as should be the case at the gapless critical point.

Now we need $K_1(T, m_0 = \Theta T)$. Simple power counting in (3.62) shows that K_1 is linearly divergent for large Λ . Moreover, the linear Λ term is $K_1(0, 0)$, which from (4.6), must be subtracted out. However, upon using the explicit results in (4.3) for Π and $\partial\Pi/\partial m_0$ in (3.62), one finds that K_1 is in fact only logarithmically divergent! The absence of any terms of order $T/(q, \epsilon_n)^2$ (which are allowed by naive power counting) in the asymptotic expansion of Π was crucial in obtaining this surprising result. The dangerous $T/(q, \epsilon_n)^2$ terms are, in fact, present at all values of m_0 other than ΘT . Even for this special value of m_0 , there is linear Λ contribution to K_1 from q, ϵ_n of order Λ . However it was precisely these contributions that were dropped when Π was evaluated in the limit of infinite cutoff. Since we are interested only in $K_1(T, m_0) - K_1(0, 0)$, we blithely neglect such contributions, and simply evaluate K_1 as defined in (3.62) using the values of Π and $\partial\Pi/\partial m_0$ obtained above. The integral is only logarithmically divergent and can be evaluated in a manner similar to Σ and K_3 . At the end, we obtained from this the needed result for m :

$$\frac{m^2}{T^2} = \Theta^2 + \eta\Theta^2 \log\left(\frac{\Lambda}{T}\right) + \frac{0.21346}{N}. \quad (4.7)$$

We will now describe the universal scaling results obtained by combining the above with the results of Sec III B. The factors of $\log(\Lambda)$ were found to cancel out of all universal quantities.

A. Correlation length and structure factor

For the correlation length we obtained

$$\frac{1}{T\xi} \equiv X_1(\infty) = \Theta \left(1 + \frac{0.2373}{N}\right) \quad (4.8)$$

The residue of the structure factor in the vicinity of the pole in the complex k plane at i/ξ is contained in the following result for the scaling function Ξ_1 of the structure factor (defined in (1.28))

$$\Xi_1(\bar{k}, \infty) = \left(1 + \frac{0.4415}{N}\right) \frac{1}{\bar{k}^2 + X_1^2(\infty)}; \quad \text{for } \bar{k} \text{ near } iX_1(\infty). \quad (4.9)$$

Our numerical results for the full scaling function $\Xi_1(\bar{k}, \infty)$ for real \bar{k} are presented in Fig. 4. Analytic forms can be obtained in the limit of large and small \bar{k}

$$\begin{aligned} \Xi_1^{-1}(\bar{k}, \infty) &= 0.860818 + \frac{0.3697}{N} \\ &\quad + \bar{k}^2 \left(0.864674 - \frac{0.079}{N}\right); \quad \bar{k} \ll 1, \end{aligned} \quad (4.10)$$

$$\Xi_1(\bar{k}, \infty) = \frac{\Gamma((1-\eta)/2)}{\Gamma(1-\eta/2)} \frac{A_Q}{2\sqrt{\pi}\bar{k}^{1-\eta}}; \quad \bar{k} \gg 1. \quad (4.11)$$

This last result for the behavior of $\Xi_1(\bar{k}, \infty)$ for large \bar{k} required knowledge of the asymptotic properties of the scaling function Φ_{1s} for the dynamic staggered susceptibility discussed in Section IV C below; the constant A_Q is given in (4.17).

For experimental comparisons, it is convenient to express $S(k)$ directly in terms of $k\xi$, where ξ is the actual correlation length. From (1.27), (1.29), (4.10) and (4.11), we obtain

$$\begin{aligned} S(k) &= \frac{N_0^2}{\rho_s} \left(\frac{Nk_B T}{2\pi\rho_s}\right)^\eta \frac{\sqrt{5}}{2} \frac{\xi}{(1+k^2\xi^2)^{1/2}} \left(1 - \frac{0.1925}{N}\right) \\ &\quad \times \begin{cases} 1 - \left(1 - \frac{0.100}{N}\right) \frac{\Theta}{\sqrt{5}} k^2; & k\xi \ll 1, \\ \frac{(k\xi)^\eta}{\sqrt{5}} \left(1 + \frac{0.267}{N}\right); & k\xi \gg 1. \end{cases} \end{aligned} \quad (4.12)$$

B. Uniform susceptibility

For the scaling function Ω_1 , (see (1.24)), of the static uniform susceptibility we obtained

$$\Omega_1(x_1 \rightarrow \infty) = \frac{\sqrt{5}}{\pi} \log \left(\frac{\sqrt{5} + 1}{2} \right) \left[\left(1 - \frac{0.6189}{N} \right) + \frac{4}{5x_1} \right], \quad (4.13)$$

We have also performed Monte Carlo simulations of a lattice version of the $O(3)$ sigma model which are described in Appendix C. This yielded $\Omega_1(\infty) = 0.25 \pm 0.04$, in good agreement with the above result.

C. Staggered Susceptibility

We first describe some asymptotic limits of the two-parameter scaling function $\Phi_{1s}(\bar{k}, \bar{\omega}, \infty)$. For small \bar{k} we have

$$\begin{aligned} \text{Re}\Phi_{1s}^{-1}(\bar{k}, 0, \infty) &= \Theta^2 \left(1 + \frac{0.4830}{N} \right) \\ &+ \bar{k}^2 \left(1 - \frac{0.0001}{N} \right) ; \quad \bar{k} \ll 1. \end{aligned} \quad (4.14)$$

Our numerical accuracy is not sufficient to rule out zero $1/N$ correction to the coefficient of \bar{k}^2 ; the small value obtained for this correction appears to be accidental. At large arguments we found

$$\begin{aligned} \Phi_{1s}^{-1}(\bar{k}, i\bar{\omega}, \infty) &= (\bar{k}^2 + \bar{\omega}^2) \left[1 - \frac{\eta}{2} \log(\bar{k}^2 + \bar{\omega}^2) \right. \\ &\left. + \eta \left(\log \left(\frac{8}{\pi} \right) + \frac{1}{3} \right) \right] ; \quad \bar{k}, \bar{\omega} \gg 1. \end{aligned} \quad (4.15)$$

We expect that this logarithmic series can be exponentiated. Performing the exponentiation, followed by an analytic continuation to real frequencies we get finally

$$\Phi_{1s}(\bar{k}, \bar{\omega}, \infty) = \frac{A_Q}{(\bar{k}^2 - \bar{\omega}^2)^{1-\eta/2}} ; \quad \bar{k}, \bar{\omega} \gg 1, \quad (4.16)$$

where the universal number A_Q is given by

$$A_Q = 1 - \eta \left(\log \left(\frac{8}{\pi} \right) + \frac{1}{3} \right) \quad (4.17)$$

to order $1/N$.

We turn finally to the determination of the scaling function $\Phi_{1s}(\bar{k}, \bar{\omega}, \infty)$ for arbitrary \bar{k} , $\bar{\omega}$. As analytic evaluation is clearly impossible, we will have to resort to numerical computations. Moreover, as it is not easy to analytically continue numerical data, we will perform the numerical computations directly at real frequencies. There are some interesting issues which arise from the interplay between the analytic continuation, finite-temperature

effects, and ultraviolet divergences. These issues do not appear to have been discussed elsewhere before, and it appears worthwhile to present some details.

Our strategy will be as follows: we will start with the key observation that to order $1/N$ $\text{Im}\Sigma$ is free of ultraviolet divergences and that

$$\text{Im}\Phi_{1s}^{-1}(\bar{k}, \bar{\omega}, \infty) = \text{Im}\bar{\Sigma}(\bar{k}, \bar{\omega}). \quad (4.18)$$

Therefore $\text{Im}\Phi_{1s}^{-1}$ can be obtained by a direct evaluation of (4.18). All ultraviolet divergences and Λ dependences are in fact in the real part of self-energy. Next we note that Φ_{1s}^{-1} is analytic as a function of $\bar{\omega}$ in the upper-half frequency plane. However, we will find that because $\text{Im}\Phi_{1s}^{-1} \sim \bar{\omega}^2$ for large $\bar{\omega}$, its Kramers-Kronig transform is not convergent and cannot be directly used to obtain the real part. Instead, we will use the analytic information contained in the large $\bar{\omega}$ behavior in (4.15) to perform an appropriate subtraction, and take the Kramers-Kronig transform of the remainder.

First some details on the evaluation of $\text{Im}\bar{\Sigma}$. From the results for Σ in Section III B, we obtain after and analytically continuation to real frequencies

$$\begin{aligned} \text{Im}\bar{\Sigma}(\bar{k}, \bar{\omega}) &= \frac{1}{4\pi^2 N} \int d^2\bar{q} \int_0^\infty d\bar{\Omega} \text{Im} \left(\frac{1}{\Pi(\bar{q}, \bar{\Omega})} \right) \\ &\times \frac{1}{\bar{\epsilon}_{\bar{q}+\bar{k}}} \left[|n_{\bar{q}+\bar{k}} - n_{\bar{\Omega}}| \delta(\bar{\omega} - |\bar{\epsilon}_{\bar{q}+\bar{k}} - \bar{\Omega}|) \right. \\ &\quad \left. + (1 + n_{\bar{q}+\bar{k}} - n_{\bar{\Omega}}) \delta(\bar{\omega} - \bar{\epsilon}_{\bar{q}+\bar{k}} - \bar{\Omega}) \right]. \end{aligned} \quad (4.19)$$

Here $\bar{\epsilon}_{\bar{k}} = (\bar{k}^2 + \Theta^2)^{1/2}$, $\bar{\omega} > 0$ ($\text{Im}\bar{\Sigma}$ is an odd function of $\bar{\omega}$), $n_{\bar{k}} = n(\bar{\epsilon}_{\bar{k}})$ is the Bose function, and there is no cutoff in the \bar{q} integration. The propagator $1/\Pi(\bar{q}, \bar{\Omega})$ is simply $1/\Pi$ in rescaled variables. Thus from (3.56) we get $\text{Im}\Pi$:

$$\begin{aligned} \text{Im}\Pi(\bar{q}, \bar{\Omega}) &= \frac{1}{16\pi} \int d^2\bar{p} \frac{1}{\bar{\epsilon}_{\bar{p}+\bar{k}} \bar{\epsilon}_{\bar{q}}} \\ &\left[|n_{\bar{p}+\bar{k}} - n_{\bar{p}}| \delta(\bar{\Omega} - |\bar{\epsilon}_{\bar{p}+\bar{k}} - \bar{\epsilon}_{\bar{q}}|) \right. \\ &\quad \left. + (1 + n_{\bar{p}+\bar{k}} + n_{\bar{p}}) \delta(\bar{\Omega} - \bar{\epsilon}_{\bar{p}+\bar{k}} - \bar{\epsilon}_{\bar{q}}) \right], \end{aligned} \quad (4.20)$$

where $\bar{\Omega} > 0$ ($\text{Im}\Pi$ is an odd function of $\bar{\Omega}$), and there is no cutoff in the \bar{p} integration. The real part $\text{Re}\Pi$ can be obtained by a Kramers-Kronig transform of $\text{Im}\Pi$ (the frequency integral is free of ultraviolet divergences), which can then be used to determine $\text{Im}(1/\Pi)$. Note all of the integrals above defining $\text{Im}\bar{\Sigma}$ are pure numbers and amenable to a direct numerical evaluation, which we undertook. The presence of delta-functions in the integrand considerably speeded up the numerical computations.

Next, we turn to $\text{Re}\Phi_{1s}^{-1}$. We deduce from (4.15) that for momenta \bar{k} fixed, but $\bar{\omega} \rightarrow \infty$ we must have

$$\begin{aligned} \text{Re}\Phi_{1s}^{-1} &= \frac{\eta}{2} \left(\bar{\omega}^2 \log \bar{\omega}^2 - A_Q^{-1} \bar{\omega}^2 - \mu_1(\bar{k}) \log \bar{\omega}^2 \right) \\ &\quad + \mu_2(\bar{k}) + \dots, \\ \text{Im}\Phi_{1s}^{-1} &= -\frac{\pi\eta}{2} \text{sgn}\bar{\omega} \left(\bar{\omega}^2 - \mu_1(\bar{k}) + \dots \right). \end{aligned} \quad (4.21)$$

where the functions $\mu_{1,2}(\bar{k})$ are unknown. We fit the numerically computed $\text{Im}\Phi_{1s}^{-1}$ to the above asymptotic form, and thence obtained $\mu_1(\bar{k})$. Then we defined the function $P(\bar{k}, \bar{\omega})$ by

$$P(\bar{k}, \bar{\omega}) \equiv \text{Im}\Phi_{1s}^{-1}(\bar{k}, \bar{\omega}) + \frac{\pi\eta}{2} \text{sgn}(\bar{\omega}) (\bar{\omega}^2 - \mu_1(\bar{k})). \quad (4.22)$$

The terms on the right-hand side have been chosen so that P falls off sufficiently fast at large $\bar{\omega}$ for its Kramers-Kronig transform to be well defined. Then, using the analyticity of Φ_{1s}^{-1} in the upper-half plane, we can conclude

$$\begin{aligned} \text{Re}\Phi_{1s}^{-1}(\bar{k}, \bar{\omega}) = \mathcal{P} \int_{-\infty}^{\infty} \frac{d\Omega}{\pi} \frac{P(\bar{k}, \Omega)}{\Omega - \bar{\omega}} + \frac{\eta}{2} (\bar{\omega}^2 \log \bar{\omega}^2 \\ - A_Q^{-1} \bar{\omega}^2 - \mu_1(\bar{k}) \log \bar{\omega}^2) + \mu_2(\bar{k}); \end{aligned} \quad (4.23)$$

this determines $\text{Re}\Phi_{1s}^{-1}(\bar{k}, \bar{\omega})$ upto the additive frequency-independent function $\mu_2(\bar{k})$. Finally, $\mu_2(\bar{k})$ was fixed by evaluating $\text{Re}\Phi_{1s}^{-1}(\bar{k}, \bar{\omega} = 0)$ by an independent method: we determined it directly from the expression (3.55) - unlike the computations just discussed, the frequency sums were evaluated by a direct summation along the imaginary frequency axis and a straightforward numerical evaluations of the relevant Feynman integrals.

This completes our discussion of the derivation $\Phi_{1s}(\bar{k}, \bar{\omega}, \infty)$. The numerical computations are summarized in Fig. 3.

One important feature of Fig. 3, which hasn't been discussed so far, is the behavior of $\text{Im}\Phi_{1s}$ at small frequencies. This can be determined directly from the expressions (4.19) and (4.20) for $\text{Im}\bar{\Sigma}$. We found

$$\text{Im}\Phi_{1s}(\bar{k} = 0, \bar{\omega}, \infty) \sim \frac{1}{N} \exp\left(-\frac{3\Theta^2}{2|\bar{\omega}|}\right), \quad (4.24)$$

while

$$\text{Im}\Phi_{1s}(|\bar{\omega}| < \bar{k}, \infty) \sim \frac{1}{N} \bar{\omega} \exp\left(-\frac{3\Theta^2}{2|\bar{k}|}\right). \quad (4.25)$$

These peculiar singularities are probably artifacts of large N expansion, because they arise from the strong constraints imposed by the delta functions in (4.19,4.20) and the difficulty in satisfying them at small momenta; in other words energy-momentum conservation drastically reduces the phase space for emission/absorption of spin-waves with the spectrum $\bar{\omega} = (\bar{k}^2 + \Theta^2)^{1/2}$. Actually, for self-consistent calculations, we have to include the damping of intermediate excitations, which lifts the restrictions imposed by the delta functions. This should probably give $\text{Im}\Phi \sim \bar{\omega}$ for small $\bar{\omega}$, as in naive expectations. Note that in an exactly solvable 1 + 1 dimensional model of a quantum phase transition, where analogous scaling functions can be computed, no such singularities appear⁷⁰.

D. Local Susceptibility and NMR Relaxation

Having obtained scaling results for the staggered susceptibility, we can now easily obtain properties of the local susceptibility χ_L . The scaling function, F_1 , for $\text{Im}\chi_L$ was defined in

(1.31). We determined F_1 by performing the integration in (1.32) numerically. Our result for $N = 3$ was shown in Fig. 5. From our numerical computation we find for small frequencies

$$F_1(\bar{\omega}) = \text{sgn}(\bar{\omega}) \frac{0.06}{N} |\bar{\omega}|^{1-\eta} ; \quad |\bar{\omega}| \ll 1. \quad (4.26)$$

The power of $\bar{\omega}$ at small $\bar{\omega}$ is fixed by the requirement that $\text{Im}(\chi_L(\omega)) \sim \omega$ for small ω . For large $\bar{\omega}$, we use the large \bar{k} , $\bar{\omega}$ result for Φ_{1s} in (4.15), and (1.32) to deduce that

$$\begin{aligned} F_1(\bar{\omega}) &= \frac{1}{|\bar{\omega}|^{1-\eta}} \int \frac{d^2 \bar{k}}{4\pi^2} \frac{A_Q}{(\bar{k}^2 - \bar{\omega}^2)^{1-\eta/2}} \\ &= \frac{A_Q}{4\pi} \sin\left(\frac{\pi\eta}{2}\right) \frac{\text{sgn}(\bar{\omega})}{|\bar{\omega}|^\eta} \int_0^{|\bar{\omega}|} \frac{\bar{k} d\bar{k}}{(\bar{\omega}^2 - \bar{k}^2)^{1-\eta/2}} \\ &= \text{sgn}(\bar{\omega}) \frac{A_Q}{4} \frac{\sin(\pi\eta/2)}{\pi\eta/2} ; \quad |\bar{\omega}| \gg 1. \end{aligned} \quad (4.27)$$

Thus $F_1(\bar{\omega})$ tends to a universal constant for large $\bar{\omega}$.

From (1.36) and (4.26) we find that the scaling function $R_1(x_1)$ for the NMR relaxation in (1.35) satisfies

$$R_1(x_1 = \infty) = \frac{0.06}{N}. \quad (4.28)$$

E. Specific Heat

We consider evaluation of the expression (3.71) for the free energy density \mathcal{F} at $g = g_c$. We will of course only be interested in $\mathcal{F}(T) - \mathcal{F}(0)$ which is finite as $\Lambda \rightarrow \infty$.

We will need the value of $\Pi(k, i\omega)$ at $T = 0$. From the result (4.3)

$$\Pi(k, i\omega)|_{T=0} = \frac{1}{8(q^2 + \omega^2)^{1/2}} ; \quad q, \omega \ll \Lambda. \quad (4.29)$$

Using this result, and the representation (3.36) for g_c we get from (3.71)

$$\begin{aligned} \mathcal{F}(T) - \mathcal{F}(0) &= \frac{NT}{2} \sum_{\omega_n} \int \frac{d^2 k}{4\pi^2} \left[\log(k^2 + \omega_n^2 + m_0^2) + \frac{1}{N} \log(\Pi(k, i\omega_n)) \right] \\ &\quad - \frac{N}{2} \int \frac{d\omega d^2 k}{8\pi^3} \left[\log(k^2 + \omega^2) - \frac{1}{2N} \log(8(k^2 + \omega^2)) + \frac{m_0^2}{k^2 + \omega^2} \right]. \end{aligned} \quad (4.30)$$

Repeated applications of Poisson summation formula⁶⁵ simplifies this result to

$$\begin{aligned} \mathcal{F}(T) - \mathcal{F}(0) &= NT \int \frac{d^2 k}{4\pi^2} \left[\log\left(1 - e^{-\sqrt{k^2 + m_0^2}/T}\right) - \frac{1}{2N} \log\left(1 - e^{-|k|/T}\right) \right] \\ &\quad + \frac{T}{2} \sum_{\omega_n} \frac{d^2 k}{4\pi^2} \log\left(8(\omega_n^2 + k^2)^{1/2} \Pi(k, i\omega_n)\right) \\ &\quad + \frac{N}{2} \int \frac{d^3 P}{8\pi^3} \left[\log\left(\frac{P^2 + m_0^2}{P^2}\right) - \frac{m_0^2}{P^2} \right]. \end{aligned} \quad (4.31)$$

All the integrals and summations in this last expression can be shown to be finite in the limit $\Lambda \rightarrow \infty$ after using the asymptotic expansion of Π in (4.3). The absence of any terms of order $T/(q, \epsilon_n)^2$ in (4.3) is again quite crucial; the structure of the T^3 term in (4.3) is also such that all potentially dangerous $\log(\Lambda)$ terms cancel. The frequency summation and momentum integration in (4.31) were performed numerically and led to a result proportional to T^3 . We then evaluated the specific heat and obtained

$$\Psi_1(\infty) = \frac{4N}{5} - 0.3344. \quad (4.32)$$

V. RENORMALIZED CLASSICAL REGION

We now proceed to the calculation of the scaling functions in the region where the ground state is ordered ($g < g_c$) and the temperature satisfies $Nk_B T \ll 2\pi\rho_s$, i.e. $x_1 \ll 1$. Under these conditions, the Josephson correlation length $\xi_J \sim \rho_s^{-1}$ is much smaller than $\hbar c/k_B T$. At the shortest scales, the antiferromagnet possesses $D = 2 + 1$ critical spin fluctuations which continue to be described by the scaling function Φ_{1s} in (1.37). The crossover to the Goldstone region (see Fig. 2) occurs at scales $k\xi_J \sim 1$ ($\omega\xi_J/c \sim 1$). In this regime, the dynamics is governed by rotationally-averaged spin-wave fluctuations about a Neel-ordered ground state. We will focus in this section on the second crossover (Fig. 2), which occurs at the correlation length ξ ($\xi \gg \xi_J, \hbar c/(k_B T)$) to a fully disordered antiferromagnet. At scales larger than ξ , all correlations decay exponentially in space and the low-energy dynamics is purely relaxational. For a qualitative description, one can neglect quantum effects in the vicinity of this crossover, and study a simplified, purely classical version of the problem - the classical lattice rotor model¹². We will see, however, that for a complete quantitative description, quantum effects cannot be neglected at *any* k .

A detailed study of the staggered spin correlations in the renormalized classical region was performed by Chakravarty *et. al.*¹² in the framework of the perturbative renormalization group approach for a classical rotor model. In this approach, one starts the description at relatively short spatial and time scales where there is a perfect short-range Neel order, and one can distinguish between the longitudinal and transverse susceptibilities. At these short scales, the thermal coupling constant $g_T = k_B T/\rho_s$, which measures the strength of thermal fluctuations, is small (notice that in two dimensions, g_T is a dimensionless quantity). One then performs RG calculations to see how g_T grows at larger scales. The scale where the running coupling constant becomes of the order of unity is identified with the inverse correlation length ξ . At larger scales, perturbative approach is unapplicable but it is assumed^{71,12} that ξ is the only large scale in the problem and the behavior at $k < \xi^{-1}$ is not very different from that at $k = \xi^{-1}$. This assumption has been explicitly verified by the Bethe-ansatz solution of the $O(3)$ sigma model in 2 dimensions⁷².

The $1/N$ expansion, which we use here, attacks the same problem but from a different perspective. We start with the Green's function which satisfies the mean-field equation for the saddle point. The structure of the saddle-point equation in Section III A shows that the symmetry remains unbroken at all finite T . The mean-field solution has a gap for quasiparticle excitations which we identified, at $N = \infty$, with the inverse correlation length. In other

words, the correlation length is finite from the very beginning. An obvious consequence is that the spin susceptibilities are isotropic functions in the spin space: $\chi_{ij}(q, \omega) \propto \delta_{ij}$. This is indeed what we expect from the true scaling functions in 2D antiferromagnet at finite T (Eqn 1.10a). On the other hand, the temperature dependences of observables are not necessarily correctly reproduced by the infinite N theory. We will show below that the perturbative $1/N$ expansion for $x_1 \ll 1$ is actually an expansion in $1/(N-2) \log x_1$. We assume that the logarithmic terms can be exponentiated; the $1/N$ expansion thus yields corrections in the form of extra powers of temperature: $x_1^{1/(N-2)}$. For $N = 3$, the power $1/(N-2) = 1$, and there will be substantial changes in the temperature dependences of the observables, and in particular, of the correlation length.

Most of our results for the staggered dynamic susceptibility agree with the results of the RG treatment for the classical lattice rotor model (some minor discrepancies with Chakravarty *et. al.*¹² are found however). We are also able to go beyond previous results and obtain explicit expressions for various pre-factors and scaling functions up to the two-loop level. For the uniform susceptibility, we have calculated the temperature dependence of χ_u^{st} in a quantum antiferromagnet and found a linear T dependence at low T , with a universal slope. We emphasize that the temperature dependence of χ_u^{st} is a purely quantum effect. It was absent in previous studies of the classical lattice rotor model^{11,12} which had (for $N = 3$) $\chi_u^{\text{st} \alpha\beta} = \chi_{\perp}(\delta_{\alpha\beta} - \langle n_{\alpha} n_{\beta} \rangle) \equiv \frac{2}{3} \chi_{\perp} \delta_{\alpha\beta}$ (χ_{\perp} is the transverse susceptibility at $T = 0$).

We now proceed to a more detailed discussion of $1/N$ expansion. As in the quantum-critical region, we will use the result (4.2) for the value of N_0^2/ρ_s at $T = 0$, to provide a counterterm for the $\log \Lambda$ contributions to the universal function Φ_{1s} . However, unlike the quantum-critical region, temperature no longer sets the overall scale for fluctuations, and we find it useful to introduce a function $\tilde{\Phi}_{1s}(k, \omega)$ related to Φ_{1s} by

$$\tilde{\Phi}_{1s}(k, \omega) = \left(\frac{\hbar c}{k_B T} \right)^2 \left(\frac{N k_B T}{2\pi \rho_s} \right)^{\eta} \Phi_{1s}(\bar{k}, \bar{\omega}). \quad (5.1)$$

In terms of this function

$$\chi_s(k, \omega) = \frac{N_0^2}{\rho_s} \tilde{\Phi}_{1s}(k, \omega). \quad (5.2)$$

Next, at $x_1 \ll 1$, the typical frequencies $\omega \sim c\xi^{-1}$ are much smaller than $k_B T/\hbar$ and equal-time structure factor $S(q)$ is simply related to $\tilde{\Phi}_{1s}(k, \omega = 0)$:

$$\begin{aligned} S(k) &= \frac{T}{\pi} \int_{-\infty}^{\infty} \frac{\text{Im} \chi_s(k, \omega)}{\omega} d\omega \\ &= k_B T \chi_s(k, \omega = 0) = \frac{k_B T N_0^2}{\rho_s} \tilde{\Phi}_{1s}(k, \omega = 0). \end{aligned} \quad (5.3)$$

The result for $\tilde{\Phi}_{1s}$ to order $1/N$ follows from (3.10) and (4.2):

$$\begin{aligned} \tilde{\Phi}_{1s}^{-1}(k, \omega) &= \left(1 - \eta \log \left(\frac{N\Lambda}{16\rho_s} \right) \right) \\ &\quad (k^2 + \omega^2 + m^2 + \Sigma(k, \omega)), \end{aligned} \quad (5.4)$$

where self-energy and mass renormalization terms ($m^2 = m_0^2 + \delta m^2$) are to be calculated as in Sec III B.

We will now describe, in outline, the computations to order $1/N$ for ξ , m , and the structure factor. We will then proceed, in the subsequent subsections, to present more precise and detailed results for these and other static and dynamic observables.

At $N = \infty$, we have from (3.27)

$$m_0 = \frac{k_B T}{\hbar c} \exp\left(-\frac{2\pi\rho_s^{N=\infty}}{Nk_B T}\right), \quad (5.5)$$

where $\rho_s^{N=\infty}$ is given by (3.25). We emphasize that m_0 is expressed here in terms of the $T = 0$ spin-stiffness constant ρ_s computed at $N = \infty$. There are however $1/N$ corrections at $T = 0$ as well, and the fully renormalized ρ_s indeed differs from (3.25). When reexpressed in terms of the total ρ_s at $T = 0$, m_0 by itself acquires a correction of the order of $1/N$; this correction will be important later as a counterterm for the leading ultraviolet divergence of $m = 1/\xi$.

At $N = \infty$, the value of the correlation length, ξ , is given simply by $\xi = 1/m_0$. Comparing Eqn (3.27) with the results of previous perturbative approaches, we see that neither the numerical factor in the exponent nor the temperature dependence of the prefactor in ξ agree with the results of the two-loop RG analysis of Chakravarty *et. al.*¹². As we already discussed above, this is not surprising because their analysis was done for the particular case of $N = 3$. The two-loop β -function for arbitrary N was first calculated by Brezin and Zinn-Justin⁷³ in a perturbative expansion about the ordered state, and their result for the correlation length is

$$\xi \sim \frac{\hbar c}{k_B T} \left(\frac{k_B T(N-2)}{2\pi\rho_s}\right)^{1/(N-2)} \exp\left(\frac{2\pi\rho_s}{(N-2)k_B T}\right). \quad (5.6)$$

At $N = \infty$, this expression coincides with m_0 , as it should. Further, if we formally expand the r.h.s. of (5.6) in $1/N$, we find terms of the form $(1/(N-2)) \log(k_B T/(\hbar c m_0))$ and $(1/(N-2)) \log(\log(k_B T/(\hbar c m_0)))$. We therefore anticipate that the same terms should appear in the $1/N$ expansion. This is indeed what we found in our calculations, as we now demonstrate.

We first observe that all $\log(k_B T/(\hbar c m_0))$ terms in the $1/N$ expansion come from integration over spatial scales which are much larger than the scale set by the temperature. Accordingly, performing the calculations with the logarithmic accuracy, we can restrict the evaluation of Σ and δm^2 to a classical lattice rotor model; this implies that we restrict the summation over ω to the contribution at $\omega = 0$ only and set $k_B T/\hbar c$ as the upper cutoff in the momentum integration. This substantially simplifies the calculations and we easily obtain from (3.56)

$$\Pi(q, 0) = \frac{k_B T}{\pi q \sqrt{q^2 + 4m_0^2}} \log \frac{q + \sqrt{q^2 + 4m_0^2}}{2m_0}. \quad (5.7)$$

Substituting this expression into (3.55), performing the integration, and using (5.5) for m_0 , we obtain

$$\Sigma_{k,0} = \frac{k^2}{N} \log \lambda_k + \dots; \quad \lambda_k = \frac{\log[k_B T / (\hbar c m_0)]}{\log[\sqrt{k^2 + m_0^2}/m_0]}, \quad (5.8)$$

where dots stand for the terms of higher order in $1/N$, nonlogarithmic classical contributions, and for quantum contributions. Note that as written, (5.8) is valid only for $k \gg m_0$; for $k = \mathcal{O}(m_0)$, we have with the logarithmic accuracy $\lambda_k = \lambda_m = \log[k_B T / (\hbar c m_0)]$. We now substitute (5.8) into (3.61) and, using the smallness of $\hbar c m_0 / k_B T$, obtain after some algebra

$$\delta m^2 = \frac{m_0^2}{N} \left[-4 \log \frac{k_B T}{\hbar c m_0} + 3 \log \lambda_m \right] + \dots \quad (5.9)$$

Next, we have to show that (i) the actual expansion holds in $1/(N-2)$ rather than in $1/N$ and (ii) the logarithmic series are geometrical and therefore can be exponentiated. In principle, to prove any of these statements, one has to examine the structure of the perturbative expansion up to infinite order in $1/N$. This is a rather difficult problem to analyze and we will be content with demonstrating that both expectations are consistent with the perturbative results up to order $1/N^2$. Specifically, we computed $1/N^2$ logarithmic corrections to $\Sigma_{k,0}$. The computational procedure is tedious but straightforward. We followed the general procedure described by Polyakov⁶⁷: we identified various regions of virtual momenta which contribute to $\Sigma_{k,0}$ with logarithmic accuracy and, evaluating the integrals, obtained:

$$\begin{aligned} k^2 + \Sigma_{k,0} &= k^2 \left[1 + \frac{1}{N} \left(1 + \frac{2}{N} + \dots \right) \log \lambda_k \right. \\ &\quad \left. + \frac{1}{2N^2} \log^2 \lambda_k + \dots \right] \\ &\rightarrow k^2 (\lambda_k)^{1/(N-2)}, \end{aligned} \quad (5.10)$$

precisely as we anticipated. We didn't perform $1/N^2$ calculations for δm^2 , but it is very likely that the expansion for the mass is similar to that for $\Sigma_{k,0}$. We assume that this is the case, and assemble the $1/N$ corrections to m^2 into logarithmic and double logarithmic series. This yields

$$\begin{aligned} m^2 &= \left(\frac{k_B T}{\hbar c} \right)^2 \left(\frac{\hbar c m_0}{k_B T} \right)^2 \left(1 - \frac{2}{N-2} \log \left(\frac{k_B T}{\hbar c m_0} \right) \right. \\ &\quad \left. + \dots \right) \left(1 + \frac{3}{N-2} \log \lambda_m + \dots \right) \\ &= \left(\frac{k_B T}{\hbar c} \right)^2 \left(\frac{\hbar c m_0}{k_B T} \right)^{2N/(N-2)} (\lambda_m)^{3/(N-2)}. \end{aligned} \quad (5.11)$$

In writing the last line we also assumed that the value of m_0 in double logarithmic terms can be replaced by the total mass m . The verification of this assumption requires a computation of finite contributions to order $1/N^2$ which we didn't perform. We now assemble the contributions in (5.4), (5.10) and (5.11) and obtain

$$\tilde{\Phi}_{1s}(k, \omega = 0) \propto \frac{\lambda_k^{-1/(N-2)}}{k^2 + \xi^{-2}}, \quad (5.12)$$

where with logarithmic accuracy

$$\xi \propto \left(\frac{\hbar c}{k_B T} \right) \left(\frac{k_B T (N-2)}{2\pi\rho_s} \right)^{1/(N-2)} \exp\left(-\frac{2\pi\rho_s}{(N-2)k_B T} \right). \quad (5.13)$$

This agrees with the two-loop RG result (5.6). From (5.12) and (5.3), the equal-time structure factor is

$$S(k) \propto \xi^2 \left(\frac{k_B T (N-2)}{2\pi\rho_s} \right)^{(N-1)/(N-2)} \frac{(1 + \frac{1}{2} \log(1 + (k\xi)^2))^{1/(N-2)}}{1 + (k\xi)^2}. \quad (5.14)$$

For $N = 3$, this coincides with the result of Chakravarty *et. al.*¹².

An advantage of the $1/N$ expansion is that we can go further than (5.12-5.14) and calculate not only logarithmic contributions in $1/N$, but also the regular ones. For this type of calculation, the classical approximation is not sufficient and one has to consider the full quantum problem. The computations are lengthy but straightforward. We will skip the details here: interested readers can obtain a fuller description of the intermediate steps directly from the authors. We will list here only a catalog of the results similar to Eqn (4.5)

$$m^2 = Z m_0^2 \left[1 - \frac{4}{N} \log \frac{k_B T}{\hbar c m_0} + \frac{4}{N} \log \log \frac{k_B T}{\hbar c m_0} + \frac{2}{N} (3 \log 2 - 1 + C + 0.3841) \right], \quad (5.15)$$

$$m_0^2 + \Sigma(k = im_0, 0) = Z^{-1} m_0^2 \left[1 - \frac{2}{N} \log \log \frac{k_B T}{\hbar c m_0} - \frac{2}{N} 0.3841 \right],$$

$$1 + \frac{\partial \Sigma(k \rightarrow 0, 0)}{\partial k^2} = Z \left[1 + \frac{2}{N} \log \log \frac{k_B T}{\hbar c m_0} + \frac{2}{N} 0.3518 \right],$$

$$k^2 + \Sigma(k \gg \xi^{-1}, 0) = Z k^2 \left[1 - \frac{1}{N} \log \left(1 + \frac{1}{2} \log(1 + (k\xi)^2) \right) + \frac{2}{N} \log \log \frac{k_B T}{\hbar c m_0} + \frac{1.9561}{N} \right],$$

$$1 - \frac{\partial \Sigma(k = im_0, 0)}{\partial k^2} = Z^{-1} \left[1 - \frac{2}{N} \log \log \frac{k_B T}{\hbar c m_0} + \frac{0.2385}{N} \right],$$

$$Z = \left(1 + \eta \log \frac{N\Lambda}{16\rho_s} \right) \left[1 - \frac{1}{N} \log \log \frac{k_B T}{\hbar c m_0} - \frac{0.9561}{N} \right]. \quad (5.16)$$

Here C is the Euler constant $C \approx 0.5772$. As before, we use these results to evaluate universal functions for various observables.

A. Correlation length and equal-time structure factor

We start with the scaling function for the correlation length. From (5.15, 5.16), we find

$$\xi = \xi_0 \left(\frac{\hbar c}{k_B T} \right) \left(\frac{k_B T (N-2)}{2\pi\rho_s} \right)^{1/(N-2)} \times \exp \left(-\frac{2\pi\rho_s}{(N-2)k_B T} \right), \quad (5.17)$$

where ξ_0 has a rather simple form

$$\xi_0 = 1 - \frac{(3 \log 2 - 1 + C)}{N}. \quad (5.18)$$

The same result was recently obtained in a different way by Hasenfratz and Niedermayer²⁵. They deduced ξ by comparing the free energy of the Heisenberg antiferromagnet in moderate magnetic fields with the Bethe-ansatz solution for the $O(N)$ sigma model^{72,74}. Moreover, they argued on the basis of the numerical analysis, that the $1/N$ result for ξ_0 is in fact the first term in the $1/N$ expansion for

$$\xi_0 = \left(\frac{e}{8} \right)^{1/(N-2)} \Gamma(1 + 1/(N-2)), \quad (5.19)$$

where $\Gamma(\dots)$ is the Gamma-function. The numerical evidence for (5.19) is rather convincing and we will use (5.19) for the experimental comparisons in Sec VII.

Further, the equal-time structure factor is given by (5.3) and using (5.16) we obtain

$$S(k) = S(0) f(k\xi), \quad (5.20)$$

where

$$S(0) = 2\pi N_0^2 \left(\frac{k_B T}{2\pi\rho_s} \right) \left(\frac{(N-2)k_B T}{2\pi\rho_s} \right)^{1/(N-2)} \times \xi^2 \left(1 + \frac{0.188}{N} \right), \quad (5.21)$$

and $f(k\xi)$ is a universal scaling function introduced first by Chakravarty *et. al.*¹², for which we obtain

$$f(k\xi) = \frac{1}{1 + (k\xi)^2} \times \begin{cases} 1 + \frac{0.065}{N} (k\xi)^2; & k\xi \ll 1, \\ \frac{N-1}{N} \left(1 - \frac{0.188}{N} \right) \left(1 + \frac{1}{2} \log(1 + (k\xi)^2) \right)^{1/(N-2)} & ; \xi^{-1} \ll k \ll \xi_J^{-1}. \end{cases} \quad (5.22)$$

At $k\xi \gg 1$, i.e., in the ‘Goldstone’ region, (5.20) reduces to

$$S(k) \approx \frac{k_B T N_0^2}{\rho_s k^2} \left(\frac{N-1}{N} \right). \quad (5.23)$$

For $N = 3$ this agrees with the result obtained by Chakravarty *et. al.*¹² (their definition for $S(k)$ differs from ours by a factor of N). Clearly, Eqn (5.23) is nothing but the rotationally averaged result for the Neel-ordered antiferromagnet. In the ordered state, there are $N - 1$ gapless transverse spin waves which contribute to the low-energy part of $S(k)$ and one longitudinal component of fluctuations which has a finite gap and does not contribute at low energies. Rotational averaging then gives a factor $(N - 1)/N$, as in (5.23).

Though our results are very similar to the scaling theory¹², we observe that the two limits in (5.22) cannot be assembled into the single one-parameter interpolation form for $f(k\xi)$ suggested by Tyc *et. al.*¹³. This is not surprising however because the one-parameter scaling function was introduced as a convenient, but approximate way to interpolate between $k\xi \gg 1$ and $k\xi \ll 1$, where the behavior of $S(k)$ is known from the hydrodynamic considerations.

Further, we emphasize that ρ_s and N_0 in (5.21) are the fully renormalized spin-stiffness and sublattice magnetization at $T = 0$. Only in this case, all ultraviolet $\log \Lambda$ divergences in $1/N$ corrections to ξ and $S(k)$ are canceled out. Finally, in obtaining the universal functions (5.17, 5.22), we actually didn't use the condition $\rho_s \ll J$. It thus appears that at least to first order in $1/N$, the universal behavior holds for arbitrary ρ_s , i.e., in the whole renormalized classical region. This is a remarkable property of the quantum sigma model, and the arguments that the universality at all g may hold at arbitrary N were elegantly displayed in the analyses of Hasenfratz *et. al.*^{25,26}. In any event, this implies that our results for the renormalized classical region, which were obtained in a theory valid near $g = g_c$, are in fact valid at small T for all $g < g_c$.

B. Uniform susceptibility

We turn next to the calculation of the static uniform susceptibility. The expression for χ_u valid at arbitrary x_1 was given in (3.68) and (3.70). In the renormalized classical region, it is convenient to introduce $\tilde{\Phi}_{1u} \equiv k_B T \Phi_{1u}(0, 0, x_1)$ such that

$$\chi_u(0, 0) = \left(\frac{g\mu_B}{\hbar c}\right)^2 \tilde{\Phi}_{1u}. \quad (5.24)$$

We then use $n_{m_0} \approx k_B T / \hbar c m_0$, and obtain for $\tilde{\Phi}_{1u}$

$$\tilde{\Phi}_{1u} = \tilde{\Phi}_{1u}^\infty - K_3 - \frac{k_B T}{m_0^2} (m^2 - m_0^2), \quad (5.25)$$

where $\tilde{\Phi}_{1u}^\infty$, given in (3.13), is the contribution at $N = \infty$ and the remaining terms are $1/N$ corrections. For $\tilde{\Phi}_{1u}^\infty$ we have

$$\tilde{\Phi}_{1u}^\infty = -2(\hbar c)^2 \int \frac{d^2 k}{4\pi^2} n'_k = \frac{k_B T}{\pi} \left(\log \frac{k_B T}{\hbar c m_0} + 1\right). \quad (5.26)$$

Using the expression for m_0 at small x_1 , we can rewrite the $N = \infty$ result for χ_u^{st} as

$$\chi_u^{\text{st}} = \left(\frac{g\mu_B}{\hbar}\right)^2 \left(\frac{2}{N} \chi_\perp + \frac{1}{\pi c^2} k_B T\right), \quad (5.27)$$

where $\chi_{\perp} \equiv \rho_s c^2$ is the transverse susceptibility. We see that in the limit of vanishing temperature, χ_u^{st} is precisely the rotationally averaged uniform susceptibility of the ordered antiferromagnet. This is likely to be the exact result, and we expect that all $1/N$ corrections at $T = 0$ can be assembled into the renormalization of χ_{\perp} . On the other hand, the temperature dependence of χ_u^{st} is a purely quantum effect (it is entirely due to the second term in (5.26)) and $1/N$ corrections to $d\chi_u^{\text{st}}/dT$ are indeed possible. We also observe that the slope of χ_u^{st} versus T at $N = \infty$ is twice as large as in the mean-field Schwinger boson approach^{62,75}. This is not surprising however, because the mean-field Schwinger boson theory is the $N = \infty$ limit for a σ -model of the N -component *complex* unit field defined on the CP^{N-1} manifold. This model is isomorphic to $O(3)$ sigma-model only at a particular value of $N = 2$ and there is no reason why the $N \rightarrow \infty$ limits of the two theories should be the same. One of main technical points of this paper is that the $1/N$ corrections in the $O(N)$ theory are numerically quite small, making it a superior approach to make precise numerical predictions.

The corrections to $\tilde{\Phi}_{1u}$ were computed in the same way as for the correlation length and equal-time structure factor. We skip the details of calculations and discuss only the results. As before, we found that all divergent contributions in the ultraviolet are canceled out when the result is expressed in terms of the fully renormalized transverse susceptibility at $T = 0$. We have explicitly checked that there are no other corrections at $T \rightarrow 0$ besides the renormalization of χ_{\perp} . Moreover, we did not find any logarithmic corrections to the temperature dependent part of χ_u^{st} which might have change the power of the leading T -dependent correction. This result is likely to be valid to arbitrary order in $1/N$ although the proof is lacking. At the same time, we did find the finite correction to the $\tilde{\Phi}_{1u}$ and our result for χ_u^{st} valid to order $1/N$ is

$$\chi_u^{\text{st}} = \left(\frac{g\mu_B}{\hbar}\right)^2 \left(\frac{2}{N}\chi_{\perp} + \left(\frac{N-2}{N}\right)\frac{k_B T}{\pi c^2}\right). \quad (5.28)$$

The renormalization factor, $(N-2)/N$, of the linear T term is likely to be correct to all orders in $1/N$. The argument is that in the XY case ($N = 2$), the spin-wave analysis for χ_u^{st} is free from divergences⁷⁶ and predicts a cubic, rather than linear dependence on T $\chi_u^{\text{st}} = \chi_u^{\text{st}}(0) + \mathcal{O}(T^3)$. We also note that for $N = 3$, the renormalization factor is $1/3$ and the slope of χ_u^{st} is therefore significantly reduced from the $N = \infty$ result and now differs substantially from the slope of χ_u^{st} in the quantum critical regime. We will use this later in Sec. VII for the interpretation of the experimental data.

C. Dynamic staggered structure factor

The calculations of the dynamic susceptibility proceed along the same lines as in Sec. IV. We use integral representation of the polarization operator continued to the real axis, and compute the retarded self-energy. The calculations are rather lengthy, so we skip the details and focus only on the results: details of the intermediate steps can be obtained directly from the authors. At $k\xi \gg 1$, we obtained

$$\chi_s(k, \omega) = \frac{N-1}{N} \frac{(\hbar c_k)^2 N_0^2}{\rho_s} \frac{\rho_s^k}{\rho_s} \frac{1}{\epsilon_k^2 - (\omega + i\gamma_{k,\omega})^2}, \quad (5.29)$$

where $\epsilon_k = (\hbar c_k)^2(k^2 + \xi^{-2})$, $c_k^2 = \rho_s^k/\chi_\perp^k$. We have introduced here the k -dependent spin stiffness, ρ_s^k , and spin susceptibility, χ_\perp^k , which are values of these observables at the momentum scale k . In the present $1/N$ expansion, they are given by

$$\rho_s^k = \frac{(N-2)k_B T}{2\pi} \left[\varrho + \frac{1}{2} \log(1 + (k\xi)^2) \right], \quad (5.30)$$

and

$$\chi_\perp^k = \chi_\perp \left[\frac{2}{N} + \frac{N-2}{N} \left(\frac{\rho_s^k}{\rho_s} \right)^{N/(N-2)} \right]. \quad (5.31)$$

The dimensionless, numerical variable ϱ was found, to first order in $1/N$, to be $\varrho = 1$ and *independent* of the ratio of $\omega/\hbar ck$ as long as this ratio is less than 1. Eqn.(5.30) (with $\varrho = 1$) coincides with the one-loop result for the running spin-stiffness inferred from the RG equation for the static coupling constant¹². It was suggested by Tyc *et. al.*¹³ that the two-loop corrections may lead to $\varrho \neq 1$. In our approach, the same is likely to happen from higher order terms in the $1/N$ expansion; dependence of ϱ on the ratio $\omega/\hbar ck$ is also possible. Furthermore, we have checked that Eqn (5.31) coincides with the perturbative result for the transverse susceptibility measured on the momentum scale k (and frequency scale ck). The first term in (5.31) is the exact result at $T = 0$, which we already obtained in the previous subsection. The second term (which, we emphasize, is also a classical contribution) actually accounts for the difference between transverse and longitudinal susceptibility measured at finite momentum *and* frequency. In this situation, we probe the system at finite spatial and time scales where the system appears Néel ordered. The temperature dependence of this term for $N = 3$ is the same as in the scaling approach¹² and, in fact, can be deduced directly from the diagrammatic expression of χ_u^{st} in Sec. IIIB if k and ω are both small but finite.

The $1/N$ result for the damping rate $\gamma_{k,\omega}^{1/N}$ is given by

$$\gamma_{k,\omega} = \frac{\pi}{2} \frac{\hbar c_k k}{N-2} \eta_{k,\omega} \left(\frac{(N-2)k_B T}{2\pi \rho_s^k} \right)^2 \left(\log \frac{k_B T}{\hbar ck} \right), \quad (5.32)$$

where $\eta_{k,\omega}$ ($=1$ for on-shell excitations) is a smooth function of the ratio $\omega/c_k k$. This result for the damping rate agrees with the lowest-order perturbative calculations by Tyc and Halperin⁷⁷. They, however, have shown that the logarithmic dependence on the quasiparticle momentum k in (5.32) is actually an artifact of the Born approximation. Significant corrections to the self-energy term arise from the damping of intermediate excitations. Neglecting this damping is a legitimate approximation only if the damping rate is smaller than the energy of the incoming quasiparticle. Let us define the momentum scale for intermediate states, q_m , such that $\gamma_{q_m} = \epsilon_k$. Clearly then, the lowest-order calculations are valid for $q < q_m$, but damping of intermediate states must be included for $q > q_m$. A simple estimate based on Eqn. (5.32) yields $q_m \sim k(\rho_s^k/T)^2$. A careful consideration⁷⁷ then demonstrated that q_m has to be taken as the upper cutoff in the momentum integral leading to (5.32), and k -dependent logarithm in (5.32) has to be substituted by the self-consistent expression

$$\log \frac{k_B T}{\hbar c k} \rightarrow \log q_m/k \rightarrow \log \left[\frac{2}{\pi} \left(\frac{2\pi \rho_s^k}{(N-2)k_B T} \right)^2 \right] \quad (5.33)$$

The self-consistent result is then

$$\gamma_{k,\omega} = \frac{\pi}{2} \frac{\hbar c_k k}{N-2} \bar{\eta}_{k,\omega} \left(\frac{(N-2)k_B T}{2\pi \rho_s^k} \right)^2 \left[2 \log \frac{2\pi \rho_s^k}{(N-2)k_B T} + \Gamma \right], \quad (5.34)$$

where $\bar{\eta}_{k,\omega}$ (=1 for on-shell excitations) is a smooth function of the ratio $\omega/c_k k$, which generally differs from η , and Γ is a pure number of order unity.

We return to consideration of the dynamic susceptibility $\chi_s(k, \omega)$ but now at momenta other than $k\xi \gg 1$. At $k\xi \sim 1$ the naive $1/N$ expansion is not terribly useful because the scale $q_m \sim \mathcal{O}(\xi^{-1})$, and the damping of intermediate excitations cannot be neglected at any momentum. We have therefore little to add here to the results of Ref^{12,77} who used the dynamic scaling hypothesis⁷⁸ to study this region. The content of this hypothesis is that there is only one large spatial scale in the problem, namely the correlation length, and the damping of excitations becomes comparable to the real part of the spectrum at $k\xi = \mathcal{O}(1)$. Indeed, if we use our result (5.34) for $\gamma_{k,\omega}$, which is strictly speaking valid only for $k\xi \gg 1$, and extend it down to $k\xi \mathcal{O}(1)$, this is precisely what happens. The ratio $\gamma_{k,\omega}/\epsilon_k$, which behaves as $(T/\rho_s^k)^2 \log \rho_s^k/T$ at large $k\xi$, becomes of the order of unity at the scale of $k\xi = \mathcal{O}(1)$. This happens because ρ_s^k in (5.30) is renormalized substantially downward at small k and eventually becomes $\sim k_B T$ ⁷⁹.

Notice also that χ_{\perp}^k tends to a finite value as k approaches zero. As a result, c_k decreases with k , and for $k\xi = \mathcal{O}(1)$, we have $c_k \sim c \sqrt{k_B T/2\pi \rho_s}$ independent of N . This last result illustrates an important feature of the $1/N$ expansion in the renormalized-classical region. The N -independent result for c_k is inconsistent with our earlier $N = \infty$ analysis in Sec III A which is completely Lorentz-invariant and has a T -independent value of c . This apparent contradiction is a consequence of the non-commutativity of the $T \rightarrow 0$ and $N \rightarrow \infty$ limits. The key point is that the $T = 0$ static uniform susceptibility in the $O(N)$ sigma model scales as $\mathcal{O}(1/N)$ (Eqn (5.28)) and therefore vanishes at $N = \infty$. In view of this, one has to proceed to the next order in the expansion over $1/N$ (as we did) to check that there is indeed a breakdown of Lorentz-invariance at small but finite T .

D. NMR relaxation

The assumption about the functional form of $\chi_s(k, \omega)$ at small k is a key ingredient which makes possible the calculation of the antiferromagnetic contribution to the spin-lattice relaxation rate. Using the definition of $1/T_1$ in (1.34) and performing the integration in (5.29), we obtain

$$\frac{1}{T_{1s}} = \lambda \frac{A_{\pi}^2 N_0^2}{(N-2)\hbar} \left(\frac{2}{N} \right)^{1/2} \left(\frac{\xi}{\hbar c} \right)$$

$$\left(\frac{(N-2)k_B T}{2\pi\rho_s} \right)^{N/(2N-4)}, \quad (5.35)$$

where λ is a numerical factor whose calculation requires us to know the precise form of $\chi_s(k, \omega)$ at $k\xi = O(1)$. The functional form of $1/T_{1s}$ in (5.35) is identical to that obtained by Chakravarty and Orbach²⁷ on the basis of the scaling approach of Chakravarty *et al.* They also estimated the value of numerical factor to be $\lambda N_0^2 \approx 0.61$ (for $N = 3$) by fitting the scaling forms of Chakravarty *et al.*¹² and Tyc *et al.*¹³ to the numerical simulations on a classical lattice rotor model.

E. Specific heat

A simple inspection of the free energy (3.71) in the renormalized classical regime shows that the dominant contribution to $\mathcal{F}(T) - \mathcal{F}(0)$ comes from the region of magnon frequencies comparable with the temperature. In this region, m_0 in (3.71) can be neglected compared to $k^2 + \omega^2$, and we obtain

$$\Pi(k, i\omega) = \frac{2\rho_s}{N} \frac{1}{k^2 + \omega^2}. \quad (5.36)$$

The free energy (3.71) is then easily seen to be precisely the same as that of a gas of $N - 1$ gapless Bose degrees of freedom. By definition, (1.10c), $\Psi_1(T \rightarrow 0)$ is a measure of the number of such modes in the ground state. We have therefore

$$\Psi_1(x_1 \ll 1) = N - 1. \quad (5.37)$$

It can be shown using the above results that x_1 dependent corrections to Ψ_1 are suppressed by a factor e^{-1/x_1} .

VI. QUANTUM DISORDERED REGION

The section will present computations of $1/N$ corrections to the staggered susceptibility. We will not compute $1/N$ corrections to the uniform susceptibility and the specific heat: both these quantities are suppressed by factors of $e^{-\Delta/(k_B T)}$ at low temperatures, and are well described by the $N = \infty$ theory in Section. III A 2 - $1/N$ corrections will lead to innocuous numerical prefactors.

As in the previous sections, the computations will be carried out with a relativistic cutoff scheme which restricts $\omega_n^2 + q^2 < \Lambda^2$. We will begin with a description of results at $T = 0$, followed by a discussion of the finite T corrections.

A. $T = 0$

An immediate simplification here is that all correlators are completely relativistic. In fact, as the ultraviolet cutoff is also relativistic, this is also true at frequencies and momenta

of the order of Λ . All Green's functions are therefore dependent only upon a relativistic 3-momentum Q , related to the usual momentum, q , and real frequency, ω , by

$$Q^2 = q^2 - (\omega + i\varepsilon)^2. \quad (6.1)$$

Here ε is a positive infinitesimal.

An important feature of $\chi_s(Q)$ has already been discussed in Section II B: there is a perfect spin-1 quasiparticle pole at $\omega = \sqrt{q^2 + \Delta^2}$. From (3.54) we deduce that the residue, \mathcal{A} at this pole is (to order $1/N$)

$$\mathcal{A} = \frac{g\tilde{S}^2}{N} \left(1 - \frac{\partial \Sigma(Q^2 = -\Delta^2)}{\partial Q^2} \right). \quad (6.2)$$

We turn therefore to an evaluation of Σ . This will be obtained from the results of Section III B evaluated at $T = 0$ with $m_0 = \Delta$. From (3.56) it is easy to obtain the exact result for Π

$$\Pi(Q) = \frac{1}{4\pi Q} \arctan \left(\frac{Q}{2\Delta} \right). \quad (6.3)$$

Next, (3.55) can be reduced to a one-dimensional integral for $\Sigma(Q)$

$$\Sigma(Q) = \frac{1}{2\pi^2} \int_0^\Lambda \frac{P^2 dP}{\Pi(P)} \left[\frac{1}{2PQ} \log \left(\frac{(P+Q)^2 + \Delta^2}{(P-Q)^2 + \Delta^2} \right) - \frac{2}{P^2 + \Delta^2} \right]. \quad (6.4)$$

From this result, numerical and analytic manipulations show

$$\begin{aligned} \frac{\partial \Sigma(Q^2 = -\Delta^2)}{\partial Q^2} &= \eta \log \left(\frac{\Lambda}{\Delta} \right) - \frac{0.4817408231574}{N} \\ \Sigma(Q^2 \gg \Delta^2) &= Q^2 \left[\eta \log \left(\frac{\Lambda}{Q} \right) + \frac{8}{3\pi^2 N} \right]. \end{aligned} \quad (6.5)$$

The first result can be combined with (4.2) to obtain the result (1.22) for Z_Q , while the second is closely related to the fourth equation in (4.5).

B. $T > 0$

We present here results for the local susceptibility $\text{Im}\chi_L(\omega)$ at very small ω . Clearly, because of the presence of gap, Δ , we have $\text{Im}\chi_L(\omega < \Delta)|_{T=0} = 0$. Thus the entire contribution below comes from thermally excited quasiparticles. From the definition (1.16) of χ_L and (3.54) we have to order $1/N$

$$\text{Im}\chi_L(\omega \rightarrow 0) = \frac{g\tilde{S}^2}{N} \int \frac{d^2k}{4\pi^2} \frac{\text{Im}\Sigma(k, \omega)}{(k^2 + \Delta^2)^2} \quad (6.6)$$

Using the integral representation of the polarization operator, it is not difficult to obtain that in the quantum disordered region ($T \ll \Delta$)

$$\text{Im}\Sigma(k, \omega \rightarrow 0) = \frac{2\omega}{NT} \int \frac{d^2q}{4\pi^2} \frac{e^{-\epsilon_{k+q}/T}}{\epsilon_{k+q}} \text{Im}\Pi^{-1}(q, \epsilon_{k+q}), \quad (6.7)$$

where, as before $\epsilon_k = \sqrt{k^2 + m_0^2}$. Note that ϵ_k and Π now have to be evaluated at $m_0 = \Delta$.

It now remains to evaluate $\text{Im}\Pi^{-1}$. We will begin by considering $\text{Im}\Pi$. From the generalization of (4.20) to the quantum disordered region we find the following important contributions to $\text{Im}\Pi$ for $T \ll \Delta$

$$\begin{aligned} \text{Im}\Pi(q, \epsilon_{k+q}) &= \text{Im}\Pi(q, \epsilon_{k+q})|_{T=0} + \\ &+ \frac{1}{8\pi} \int d^2p \frac{n_p - n_{p+q}}{\epsilon_p \epsilon_{p+q}} \delta(\epsilon_{p+q} - \epsilon_p - \epsilon_{k+q}), \end{aligned} \quad (6.8)$$

where $\Pi|_{T=0}$ was obtained earlier in (6.3). In principle, the T dependent corrections to $\text{Re}\Pi$ can be obtained by a Hilbert transform of (6.8); however, we found that these contributed subdominant corrections to $\text{Im}\chi_L/\omega$ in the limit $T \ll \Delta$.

We can now compute $\text{Im}\chi_L$ by combining (6.3), (6.6), (6.7) and (6.8). We omit the details and give the final result

$$\begin{aligned} \text{Im}\chi_L(\omega \rightarrow 0) &= \omega \frac{\mathcal{A}T}{4N\Delta^2} e^{-2\Delta/T} \left[\frac{1}{\arctan^2(1/\sqrt{2})} \right. \\ &\left. + \frac{4}{\log^2(\Delta/T)} + \mathcal{O}\left(\frac{1}{\log^3(\Delta/T)}\right) \right]. \end{aligned} \quad (6.9)$$

Note that the first term in the brackets is due to the temperature dependent part of $\text{Im}\Pi$, while the logarithmical terms come from the real and imaginary parts of $\Pi|_{T=0}$. This result can be combined with the definitions in Section ID5 to obtain the small argument limit of the scaling function F_2 .

VII. COMPARISON WITH EXPERIMENTS

In this Section, we compare our theoretical results with the available experimental data for undoped, and weakly doped $La_{2-x}Sr_xCuO_4$ and the numerical results for 2D $S = 1/2$ Heisenberg antiferromagnets on a square lattice. But first, let us briefly summarize our findings.

We presented above the general forms for uniform and staggered susceptibilities in a two-dimensional quantum antiferromagnet which has $\rho_s \ll J$. The explicit crossover functions were calculated at $N = \infty$ and the $1/N$ corrections were examined in the limiting cases of $x_1 \gg 1$ and $x_1 \ll 1$, where $x_1 = Nk_B T / (2\pi\rho_s)$ is a parameter which governs the crossover between renormalized classical and quantum critical regions (for $x_1 \ll 1$, the system is in the renormalized classical region, while for $x_1 \gg 1$ it is in the quantum critical region). We found that for large values of x_1 , the perturbative expansion is regular in $1/N$. Moreover, the corrections were numerically rather small; so we expect that for the physical case of

$N = 3$, the results obtained in the first order in $1/N$ are already quite close to the exact values of observables. On the other hand, at small x_1 , the $1/N$ expansion is logarithmically singular - it holds in $\log x_1/N$ and eventually changes the leading singularity in some of the scaling functions at $x_1 \rightarrow 0$; the final low-T behavior is the same as in the renormalized-classical scaling theory of Chakravarty *et.al.*¹². The crossover between small and large- x_1 behavior should occur at x_1 around unity, though not necessarily at the same x_1 for various observables. For $\rho_s \ll J$, $x_1 \sim 1$ is within the validity of the long-wavelength description, and we expect that there should be a temperature range where our formulas for the quantum critical region describe the experimental data better than the renormalized classical theory. Strictly speaking, the renormalized classical theory should be valid only for $x_1 \ll 1$ when $\log x_1$ terms dominate regular perturbative corrections.

We now proceed to describe the data. Let us first discuss undoped antiferromagnet. We know from elementary spin-wave analysis that zero-point fluctuations are not divergent in two dimensions and therefore the $T = 0$ renormalization of spin-stiffness, spin-wave velocity and sublattice magnetization come primarily from the lattice scales, where we can rely on the results of spin-wave calculations. At present, two-loop spin-wave expressions are available⁸⁰. For $S = 1/2$, they yield the values of ρ_s , χ_\perp and N_0 , which are practically undistinguishable from the results obtained in numerical simulations⁸¹:

$$\rho_s = 0.181J; \quad \chi_\perp = \left(\frac{g\mu_B}{\hbar}\right)^2 \frac{0.514}{8Ja^2}; \quad N_0 = 0.307, \quad (7.1)$$

where a is the lattice spacing. Hence $2\pi\rho_s \approx 1.13J$ and we therefore expect that quantum critical expressions should work for $k_B T > 0.35J \div 0.4J$. The expected crossover temperature is indeed not very small, but it is still significantly lower than J ; in other words we may reasonably expect our long-wavelength description to continue to be valid for $x_1 \geq 1$. Notice that our result for ρ_s differs from $\rho_s \approx 0.15$ used by Chakravarty *et.al.*¹². The reason is that Chakravarty *et.al.* extracted the value of ρ_s from one-loop spin-wave results extended to $S = 1/2$, while our estimate of ρ_s is based on a two-loop spin-wave calculations.

We now discuss what happens at nonzero doping. First, a mean-field analysis based on Hubbard model predicts that antiferromagnetism is destroyed at arbitrary small concentration of holes⁸². However, more sophisticated considerations show^{84,85} that there is in fact no discontinuity in the immediate vicinity of half-filling, and one needs a finite, though small, concentration of holes to destroy antiferromagnetic ordering. There are several possible scenarios of the doping-induced loss of Néel order:

(i) There is a $T = 0$ transition from the Néel state to a incommensurate magnetically ordered state⁸³⁻⁸⁶; or

(ii) The Néel state is destroyed by quantum fluctuations and the system enters a quantum disordered spin-fluid with commensurate correlations. Only at a larger doping do incommensurate correlations appear.

A recent self-consistent two-loop calculation⁸⁷ on the Shraiman-Siggia⁸³ model displays both sequences of transitions depending on the strength of the coupling between fermions and n -field.

The two scenarios differ primarily in their predictions for the behavior in the non Néel-ordered state; in both approaches, the spin-stiffness decreases with doping and vanishes at the critical point, while the spin-wave velocity remains finite at the transition. Thus, in any

event, the main effect of small doping is simply to decrease the bare spin-stiffness of the antiferromagnet. Moreover, the self-consistent analysis mentioned above^{21,87} shows that the holes do not modify the critical properties of a Néel to quantum spin-fluid transition. Thus, the universal scaling functions computed in this paper can be used unchanged to describe this transition in doped antiferromagnets.

A further, important, complication that has to be considered in realistic doped antiferromagnets is the effect of randomness. All cuprate antiferromagnets have randomly placed dopant ions which will perturb the properties of the two-dimensional antiferromagnet. Randomness has been argued to be a relevant perturbation near the pure phase transition of the $O(3)$ sigma model²¹. It thus necessarily changes the universality class of the fixed point and also pushes the transition to smaller doping concentrations. In Appendix A we have presented a phenomenological discussion of the expected scaling properties of the random fixed point.

However, we may conjecture (though we have no strong theoretical arguments for this) that the effects of randomness are important only at low temperatures in the immediate vicinity of the quantum transition. At higher T the dominant effect of doping is solely the change in ρ_s and the properties of the antiferromagnet should be controlled by the pure fixed-point. We will soon see that neglecting randomness at moderate temperatures is consistent with the available experimental data in weakly doped $La_{2-x}Sr_xCuO_4$. Of course, this simple approach will eventually fail at large doping. Crudely, we may take the largest possible x as one where ρ_s would vanish in the absence of randomness. We will estimate from the data that this x to be somewhat larger than 0.04.

An important consequence of the decrease of ρ_s with doping is that x_1 becomes larger at the same T . Hence the crossover between renormalized-classical and quantum-critical behavior occurs at lower T . Consequently, there should be a wider temperature range where our predictions for quantum-critical region should describe experiments better than the renormalized-classical theory.

We now consider separately the experimental data for various observables.

A. Uniform susceptibility

We start with the uniform susceptibility, χ_u^{st} . This quantity has no logarithmic corrections in the renormalized classical region, and is therefore an ideal candidate to test the predictions of the $1/N$ expansion. We consider first the numerical results for χ_u^{st} in the square-lattice $S = 1/2$ antiferromagnet. There have been high-temperature series expansions³², quantum Monte-Carlo³³ and finite-cluster calculations³⁴ of χ_u^{st} . Their results all show that $\chi_u^{\text{st}}(T)$ obeys a Curie-Weiss law at high T , reaches a maximum at $k_B T \sim J$ and then falls down to a finite value at $T = 0$ which is close⁸⁸ to the rotationally averaged $1/S$ result $(\hbar a/g\mu_B)^2 \chi_u^{\text{st}}(T = 0) = (2/3)(0.514/8J) \approx 0.04/J$ (a is the lattice spacing). The data at low T are not accurate enough to make a reliable theoretical fit but at higher T ($0.35J < T < 0.55J$), both series expansions and Monte-Carlo calculations report a linear temperature dependence of χ_u^{st} . The best fit to the Monte-Carlo data gives $(\hbar a/g\mu_B)^2 J \chi_u^{\text{st}} = 0.037x_1(1 + 0.775/x_1)$ (Fig. 7). We compared this behavior with the theoretical prediction for the quantum critical region, which over the range of x_1 values

used in the figure, is well approximated by the large- x_1 formula Eqn (1.24, 3.35,4.13) : $(\hbar a/g\mu_B)^2 J\chi_u^{\text{st}} = 0.037x_1(1 + \alpha/x_1)$ where $\alpha = 0.8 + \mathcal{O}(1/N)$. (We do not know the $1/N$ corrections to α ; we only know that the $1/N$ corrections modify the $1/x_1$ term to $1/x_1^{1/\nu}$.) The agreement between the slopes of the two results is remarkable. On the contrary, the slope for the renormalized classical region, Eqn (5.28), is $0.014x_1$ in clear disagreement with the numerical data at $T > 0.35J$.

We consider next measurements of $\chi_u^{\text{st}}(T)$ in weakly doped $La_{2-x}Sr_xCuO_4$. The interpretation of the experimental data requires caution^{31,89} because one has to subtract Van-Vleck, core and dia- and paramagnetic contributions from valence fermions from the measured $\chi_u^{\text{st}}(T)$. Besides, as we said above, the effects of randomness are clearly important at low T . The subtraction of extra contributions neglecting the effects of randomness was first done by Johnson³¹ who actually estimated the strength of the Van-Vleck contribution by *assuming* that at zero doping, the susceptibility should be the same as in the Monte-Carlo studies of 2D antiferromagnet. Nevertheless, his results for χ_u^{st} clearly show^{31,89} that at small doping concentrations, the susceptibility is linear in T with the slope of $(\hbar a/g\mu_B)^2 J\chi_u^{\text{st}}$ vs. x_1 about 0.043 which is close to our result (0.037). Unfortunately, we cannot definitely conclude from the experimental data whether the linear behavior with universal slope stretches up to lower T as the doping increases, which has to be the case if ρ_s decreases with the doping. We will observe this effect, however, in the data for the spin-lattice relaxation rate. Note also that at higher doping concentrations $x_1 \sim 0.1$, the experimentally measured $\chi_u^{\text{st}}(T)$ vs T flattens⁹⁰. However, at such x_1 , the system is already in the metallic phase, where our approach clearly has to be modified.

B. NMR relaxation rate

The simple Mila-Rice-Shastry model⁹¹ for hyperfine coupling in La_2CuO_4 predicts that the hyperfine coupling constant for ^{63}Cu is finite at the antiferromagnetic ordering momentum (π, π) , where the dynamic susceptibility is peaked. The region around (π, π) thus gives the dominant contribution to ^{63}Cu relaxation and we may use the long-wavelength theory for experimental comparisons. At the same time, the value of the hyperfine coupling constant in the sigma model approach cannot be inferred directly from the Knight shift measurements as in microscopic theories⁹². Instead, we have to integrate out all intermediate scales in the microscopic model for the hyperfine interaction, to obtain the coupling constant between the nuclear spin and the unit vector field in the sigma model. This renormalization is not singular, however, and the fully renormalized coupling, which we label as A_π , should not be very different from the microscopic one.

At very low T (x_1 small), the system is in the renormalized classical region. For $N = 3$, our theoretical result Eqn. (5.35) is the same as in the hydrodynamic theory of Chakravarty *et.al.*¹²

$$\frac{1}{T_1} = \sqrt{\frac{2}{3}} \lambda \frac{A_\pi^2 N_0^2}{\hbar} \frac{\xi}{\hbar c} \left(\frac{k_B T}{2\pi\rho_s} \right)^{3/2}. \quad (7.2)$$

Here λ is the numerical factor which is difficult to calculate analytically. Chakravarty and Orbach²⁷ estimated it to be $\lambda N_0^2 \approx 0.61$ by fitting the scaling forms of Chakravarty *et.al.*¹²

and Tyc *et.al.*¹³ to the numerical simulations on a classical lattice rotor model.

On the other hand, at higher temperatures ($x_1 \geq 1$) we expect the quantum critical theory to work and $1/T_1$ should behave as in Eqn (1.35, 1.36)

$$\frac{1}{T_1} = R_1(\infty) \frac{2A_\pi^2 N_0^2}{\hbar \rho_s} \left(\frac{3k_B T}{2\pi \rho_s} \right)^\eta. \quad (7.3)$$

Comparing these two forms for $1/T_1$, we observe that the predicted spin-lattice relaxation rate rapidly decreases with the temperature at low T , passes through a minimum at $x_1 \sim 1$ and then slightly increases with T . In practice, η is very small for clean systems ($\eta \approx 0.028$ ⁵¹) and therefore $1/T_1$ should be nearly independent on temperature in the quantum-critical region.

We now turn to the data. The spin-lattice relaxation rate for nuclei coupled to the antiferromagnetic order parameter of 2D $S = 1/2$ antiferromagnet was numerically studied in high- T series expansions³² and finite cluster calculations³⁴. In both cases, $1/T_1$ rapidly decreases with increasing T at high temperatures ($T \geq J/2$) and becomes weakly temperature dependent around $T \sim J/2$. In finite-cluster calculations, the subsequent growth of $1/T_1$ at lower temperatures has also been observed. Clearly, this behavior is consistent with our theoretical observations.

Experimental measurements of $1/T_1$ in undoped and weakly doped $La_{2-x}Sr_xCuO_4$ have recently been performed by Imai *et.al.*³⁰ in the temperature range 20 – 900K. For undoped system, the behavior above $T_N = 308K$, but below 700K is well fitted by (7.2) with $A_\pi = (1.33 \pm 10) 10^{-2}K$ and $J = 1590 \pm 140K$ (our estimate for A_π is slightly different from theirs³⁰ because we use the exact prefactor for the correlation length). However, at about 650K, $1/T_1$ flattens and remains practically independent of temperature up to 900K - the largest temperature reported in by Imai *et. al.*³⁰. This is indeed what we expect from $1/T_1$ in the quantum-critical region. Furthermore, the experimental T range over which $1/T_1$ is nearly T independent increases with doping: at $x = 0.04$ it stretches nearly up to 500 K. We interpret this result as an evidence that ρ_s indeed decreases with doping, thus pushing the system into larger x_1 for the same T .

For a quantitative comparison with the data, we need to know the value of $R_1(\infty)$. Direct $1/N$ calculations give $R_1(\infty) = 0.06/N$, which is too small to account for the experimental result for $1/T_1$. However, we already observed in Sec. IV C that $\text{Im}\Phi_{1s}$ calculated to leading order in $1/N$ has peculiar exponential singularities at small frequencies (Eqn. (4.24, 4.25)) which are probably artifacts of the large N expansion. These singularities substantially reduce the slope of $F_1(\bar{\omega})$ at the smallest $\bar{\omega}$ (see Fig. 5). On the other hand, no such low-frequency suppression of $F_1(\bar{\omega})$ was found in numerical studies³⁴ and in the experiments on weakly doped La compounds³⁶. In view of this, it appears reasonable to estimate the value of $R_1(\infty)$ from our result for the scaling function F_1 at slightly larger frequencies. Inspection of the numerical result for F_1 (Fig. 5) shows that $F_1(\bar{\omega})$ is linear in $\bar{\omega}$ for $\bar{\omega}$ between 0.5 and 1, and the slope yields $R_1(\infty) \approx 0.22$. Substituting this result into (7.3) and using the values of A_π and J from the low- T (renormalized-classical) fit, we obtain $1/T_1 = (3.2 \pm 0.5) \times 10^3 \text{sec}^{-1}$; this is in a good agreement with the experimental result $1/T_1 \approx 2.7 \times 10^3 \text{sec}^{-1}$.

C. Correlation length

Detailed measurements of $\xi(T)$ in pure La_2CuO_4 have been performed^{28,35,36} at low T , where the system is in the renormalized classical region. Here Eqn. (5.17) is valid and using (7.1) we obtain

$$\xi(T) \approx 0.50a \exp \left\{ \frac{1.13J}{k_B T} \right\}. \quad (7.4)$$

Chakravarty *et al.*¹² used a different numerical prefactor in (5.17) and a different value for the spin-stiffness constant. The combination of the two yielded nearly the same value of prefactor as in (7.4), but the numerical factor in the exponent was slightly different (0.94 instead of 1.13). This discrepancy is not crucial however, and both Eqn. (7.4) and the analogous expression of Chakravarty *et al.*¹² fit the experimental data between $350K$ and $560K$ rather well. The value of J has been estimated by high-energy neutron scattering measurements of the spin-wave velocity²⁹ to be $J \sim 1560K$. Hence $x_1 \sim T/590K$, and all of the experimentally accessible temperature range is within the renormalized classical region. Nevertheless, we estimated the value of ξ at the highest experimentally accessible temperature $560K$ by using the $N = \infty$ expression for the crossover function X_1 in (3.26); we obtained $\xi^{-1} = 0.023\text{\AA}^{-1}$, which is not far from the experimental value³⁶ of 0.03\AA^{-1} .

At finite doping, we expect that the crossover between the two regimes will occur at smaller temperatures; quantum-critical behavior should therefore be observable at temperatures above and around $500K$. Deep in the quantum-critical region, we expect that ξ behaves as

$$\xi^{-1} = 1.039 \frac{k_B T}{\hbar c a} \left(1 - \frac{\gamma}{x_1} \right), \quad (7.5)$$

where $\gamma \approx 1$. The $1/N$ corrections have been included in the slope but are not known for γ : they also change the subleading term to $x_1^{1/\nu}$. We fitted the data of Keimer *et al.*³⁶ at $x = 0.04$ by this formula and found satisfactory agreement with the data over the temperature range between $300K$ and $550K$. The value of ρ_s extracted from the fit: $2\pi\rho_s \sim 150K \div 300K$, is still positive, but of course is much smaller than at zero doping. Note that Keimer *et al.*³⁶, used a phenomenological form for $\xi^{-1}(T)$ which combined the renormalized-classical result at zero-doping and temperature-independent correction due to finite doping; this form agreed well with the experimental data for doping concentrations $x = 0 \div 0.04$, but the theoretical arguments behind it are unclear to us.

We also compared our results for the quantum-critical region with the numerical data for ξ in a pure 2D $S = 1/2$ Heisenberg antiferromagnet^{33,93,94}. Numerical simulations were performed up to temperatures of about $4J$; if quantum-critical behavior for ξ is present in the Heisenberg antiferromagnet in some temperature range, it should have been detected. It turns out, however, that up to $k_B T \sim J$, numerical data are well fitted by the renormalized classical theory, although the best fit³³ gives the value for the prefactor which is nearly half of that in (7.4). On the other hand, for $0.4J < k_B T < 0.6J$ (where $1/T_1$ levels off to a constant value), our pure quantum-critical result for ξ is close to the numerical one^{33,93}. The interpretation of the numerical data at higher T requires caution as these data at $k_B T > 0.6J$

are equally well fitted by the quantum-critical result $\xi^{-1} \propto x_1(1 - \gamma x_1)$ where γ is close to one⁹⁵. However, the prefactor in the fit is nearly twice as that in (7.5). We argue in a separate publication⁹⁶ that these discrepancies in the fit to the quantum-critical theory are chiefly due to nonuniversal corrections $\sim T/J$ which cannot be neglected above $0.6J$.

Separate Monte-Carlo calculations of the correlation length precisely at $\rho_s = 0$ have been performed by Manousakis and Salvador⁹⁴. They simulated the quantum $O(3)$ sigma model directly, rather than the spin-1/2 antiferromagnet. Their results yielded the value of the universal function $X_1(\infty) = 1.25$ which is not far from the result of Chakravarty *et. al.*¹², or our result in (7.5): $X_1(\infty) = 1.04$.

D. Equal-time structure factor

There are, to our knowledge, only few data available on $S(k)$. The behavior of $S(k)$ vs $k\xi$ in a 2D antiferromagnet was studied by a Quantum Monte-Carlo by Makivic and Jarrell⁹⁷. They fitted their data at $k_B T = 0.35J \div 0.42J$ by the renormalized-classical scaling formula of Chakravarty *et. al.*¹². We present another interpretation for the data. The key point is that at $k_B T = 0.42J$, the correlation length is about $5.7a$ and the magnon energy is therefore $\hbar ck/k_B T \sim 0.7(k\xi)$. We see that it becomes larger than $k_B T$ already at $k\xi \approx 1.5$, and the use of the classical description at larger k is hardly justified. We rather have to use the full quantum expression for $S(k)$ to fit the data. Clearly, at $k_B T \sim 0.4J$, the Josephson correlation length is not very different from ξ , that is at $\hbar ck > k_B T$ the system should be in the quantum-critical regime. However, we found above that the $1/N$ corrections to $S(k)$ in this regime are very small, even for $N = 3$, and for experimental comparisons we may well use the scaling function for $S(k)$ computed at $N = \infty$. For $k_B T = 0.42J$, we have the following theoretical prediction, valid in both the quantum-critical and renormalized-classical regions, from (1.28) and (3.30)

$$S(k) = \bar{S} \frac{\coth[\alpha\sqrt{1 + (k\xi)^2}]}{\sqrt{1 + (k\xi)^2}}, \quad (7.6)$$

where $\alpha = \hbar c/2k_B T\xi \sim 0.35$ and $\bar{S} = (N_0^2/\rho_s)(\hbar c\xi/2a^2) \approx 2.48$. We fitted the Monte-Carlo data by (7.6), using the overall factor \bar{S} as the only adjustable parameter; we found very good agreement with the simulations not only for $\hbar ck > k_B T$, but for all k (Fig. 8). However, the value of \bar{S} in the fit is $\bar{S} = 3.61$, which is somewhat larger than our $N = \infty$ result of 2.48. As yet, we have no explanation for the discrepancy, and therefore cannot judge from the data whether at intermediate k the system is in the quantum-critical or in the Goldstone regime ($S(k)$ in the quantum-critical regime is very close to the $N = \infty$ result, while in the Goldstone regime, $S(k)$ chiefly differs from its value at $N = \infty$ by the factor $(N - 2)/N = 2/3$). At the same time, the good agreement we found in the momentum dependence of $S(k)$ is clearly consistent with our conjecture that at $k_B T \sim 0.4J$, the antiferromagnet is very near the crossover between renormalized-classical and quantum-critical regimes.

Experimental data for energy-integrated $S(k)$ are available³⁶ for pure La_2CuO_4 . Clearly, the experimental temperature dependence for the correlation length was inferred from these data. The experiments³⁶ were performed in the temperature range of $T < 560K$, where

$x_1 < 1$. The momentum dependence of $S(k)$ was reported to be well described by a simple Lorentzian $S(k) = S(0)/(1+(k\xi)^2)$, and the temperature dependence of $S(0)$ agreed with the renormalized-classical result $S(0) \propto T^2\xi^2$. The absolute value of $S(0)$ was not determined in the experiments, so we cannot compare the experimental result at highest accessible temperature with the theoretical expression in the quantum-critical region, as we did for the correlation length. The data on $S(0)$ at finite doping have not been reported, to the best of our knowledge.

E. Local susceptibility

Finally, we consider the experimental data on the momentum-integrated dynamical susceptibility $\text{Im}\chi_L(\omega) = \int d^2k \text{Im}\chi_s(k, \omega)$. Extensive experimental measurements were done^{35,36} for $La_{1.96}Sr_{0.04}CuO_4$ in a frequency range $\omega = 2 \div 45\text{mev}$ and for temperatures $10 < k_B T < 500K$. They showed that the experimental data at all values of ω and $k_B T$, obeyed the following functional form to reasonable accuracy

$$\text{Im}\chi_L(\omega) = I(|\omega|)F(\omega/T). \quad (7.7)$$

This form is in agreement with the theoretical scaling form (1.31, 1.32) for clean systems, or (A10, A19) from Appendix A for random systems; further, we arrive at the theoretical prediction that $I \sim |\omega|^\mu$. The exponent $\mu = \eta > 0$ in clean systems, while we expect $\mu < 0$ in random systems^{3,21}. Experimentally, it was found that I was approximately ω independent at the larger frequencies; this is consistent with our results for the clean antiferromagnet in which $\mu = \eta$ is very small. At smaller frequencies, I showed significant frequency dependence which could be well fit by an exponent $\mu = -0.41 \pm 0.05$. Such a behavior is clear evidence of the importance of randomness at low frequencies and low temperatures²¹. Note also that the scaling plot to test the ω/T dependence of the function F shows rather good collapse of the data for a wide range of values of ω/T ^{35,36}, thus giving strong evidence of the presence of quantum-criticality. The universal scaling functions at the pure and random fixed points probably have a rather similar shape, and thus the presence of disorder does not effect the scaling plot very much. It is only the exponent μ which is particularly sensitive to disorder.

We emphasize, then, that this experimental data clearly shows the presence of quantum-criticality and suggests that the effects of randomness are important only at low energies; at high enough ω or $k_B T$ one can successfully fit the data at $x = 0.04$ by the quantum-critical theory for a clean antiferromagnet.

VIII. CONCLUSIONS

We conclude the paper by recalling some highlights of our results.

We have presented the general theory of clean, two-dimensional, quantum Heisenberg antiferromagnets which are close to the zero-temperature quantum transition between ground states with and without long-range Néel order. While some of our discussion was more general, the bulk of our theory was restricted to antiferromagnets in which the Néel order is described by a 3-vector order parameter. For Néel-ordered states, ‘nearly-critical’ means

that the ground state spin-stiffness, ρ_s , satisfies $\rho_s \ll J$, where J is the nearest-neighbor exchange constant, while ‘nearly-critical’ quantum-disordered ground states have an energy-gap, Δ , towards excitations with spin-1, which satisfies $\Delta \ll J$. The allowed temperatures, T , are also smaller than J , but *no* restrictions are placed on the values of $k_B T/\rho_s$ or $k_B T/\Delta$.

Our results followed from some very general properties of the $T = 0$ quantum fixed point separating the magnetically-ordered and quantum-disordered phases. These properties are expected to be valid in both undoped and doped antiferromagnets, though not in the presence of randomness. They are (i) the spin-wave velocity, c , is non-singular at the fixed-point (i.e., the dynamical critical exponent $z = 1$); for the case of a vector order parameter this implies that the critical field-theory has the Lorentz invariance of 2+1 dimensions; (ii) on the ordered side of the transition, there is a Josephson correlation length, ξ_J , related to the $T = 0$ spin stiffness ρ_s by the hypothesis of ‘two-scale factor’ universality which implies that $\rho_s = \hbar c \Upsilon/\xi_J$, where the number Υ is dimensionless and universal; (iii) turning on a finite temperature places the critical field theory in a slab geometry which is infinite in the two spatial directions, but of finite length, $L_\tau = \hbar c/(k_B T)$, in the imaginary time (τ) direction. The consequences of a finite T can therefore be deduced by the principles of finite-size scaling.

Under these circumstances, we showed that the wavevector/frequency-dependent uniform and staggered spin susceptibilities, and the specific heat, are completely universal functions of just three thermodynamic parameters. On the ordered side, these three parameters are ρ_s , the $T = 0$ spin-wave velocity c , and the ground state staggered moment N_0 ; previous works have noted the universal dependence of the susceptibilities on these three parameters only in the more restricted regime of $k_B T \ll \rho_s$. On the disordered side the three thermodynamic parameters are Δ , c , and the spin-1 quasiparticle residue \mathcal{A} .

We have calculated the universal scaling functions by a $1/N$ expansion on the $O(N)$ quantum non-linear sigma model, and by Monte Carlo simulations. For ρ_s finite, these scaling functions demonstrate the crossover behavior between the renormalized classical regime, when thermal fluctuations are dominant, to the quantum-critical regime, where the dynamics is governed by the renormalization group flows near the $T = 0$ quantum fixed point. For small $k_B T/\rho_s$, the T -dependence of our results was similar to those already obtained by Chakravarty *et al*¹². For large $k_B T/\rho_s$, most of our results were new. We found that the crossover between the renormalized-classical and quantum-critical regimes occurs at $x_1 \sim 1$, where $x_1 = N k_B T/2\pi\rho_s$. In a square lattice, $S = 1/2$ Heisenberg antiferromagnet, $2\pi\rho_s \approx 1.13J$, and quantum-critical behavior therefore should be seen at $k_B T \geq 0.4J$. We compared our quantum-critical results with a number of numerical simulations and experiments on undoped and lightly-doped $La_{2-\delta}Sr_\delta CuO_4$ in the intermediate temperature range, and found good agreement with the data, particularly for uniform susceptibility, NMR relaxation rate and equal-time structure factor. It appears, therefore, that the use of a ‘small’ ρ_s point-of-view is quite reasonable even for a pure square lattice, $S = 1/2$ Heisenberg antiferromagnet - while ordered at $T = 0$, this system is evidently close to the point where long-range order vanishes. A small ρ_s approach also appears to be appropriate for lightly-doped antiferromagnets.

ACKNOWLEDGMENTS

This research was supported by NSF Grants No. DMR-8857228 and DMR-9224290, and by a fellowship from the A.P. Sloan Foundation. We are pleased to thank R. Birgeneau, S. Chakravarty, D. Fisher, E. Fradkin, P. Hasenfratz, T. Imai, B. Keimer, M. Makivic, E. Manousakis, A. Millis, H. Monien, A. Ramirez, N. Read, A. Sokol and R. Shankar for useful discussions and communications.

APPENDIX A: RANDOM ANTIFERROMAGNETS AND ANISOTROPIC SCALING

This appendix will present a brief discussion of the extension of the results of this paper to the case of random antiferromagnets. We will restrict our attention to systems in which the randomness preserves the Heisenberg spin symmetry *i.e.* antiferromagnets with random exchange constants J_{ij} .

Random impurities induce perturbations on the clean system which are uncorrelated in the spatial directions but fully correlated along the imaginary time direction. This has the immediate consequence of breaking the long-distance Lorentz invariance of the pure system. It therefore becomes necessary to allow for anisotropic scaling in space-time at the quantum fixed point. It is conventional to introduce a dynamic scaling exponent z such that characteristic frequencies, ω , scale with the characteristic wavevector k as

$$\omega \sim k^z \tag{A1}$$

in the critical region.

It is important to distinguish to two distinct classes of magnetically ordered phases that can occur in random antiferromagnets: these are (*i*) Néel ordered and (*ii*) spin-glass ground states. In the first of these the ordering moment has a definite orientation on each of the lattice sites. In the spin-glass, there is a long-lived moment on each site, but its orientation is random. We will consider the properties of the transition of these two magnetically-ordered states to a spin-fluid in turn:

1. Néel order

We present here some phenomenological scaling ansatzes for the quantum phase transition from a Néel ordered state to a spin-fluid in a random antiferromagnet. The scaling arguments are similar to those employed for the superfluid to bose-glass transition by Fisher *et. al.*⁹⁸, although they did not discuss the issue of universal amplitudes. We will restrict our attention to the magnetically-ordered side $g < g_c$. The magnetically disordered side is expected to be gapless⁹⁹ and its properties will not be discussed here. We also note that little explicit reference to randomness will be made here, its main role being the introduction of a $z \neq 1$. The results should therefore also be applicable to other quantum phase transitions in *clean* systems which have $z \neq 1$ and are below their upper critical dimensions.

We also assume below that the antiferromagnet is below its upper critical dimension and hyperscaling is valid.

As in clean systems, we expect that $T = 0$ ordered state is characterized by a Josephson length scale, ξ_J , separating the Goldstone and critical regions. As g approaches g_c , this scale must diverge as

$$\xi_J \sim (g_c - g)^{-\nu}. \quad (\text{A2})$$

At scales larger than ξ_J , the system should exhibit conventional Goldstone fluctuations with a well defined spin-wave velocity, c . However, because $z \neq 1$, the spin-wave velocity should exhibit non-trivial critical behavior as g approaches g_c :

$$c \sim (g_c - g)^{\nu(z-1)}. \quad (\text{A3})$$

The ground state is also characterized by an average ordered moment N_0 which vanishes as

$$N_0 \sim (g_c - g)^\beta, \quad (\text{A4})$$

and a spin-stiffness ρ_s which satisfies⁹⁸

$$\rho_s \sim (g_c - g)^{\nu(d+z-2)}, \quad (\text{A5})$$

where d is the spatial dimensionality. The exponent identity

$$2\beta = (d + z - 2 + \eta)\nu \quad (\text{A6})$$

generalizes (1.11) and will be useful to us below.

In the main part of the paper we showed that the three properties N_0 , ρ_s , and c , of the $T = 0$ state, completely determine the entire finite temperature form of the susceptibilities and the specific heat in clean antiferromagnets. We argue below that, remarkably, this continues to be true even in random antiferromagnets which have $z \neq 1$. The value of c helps determined the appropriate scaling between space and time even though c itself has non-trivial critical behavior.

The following discussion will specialize explicitly to the case of $d = 2$, although the generalization to arbitrary d is quite straightforward. We will also assume that $z < 2$, otherwise, the universality in the spectrum near the critical point will be broken by the higher order analytic terms in an expansion in k . As before, we will use units in which $\hbar = k_B = 1$. Of course, we are no longer free to set $c = 1$!

The application of finite-size scaling to quantum systems requires that one determine two length scales characterizing the effects of (i) the deviations from criticality, and (ii) the temperature, and write down universal functions of their ratio. The length scale characterizing deviations from criticality is clearly ξ_J . In clean systems, the length scale ξ_T characterizing the effect of a finite T was given by $\xi_T = c/T$. Scaling suggests that in systems with $z \neq 1$ we should have $\xi_T \sim T^{-1/z}$. The scaling functions will now depend on the ratio ξ_J/ξ_T . Using (A2) we see that this ratio is measured by the value of $(g_c - g)^{\nu z}/T$. However from (A5) this is the same (in $d = 2$) as ρ_s/T . Moreover, since this ratio also has engineering dimension 0, there are *no* non-universal metric factors that can appear. Thus as in clean systems, the

scaling functions will have a universal dependence upon ρ_s/T . For similar reasons, they can also depend only on ω/T .

It remains to consider the wavevector dependence of the scaling functions. By scaling, this must appear in the combination $q\xi_T \sim q/T^{1/z}$. Let us now try and determine the metric factor in front of this combination. There are two basic rules: (i) the metric factor should involve combinations of observables whose scaling dimension is 0; and (ii) the entire combination which appears in the argument of the scaling function should have engineering dimension 0. Once these rules are satisfied, one is guaranteed, by the principles of scaling, that no non-universal pre-factors remain. A little experimentation shows that the following satisfies these criteria:

$$\xi_T = \frac{c}{T} \left(\frac{T}{\rho_s} \right)^{1-1/z}. \quad (\text{A7})$$

We now have enough information to use the same steps as were used in Section II and obtain universal scaling functions of the observables. We will omit most of the intermediate steps here and go directly to the results.

Consider first the susceptibility measuring fluctuations of the order parameter, χ_s . We find

$$\chi_s(k, \omega) = \frac{N_0^2}{\rho_s} \left(\frac{c}{T} \right)^2 \left(\frac{T}{\rho_s} \right)^{2+(\eta-2)/z} \Phi_{1s} \left(\frac{ck}{T} \left(\frac{T}{\rho_s} \right)^{1-1/z}, \frac{\omega}{T}, \frac{T}{\rho_s} \right), \quad (\text{A8})$$

where Φ_{1s} is a completely universal function and there are no non-universal metric factors. We have chosen the prefactors to satisfy the convention that scaling functions should remain finite as g approaches g_c . One can verify from (A3), (A5) and (A6) that the pre-factor of the scaling function, and the coefficient of $q/T^{1/z}$ are non-singular as g approaches g_c . The scaling results for all the observables dependent upon χ_s can now be obtained in a manner similar to that used for clean antiferromagnets. We will display explicit expressions for only two of them: the correlation length ξ satisfies

$$\xi^{-1} = \frac{c}{T} \left(\frac{T}{\rho_s} \right)^{1-1/z} X_1 \left(\frac{T}{\rho_s} \right), \quad (\text{A9})$$

while the local susceptibility $\text{Im}\chi_L$ is given by

$$\text{Im}\chi_L(\omega) = \frac{N_0^2}{\rho_s} \left(\frac{T}{\rho_s} \right)^{\eta/z} F_1 \left(\frac{\omega}{T}, \frac{T}{\rho_s} \right). \quad (\text{A10})$$

Again X_1 and F_1 are completely universal functions chosen such that $X_1(\infty)$ and $F_1(\bar{\omega}, \infty)$ are finite.

The properties of the uniform susceptibility and the specific heat follow from an understanding of the hyperscaling properties of the free energy density, \mathcal{F} . A simple generalization of the arguments of Privman and Fisher⁵⁷ to anisotropic systems yields (in $d = 2$)

$$\mathcal{F} = \mathcal{F}_0 + T\xi_T^{-2}\varphi\left(\frac{T}{\rho_s}\right), \quad (\text{A11})$$

where \mathcal{F}_0 is the ground state energy, and φ is a universal function. As in Section II the following results for static uniform susceptibility χ_u^{st} and the specific heat C_V now follow

$$\begin{aligned} \chi_u^{\text{st}} &= (g\mu_B)^2 \frac{T}{c^2} \left(\frac{T}{\rho_s}\right)^{-2+2/z} \Omega_1\left(\frac{T}{\rho_s}\right), \\ C_V &= \frac{T^2}{c^2} \left(\frac{T}{\rho_s}\right)^{-2+2/z} \Psi_1\left(\frac{T}{\rho_s}\right), \end{aligned} \quad (\text{A12})$$

where Ω_1, Ψ_1 are universal functions, with $\Omega_1(\infty), \Psi_1(\infty)$ finite. Note, in particular, that the Wilson ratio, W , (Eqn. (1.25)) continues to remain a fully universal function of T/ρ_s , and has a universal value at $g = g_c$. The universality of the Wilson ratio, even in the presence of anomalous powers in χ_u^{st} and C_V , was also noted recently (using very different arguments) in the boundary critical theory of overscreened Kondo fixed points¹⁰⁰.

2. Spin-glass order

We now consider the properties of a quantum transition from a spin-glass ground state to a spin fluid. Clearly many of the properties discussed in the previous section are special to Néel ordered states and do not generalize. However measurements which are spatially local do have similar critical properties. As we do not wish to discuss the nature of the spin-glass state itself, we will restrict ourselves here to behavior in the quantum-critical region where $T \gg (g_c - g)^{z\nu}$.

A very useful measure of the local spin correlations is provided by the local spin susceptibility, $\chi_L(\omega)$ defined in (1.16). Along the imaginary frequency axis, this local susceptibility is given at the Matsubara frequencies ω_n by

$$\begin{aligned} \chi_L(i\omega_n) &= \int_0^{1/T} d\tau e^{i\omega_n\tau} C(\tau), \\ C(\tau) &= \overline{\langle \mathbf{S}_i(0) \cdot \mathbf{S}_i(\tau) \rangle}, \end{aligned} \quad (\text{A13})$$

where the bar represents an average over all the sites i . The function $C(\tau)$ can be used to distinguish the spin-glass and spin-fluid states. In the spin-fluid state $C(\tau)$ will decay to zero for large τ , will in the $T = 0$ spin-glass phase¹⁰¹ we must have

$$\lim_{\tau \rightarrow \infty} C(\tau) = q_{EA} > 0, \quad (\text{A14})$$

with q_{EA} the Edwards-Anderson order-parameter. It is conventional to define the order-parameter exponent β by the behavior of q_{EA} as g approaches g_c :

$$q_{EA} \sim (g_c - g)^\beta. \quad (\text{A15})$$

The value of q_{EA} thus fixes the behavior of $C(\tau)$ at infinite time. We can obtain the behavior of $C(\tau)$ for finite times τ by a simple application of the dynamic scaling hypothesis. We expect at $T = 0$ that

$$C(\tau) = (g_c - g)^\beta h_1(\tau |g - g_c|^{z\nu}) ; \quad T = 0, \quad (\text{A16})$$

where h_1 is a scaling function and z is the dynamic scaling exponent. Clearly we must have $h_1(x \rightarrow \infty)$ be a finite non-singular constant to satisfy (A14) and (A15). For $\tau \ll (g_c - g)^{-z\nu}$, standard critical phenomena lore requires that $C(\tau)$ become independent of $g_c - g$. This is only possible if $h_1(x) \sim x^{-\beta/z\nu}$ for small x . Putting this together with (A16) we can determine the behavior of $C(\tau)$ at $T = 0$ and $g = g_c$

$$C(\tau) \sim \frac{1}{\tau^{\beta/(z\nu)}} ; \quad T = 0, \quad \tau \ll (g_c - g)^{-z\nu}. \quad (\text{A17})$$

We can now use finite-size scaling to determine the behavior of $C(\tau)$ at finite T

$$C(\tau) = \frac{1}{\tau^{\beta/(z\nu)}} h_2(T\tau) ; \quad T^{-1}, \tau \ll (g_c - g)^{-z\nu}, \quad (\text{A18})$$

where h_2 is yet another scaling function. Finally we use (A13), to determine $\chi_L(i\omega_n)$. In general we may find that the fourier transform is dominated by non-universal contributions at short times. However, upon analytically continuing to real frequencies, we expect all these non-universal contributions to affect only the real part of χ_L , while the imaginary part is dominated by the universal long-time behavior. We therefore obtain the following generalization of (A10) to systems with spin-glass order

$$\text{Im}\chi_L(\omega) = |\omega|^\mu F_1\left(\frac{\omega}{T}\right) ; \quad T, \omega \gg (g_c - g)^{z\nu}, \quad (\text{A19})$$

where

$$\mu = -1 + \frac{\beta}{z\nu}, \quad (\text{A20})$$

and F_1 is a universal scaling function with a single non-universal overall scale. For small argument, we have $F_1(\bar{\omega}) \sim \text{sgn}(\omega)|\omega|^{1-\mu}$, while $F_1(\bar{\omega} \rightarrow \infty)$ is finite and non-singular.

In addition to the local susceptibility, the thermodynamic properties of the quantum phase transition which can be deduced from the hyperscaling properties of the free energy, are very similar in the spin-glass and the Néel ordered systems. In particular, we expect the following temperature dependence of χ_u^{st} and C_V in the quantum-critical region ($T \gg (g_c - g)^{z\nu}$ of the spin-glass to spin-fluid transition:

$$\begin{aligned} \chi_u^{\text{st}} &\sim T^{-1+d/z}, \\ C_V &\sim T^{d/z}. \end{aligned} \quad (\text{A21})$$

It follows then that the Wilson ratio W (Eqn. (1.25)) is a universal number at $g = g_c$.

APPENDIX B: BERRY PHASES AND DANGEROUSLY IRRELEVANT COUPLINGS

We have assumed in this paper that the $O(3)$ sigma model is sufficient to determine the quantum-critical scaling functions of quantum antiferromagnets. A key step in this assumption is that the Berry phases present in the antiferromagnet can be neglected. This

assumption is based on the following circumstantial evidence. After some rather involved calculations, which have been discussed at length elsewhere^{15,102}, it was shown that the primary effect of the Berry phases was to induce spin-Peierls ordering in the quantum-disordered phase of non-even-integer-spin antiferromagnets. This was shown in the context of large M calculations for $SU(M)$ antiferromagnets. Further, a key feature of this calculation was the appearance of two well-separated length scales which characterized the fully-gapped spin-fluid phase. The first of these scales was the two-spin correlation length ξ which determined the exponential decay of the equal-time spin-spin correlation function. The second was ξ_{SP} the length at which Berry phases first became effective in inducing spin-Peierls ordering. In the large M limit these two were found to be related by

$$\xi_{SP} \sim \xi^{4M\rho_1}, \quad (\text{B1})$$

where $\rho_1 = 0.062296 + \mathcal{O}(1/M)$. It is clear that for sufficiently large M (which is the only region in which we know how to perform these calculations) we have $\xi_{SP} \gg \xi$.

It was then pointed out to us by Daniel Fisher¹⁰³ that the appearance of two length-scales at a second-order phase transition, one of which is a power of the other, is a characteristic property of systems with dangerously irrelevant couplings. A dangerously irrelevant coupling is defined as one which is irrelevant at the critical fixed point separating the two phases, but is relevant at the fixed point which controls the nature of the phase one is studying. Crudely speaking, the coupling decays to a very small value at the first length scale while the system is controlled by the critical fixed point, but grows again to a value of order unity at the second, larger, length scale.

For the antiferromagnet, our assumptions then, are the following. We assume that the dangerous-irrelevancy of the Berry phase effects, found in the $SU(M)$ models, survives in the $O(3)$ sigma model. The coupling to the Berry phase terms in the action decays to a negligibly small value after renormalizing out to a scale of order $\max(c/T, c/\Delta)$. At scales larger than this, the coupling grows again, as the renormalization group flows are now in the vicinity of the strong-coupling fixed point controlling the quantum-disordered phase. However, this coupling significantly modifies only those correlation functions which are directly sensitive to the presence of spin-Peierls ordering. For all other spin-correlations (which includes all we have considered in this paper) the Berry phases can be neglected in determining the leading quantum-critical behavior.

To clarify this issue, we now present a pedagogical discussion of a simple statistical mechanical model with a dangerously irrelevant coupling. Unlike the quantum antiferromagnet, the overall structure of the renormalization group flows is well-understood in this model.

We consider the finite temperature properties of a classical, XY model on a cubic lattice. At each site we introduce a four-fold anisotropy field h_4 , which we will find is dangerously irrelevant. The model is described by the partition function Z

$$Z = \int \mathcal{D}\theta e^S, \quad (\text{B2})$$

$$S = \frac{1}{T} \sum_{\langle ij \rangle} \cos(\theta_i - \theta_j) + \sum_i h_4 \cos(4\theta_i),$$

where the sites i, j lie on a 3-dimensional cubic lattice. This model will have a phase transition at some $T = T_c$ from a high temperature paramagnetic phase to a low temperature ordered phase. It is well known that the four-fold anisotropy h_4 is irrelevant near $T = T_c$ and the phase transition is therefore in the universality class of the pure three dimensional XY model. However, it is also clear that the field h_4 surely cannot be neglected in the ordered phase. It breaks the $O(2)$ symmetry of the XY model, and must therefore destroy the Goldstone modes. Further, the common mean orientation at each site must be one of $\theta = 0, \pi/2, \pi, 3\pi/2$ and cannot be arbitrary as in the XY model. The apparently conflicting properties of the critical point and the ordered phase are reconciled by the concept of a dangerously irrelevant coupling.

Let us examine the structure of the renormalization group flows of this model for T close to T_c : we measure the deviation from criticality by the reduced temperature variable

$$t = \frac{T_c - T}{T}. \quad (\text{B3})$$

A schematic of the renormalization group flows projected onto the T, h_4 plane are shown in Fig. 9. The critical fixed point is at $t = 0$ and $h_4 = 0$. The initial growth of t away from this fixed point is given by

$$t(\ell) = te^{\ell/\nu}, \quad (\text{B4})$$

where $0 < t \ll 1$, e^ℓ is the length rescaling factor, and ν is the usual thermal critical exponent. The field h_4 is irrelevant at this critical point and will therefore decay exponentially

$$h_4(\ell) = h_4 e^{-\omega\ell/\nu}, \quad (\text{B5})$$

where h_4 is of order unity, ω is the crossover exponent associated with h_4 at the critical fixed point. The system will emerge from the critical region at the Josephson length scale ξ_J where $t(\ell = \ell_1^*) \approx 1$. From (B4) we see that

$$\xi_J = e^{\ell_1^*} = t^{-\nu}. \quad (\text{B6})$$

For $\ell > \ell_1^*$, the flow of h_4 will now be controlled by the $T = 0$ fixed point. Let us assume that h_4 is relevant at the $T = 0$ fixed point with eigenvalue $\phi > 0$ (the value of ϕ will be determined later). Then we have

$$\begin{aligned} h_4(\ell > \ell_1^*) &\approx h_4(\ell_1^*) e^{\phi(\ell - \ell_1^*)} \\ &= h_4 e^{-(\omega/\nu + \phi)\ell_1^* + \phi\ell}. \end{aligned} \quad (\text{B7})$$

Thus h_4 will return to a value of order unity when the argument of the exponent is zero. This defines a second length scale $\xi_4 = e^{\ell_2^*}$ where

$$\ell_2^* = \left(1 + \frac{\omega}{\phi\nu}\right) \ell_1^*. \quad (\text{B8})$$

The effects of the h_4 field thus become important at length scales of order ξ_4 : this is the scale at which the Goldstone modes are destroyed, and the condensate gets locked at one of $\theta = 0, \pi/2, \pi, 3\pi/2$. The scale ξ_4 is related to ξ_J by

$$\xi_4 = \xi_J^{1+\omega/(\phi\nu)}. \quad (\text{B9})$$

Additional insight can be gained by considering the scaling form for the transverse susceptibility near the transition. Assume the condensate points at $\theta = 0$. Then the transverse susceptibility satisfies the scaling form

$$\langle |\theta(k)|^2 \rangle = \frac{N_0^2}{\rho_s} \xi_J^2 \varphi(k\xi_J, c_1 h_4 \xi_J^{-\omega/\nu}), \quad (\text{B10})$$

where k is the wavevector, φ is a universal function, and c_1 is the only non-universal metric factor. For most values of $k\xi_J$ the term proportional to h_4 can be treated as a small perturbation which makes a subdominant correction to the leading critical behavior. Only at extremely small values of $k\xi_J$ does the h_4 term become important. Matching to the expected form of the incipient Goldstone modes, we should have

$$\varphi(\bar{k}, \bar{h}) = \frac{1}{\bar{k}^2 + \bar{h}}; \quad \bar{k} \ll 1. \quad (\text{B11})$$

Thus the \bar{h} term is significant for all $\bar{k} < \bar{h}^{1/2}$ or for

$$k^{-1} > \xi_4 \sim \xi_J^{1+\omega/(2\nu)}. \quad (\text{B12})$$

Comparing with (B9) we see that $\phi = 2$. The key point, of course, is that $\xi_4 \gg \xi_J$. In particular, the crossover from critical to Goldstone fluctuations occurs at a scale of order ξ_J and is described by the scaling function of the pure XY model $\varphi(\bar{k}, 0)$. Only at much larger scales does it become necessary to include the effects of the h_4 field.

APPENDIX C: MONTE CARLO EVALUATION OF QUANTUM-CRITICAL UNIFORM SUSCEPTIBILITY

It was shown in Section I that the high temperature behavior of the uniform, static spin susceptibility is given by (see (1.24))

$$\chi_u^{\text{st}}(T) = \left(\frac{g\mu_B}{\hbar c} \right)^2 k_B T \Omega_1(\infty). \quad (\text{C1})$$

The universal number $\Omega_1(\infty)$ has been evaluated so far in a $1/N$ expansion with the result (4.13). In this appendix we will describe a determination of $\Omega_1(\infty)$ at $N = 3$ by Monte Carlo simulations.

The quantum $O(3)$ non-linear sigma model is expected to be in the same universality class as the classical, Heisenberg ferromagnet on a cubic lattice. Our simulations were therefore performed at the critical point of this latter model. We considered the ensemble defined by the following partition function

$$Z = \int \prod_i d\mathbf{S}_i e^{-\mathcal{H}},$$

$$\mathcal{H} = -K \sum_{\langle ij \rangle} \mathbf{S}_i \cdot \mathbf{S}_j, \quad (\text{C2})$$

where i, j extend over the sites of a cubic lattice, and $\mathbf{S}_i = (S_{x,i}, S_{y,i}, S_{z,i})$ is a 3-component vector of unit length. We used a lattice with $L \times L \times L_\tau$ sites, with periodic boundary conditions in all three directions. The Wolff single-cluster algorithm¹⁰⁴ was used to sample the states. This simulation was carried out at the critical value $K = K_c$ at which this model has a second-order phase transition. The value of K_c is known very accurately from recent high precision Monte Carlo simulations⁵¹:

$$K_c = 0.6930. \quad (\text{C3})$$

It has been argued that χ_u^{st} is related to the stiffness, ρ_τ , of this system to twists along the τ direction. Upon examining the response of \mathcal{H} to a field that generates rotations in the $x - y$ plane, we obtain the following expression for ρ_τ

$$\rho_\tau = \frac{1}{L^2 L_\tau} \left\langle \sum_i K (S_{x,i} S_{x,i+\hat{\tau}} + S_{y,i} S_{y,i+\hat{\tau}}) - \left[\sum_i K (S_{x,i} S_{y,i+\hat{\tau}} - S_{y,i} S_{x,i+\hat{\tau}}) \right]^2 \right\rangle, \quad (\text{C4})$$

where the expectation value is to be evaluated in the ensemble defined by Z . Finally, the universal number $\Omega_1(\infty)$ is defined by

$$\Omega_1(\infty) = \lim_{L_\tau \rightarrow \infty} \left[\left(\lim_{L \rightarrow \infty} L_\tau \rho_\tau |_{K=K_c} \right) \right]. \quad (\text{C5})$$

It is crucial that the $L \rightarrow \infty$ limit be taken first, to model a quantum system which is infinite in the spatial directions. The subsequent $L_\tau \rightarrow \infty$ places the quantum system at zero temperature.

The results of our simulations are contained in Table I. Three independent simulations of 70000, 70000, and 210000, flips per spins were performed in systems upto $L = 30$ and $L_\tau = 10$. A polynomial extrapolation to $L = \infty$ at L_τ fixed yielded the results shown in the last column of Table I. Finally, a second polynomial extrapolation to $L_\tau = \infty$ was performed to yield the following estimate for $\Omega_1(\infty)$

$$\Omega_1(\infty) = 0.25 \pm 0.04. \quad (\text{C6})$$

APPENDIX D: COMPUTATIONS IN THE NÉEL STATE AT $T = 0$

In this Appendix, we derive the expressions for the $T = 0$ sublattice magnetization N_0 , and the spin-stiffness ρ_s to order $1/N$. These results will be used in the derivations of the universal scaling functions for the uniform and staggered susceptibilities in both the quantum-critical and renormalized classical regions. As in Sec III, our starting point is the functional integral for the $O(N)$ sigma model. At zero temperature, the spin rotation

symmetry is broken and the perturbative $1/N$ expansion has to be modified to account for the nonzero expectation value of the order parameter. This $1/N$ expansion has been developed by Brezin and Zinn-Justin⁷³ and we use some of their results. We first represent the unit vector field as

$$\vec{n} = \vec{\sigma}_0 + \vec{\pi}, \quad (\text{D1})$$

where $\langle \vec{\sigma}_0 \rangle$ is finite and $\vec{\sigma}_0 \cdot \vec{\pi} = 0$. The sublattice magnetization N_0 in spin- S antiferromagnet is expressed as $N_0 = \tilde{S} \langle \sigma_0 \rangle$, where $\tilde{S} = SZ_S$. The renormalization factor Z_S accounts for the order parameter fluctuations at short (lattice) scales which have to be integrated out in the mapping to sigma model from the original spin Hamiltonian on the lattice. Upon substituting (D1) into (3.1), the functional integral becomes

$$Z = \int \mathcal{D}\sigma_0 \mathcal{D}\pi_l \delta(\sigma_0^2 + \pi_l^2 - 1) \exp \left(-\frac{\rho_s^0}{2\hbar} \int d^2r \int_0^\infty d\tau \left[(\nabla_r \sigma_0)^2 + (\nabla_r \pi_l)^2 + \frac{1}{c_0^2} \left((\partial_\tau \sigma_0)^2 + (\partial_\tau \pi_l)^2 \right) \right] \right), \quad (\text{D2})$$

where the index l now runs from 1 to $N - 1$, ρ_s^0 is the bare spin-stiffness and c_0 is the bare spin-wave velocity. All of the discussion in this Appendix will use the relativistic cutoff scheme when the momenta and frequency satisfy $k^2 + \omega^2 < \Lambda^2$. In this situation, the full relativistic invariance is preserved at each order in the perturbation theory and we will not have to consider explicitly the renormalization of the spin-wave velocity. To simplify the presentation, below we use the units where $\hbar = c_0 = 1$. As in Sec III, we introduce a Lagrange multiplier λ into the functional integral to impose the constraint, and integrate over π_l . This gives

$$Z = \int \mathcal{D}\vec{\sigma}_0 \mathcal{D}\lambda \exp \left(-\frac{\rho_s^0}{2} \int d^2r \int_0^\infty d\tau \left[(\partial_\mu \sigma_0)^2 + \lambda(\sigma_0^2 - 1) \right] - \frac{N-1}{2} \log || -\partial_\mu^2 + \lambda || \right). \quad (\text{D3})$$

Here $\partial_\mu^2 = (\nabla_r)^2 + (\partial_\tau)^2$. The saddle-point equation is easily obtained by taking a variational derivative over λ and neglecting fluctuations in σ_0 . This yields

$$\frac{(N-1)}{N} g \int \frac{d^2k d\omega}{(2\pi)^3} G_0(\vec{k}, i\omega) = 1 - \langle \sigma_0 \rangle^2, \quad (\text{D4})$$

Here $g = N/\rho_s^0$ is the coupling constant and $G_0(\vec{k}, i\omega) = (k^2 + \omega^2)^{-1}$ is the zero-temperature propagator of the π_l field at $N = \infty$. The $1/N$ corrections to (D4) are calculated as described earlier⁶⁷, with the modification that we have to consider the fluctuations of σ_0 around its mean value. We find the $T = 0$ analog to the polarization operator

$$\Pi^*(k, i\omega) = \Pi(k, i\omega) + \frac{2}{g} \langle \sigma_0 \rangle^2 G_0(k, i\omega), \quad (\text{D5})$$

and the correlator of the σ_0 field:

$$\begin{aligned} \langle (\sigma_0(k, i\omega))^2 \rangle &= \langle \sigma_0 \rangle^2 \delta(\omega) \delta^2(k) \\ &+ \frac{G_0(k, i\omega)}{\rho_s^0} \left(1 - \frac{2}{g} \langle \sigma_0 \rangle^2 \frac{G_0(k, i\omega)}{\Pi^*(k, i\omega)} \right). \end{aligned} \quad (\text{D6})$$

The condition $\sigma_0^2 + \pi_l^2 = 1$, then yields

$$\begin{aligned} 1 - \langle \sigma_0 \rangle^2 &= g \int \frac{d^2 k d\omega}{(2\pi)^3} G(k, i\omega) \\ &- \frac{2\langle \sigma_0 \rangle^2}{N} \int \frac{d^2 k d\omega}{(2\pi)^3} \frac{G_0^2(k, i\omega)}{\Pi^*(k, i\omega)}. \end{aligned} \quad (\text{D7})$$

Here G is related to G_0 in the usual way:

$$G^{-1}(k, i\omega) = G_0^{-1}(k, i\omega) + \Sigma(k, i\omega), \quad (\text{D8})$$

$$\Sigma(k, i\omega) = \frac{2}{N} \int \frac{d^2 q d\epsilon}{(2\pi)^3} \frac{G_0(q, i\epsilon)}{\Pi^*(\vec{q}, i\epsilon)}. \quad (\text{D9})$$

Below, we will express N_0 directly in terms of the fully renormalized spin-stiffness. It is instructive, however, to compute the critical exponent for N_0 directly from (D7). For this we observe that the first term in the r.h.s. in (D7) is simply a constant so that with the accuracy to $1/N$,

$$\langle \sigma_0 \rangle^2 = \left(\frac{g_c - g}{g_c} \right) \left(1 + \frac{2}{N} \int \frac{d^2 k d\omega}{(2\pi)^3} \frac{G_0^2(\vec{k}, i\omega)}{\Pi^*(\vec{k}, i\omega)} \right), \quad (\text{D10})$$

where g_c is the non-universal critical coupling. The value of the integral depends on the precise form of the polarization operator at $k, \omega \sim \Lambda$, which can be very complicated. However, for the logarithmic contribution in (D10), we only need to know the form of $\Pi^*(\vec{k}, i\omega)$ for momentum and frequency well below the upper cutoff. For such k and ω the evaluation of $\Pi(k, i\omega)$ at $T = 0$ is straightforward and we obtain

$$\Pi(\vec{k}, i\omega) = \frac{1}{8\sqrt{k^2 + \omega^2}}. \quad (\text{D11})$$

We then use (D5) for Π^* and evaluate the integral in (D10) with the logarithmic accuracy. We obtain

$$\langle \sigma_0 \rangle^2 = \left(\frac{g_c - g}{g_c} \right) \left(1 + \frac{8}{N\pi^2} \log \frac{g_c}{g_c - g} \right). \quad (\text{D12})$$

The correction can be exponentiated in the usual way and we get

$$\langle \sigma_0 \rangle^2 = \left(\frac{g_c - g}{g_c} \right)^{2\beta}. \quad (\text{D13})$$

where

$$2\beta = 1 - \frac{8}{N\pi^2}. \quad (\text{D14})$$

Our next goal is to express N_0 in terms of the fully renormalized spin stiffness at $T = 0$. At $N = \infty$, we have from (3.25)

$$\rho_s = N \left(\frac{1}{g} - \frac{1}{g_c} \right). \quad (\text{D15})$$

Now we have to compute $1/N$ corrections to (D15). In principle, it is possible to evaluate ρ_s directly by calculating the response to the twist of the order parameter in the momentum space. In practice, however, it is more convenient to calculate the static susceptibility χ_\perp , which measures the response to the twist in τ -direction; the value of ρ_s then can be obtained using Lorentz invariance: $\rho_s \equiv c_0^2 \cdot \chi_\perp$.

The calculations of χ_\perp to order $1/N$ were described in Sec III B. As before, they have to be modified to account for nonzero order parameter. For $N = \infty$, we use (D1) for the n -field, substitute it into the bubble diagram in Fig. 6, and after simple manipulations obtain at $T = 0$,

$$\chi_\perp^{N=\infty} = \frac{\rho_s^0}{c_0^2} \langle \sigma_0 \rangle^2. \quad (\text{D16})$$

The calculation of $1/N$ terms proceeds along the same lines as in Sec III B. We substitute (D1), into the $1/N$ diagrams in Fig. 6 and using (D6) obtain after some algebra,

$$\chi_\perp = \chi_\perp^{N=\infty} \left(1 - \frac{2}{N} I_{T=0} \right), \quad (\text{D17})$$

where

$$I_{T=0} = \int \frac{d^2k d\omega}{(2\pi)^3} \frac{G_0^2(k, i\omega)}{\Pi^*(k, i\omega)} \frac{(k^2 - 3\omega^2)}{(k^2 + \omega^2)}. \quad (\text{D18})$$

We emphasize that the calculations at $T = 0$ are much simpler than that at finite T because in fact we have to keep only the terms $\sim \langle \sigma_0 \rangle$; all other contributions give zero after *integration* over intermediate frequency. This indeed is clearly seen from the expression for χ_\perp at finite T (Eqn (3.68)) where each term contains derivatives of the Bose functions.

Finally, from (D13) and (D14), and the definition of N_0 , we obtain:

$$\frac{N_0^2}{\rho_s} = \frac{g\tilde{S}^2}{N} \left(1 - \frac{2}{N} I_{T=0} \right). \quad (\text{D19})$$

Clearly, the value of the integral in (D18) depends on the form of $\Pi^*(k, i\omega)$ near the upper cutoff and the result for N_0^2/ρ_s is therefore model dependent. However, we explicitly showed in Sec IV that the universal functions for observables are insensitive to the behavior of Π^* at $k, \omega \sim \Lambda$. In view of this, we use in Sec IV and Sec V the result for N_0^2/ρ_s obtained from (D19) in the case when the polarization operator is computed without a cutoff in the momentum and frequency integration. Then $\Pi(k, \omega)$ is given by (D11) and performing the integration in (D18), we find

$$\frac{N_0^2}{\rho_s} = \frac{g\tilde{S}^2}{N} \left[1 - \frac{8}{3\pi^2 N} \log \left(\frac{N\Lambda}{16\rho_s} \right) \right]. \quad (\text{D20})$$

This equation we use in (4.2).

We will also need the result for ρ_s expressed in terms of the spin-stiffness at $N = \infty$. From (D14) (D10) and (D15), we obtain

$$\rho_s = \rho_s^{N=\infty} \left(1 + \frac{2}{N} \int \frac{d^2k d\omega}{(2\pi)^3} \frac{G_0^2(\vec{k}, i\omega)}{\Pi^*(\vec{k}, i\omega)} \frac{4\omega^2}{(k^2 + \omega^2)} \right). \quad (\text{D21})$$

Finally, we deduce from (D21) the critical exponent for ρ_s . For this, we perform the integration in (D21) with the logarithmic accuracy using (D11) and (D5), and exponentiate the result. We then obtain

$$\rho_s \sim \left(\frac{g_c - g}{g_c} \right)^\nu, \quad (\text{D22})$$

where

$$\nu = \frac{2\beta}{1 + \eta} = 1 - \frac{32}{3\pi^2 N}, \quad (\text{D23})$$

and $\eta = 8/(3\pi^2 N)$ is the critical exponent for spin correlations at g_c .

REFERENCES

- ¹ S. Chakravarty in *High-Temperature Superconductivity*, eds. K. Bedell, D. Coffey, D.E. Meltzer, D. Pines and J.R. Schrieffer, Addison-Wesley, p.136 (1990).
- ² E. Manousakis, *Rev. Mod. Phys.*, **63**, 1 (1991).
- ³ S. Sachdev, in *Low Dimensional Quantum Field Theories for Condensed Matter Physicists*, Proceedings of the Trieste Summer School 1992, World Scientific, to be published, and references therein. Available as paper 9303014 on cond-mat@babbage.sissa.it.
- ⁴ A.P. Ramirez, G.P. Espinosa, and A.S. Cooper, *Phys. Rev. Lett.* **64**, 2070 (1990).
- ⁵ C. Broholm, G. Aeppli, G.P. Espinosa, and A.S. Cooper, *Phys. Rev. Lett.* **65**, 3173 (1991).
- ⁶ G. Aeppli, C. Broholm, and A. Ramirez in Proceedings of the Kagomé Workshop, NEC Research Institute, Princeton, NJ (unpublished).
- ⁷ V. Elser, *Phys. Rev. Lett.*, **62**, 2405 (1990).
- ⁸ S.J. Clarke, A. Harrison, T.E. Mason, G.J. McIntyre and D. Visser, *J. Phys. Cond. Matter*, **4**, L71 (1992).
- ⁹ For a review on recent experiments see e.g. A. Harrison, in "Annual Reports on the Progress of Chemistry (Royal Soc. of Chemistry, UK), **87A**, 211, (1992); **88A**, 447, (1992).
- ¹⁰ V.L. Pokrovskii, *Adv. Phys.* **28**, 595 (1979).
- ¹¹ A.F. Andreev and V. I. Marchenko, *Sov. Phys. Usp.* **23**, 21, (1980).
- ¹² S. Chakravarty, B.I. Halperin and D.R. Nelson, *Phys. Rev. Lett.* **60**, 1057 (1988); *Phys. Rev. B* **39**, 2344 (1989).
- ¹³ S. Tyc, B.I. Halperin, S. Chakravarty, *Phys. Rev. Lett.* **62**, 835 (1989).
- ¹⁴ V. Kalmeyer and R.B. Laughlin, *Phys. Rev. Lett.*, **59**, 2095 (1987); X.G. Wen, F. Wilczek and A. Zee, *Phys. Rev. B* **39**, 11413 (1989).
- ¹⁵ N. Read and S. Sachdev, *Phys. Rev. Lett.* **62**, 1694 (1989); *Phys. Rev. B* **42**, 4568 (1990).
- ¹⁶ N. Read and S. Sachdev *Phys. Rev. Lett.* **66**, 1773 (1991); S. Sachdev and N. Read, *Int. J. Mod. Phys.* **B5**, 219 (1991).
- ¹⁷ P. Chandra, P. Coleman and A.I. Larkin, *J. Phys. Cond. Matter* **2**, 7933 (1990).
- ¹⁸ I. Affleck and J. Brad Marston, *Phys. Rev. B* **37**, 3774, (1988).
- ¹⁹ P.B. Wiegmann, *Phys. Rev. Lett.* **60**, 821, (1988); D.V. Khveshchenko and P.B. Wiegmann, *Mod. Phys. Lett. B* **4**, 17 (1990).
- ²⁰ P.W. Anderson, *Science* **235**, 1196 (1987).
- ²¹ S. Sachdev and Jinwu Ye, *Phys. Rev. Lett.* **69**, 2411 (1992).
- ²² A.V. Chubukov and S. Sachdev, *Phys. Rev. Lett.* **71**, 169 (1993); erratum, to be published.
- ²³ B. Andraka and A.M. Tsvelik, *Phys. Rev. Lett.* **67**, 2886 (1991).
- ²⁴ A.J. Millis, preprint; J.A. Hertz, *Phys. Rev. B* **14**, 525 (1976).
- ²⁵ P. Hasenfratz and F. Niedermayer, *Phys. Lett. B* **268**, 231 (1991); University of Bern preprint BUTP-92/46.
- ²⁶ P. Hasenfratz, M. Maggiore and F. Niedermayer, *Phys. Lett. B* **245**, 522 (1990); P. Hasenfratz and F. Niedermayer, *Phys. Lett. B* **245**, 529 (1990).
- ²⁷ S. Chakravarty and R. Orbach, *Phys. Rev. Lett* **64**, 224 (1990).

- ²⁸ Y. Endoh *et. al.*, Phys. Rev. B **37**, 7443 (1988); K. Yamada *et. al.*, Phys. Rev. B **40**, 4557 (1989).
- ²⁹ S.M. Hayden, G. Aeppli, H. Mook, D. Rytz, M.F. Hundley, and Z. Fisk, Phys. Rev. Lett. **66**, 821 (1991); S.M. Hayden, G. Aeppli, R. Osborn, A.D. Taylor, T.G. Perring, S.-W. Cheong, and Z. Fisk, Phys. Rev. Lett. , **67**, 3622 (1991).
- ³⁰ T. Imai, C.P. Slichter, K. Yoshimura and K. Kosuge, Phys. Rev. Lett **70**, 10002, (1993).
- ³¹ D.C. Johnson, Phys. Rev. Lett. **62**, 957 (1989).
- ³² R.R.P. Singh and M. Gelfand, Phys. Rev. B **42**, 966 (1990).
- ³³ H.Q. Ding and M. Makivic, Phys. Rev. Lett, **64**, 1449 (1990); Phys. Rev. B **43**, 3662 (1990).
- ³⁴ A. Sokol, S. Bacci and E. Gagliano, Phys. Rev. B **47**, 14646 (1993).
- ³⁵ B. Keimer, R.J. Birgeneau, A. Cassanho, Y. Endoh, R.W. Erwin, M.A. Kastner, and G. Shirane, Phys. Rev. Lett. **67**, 1930 (1991).
- ³⁶ B. Keimer, N. Belk, R.J. Birgeneau, A. Cassanho, C.Y. Chen, M. Greven, M.A. Kastner, A. Aharony, Y. Endoh, R.W. Erwin, and G. Shirane, Phys. Rev. B **46**, 14034 (1992).
- ³⁷ C.M. Varma P.B. Littlewood, S. Schmitt-Rink, E. Abrahams, and A.E. Ruckenstein, Phys. Rev. Lett. **63**, 1996 (1989).
- ³⁸ L.B. Ioffe and A.I. Larkin, Int. J. Mod. Phys. B **2**, 203 (1988).
- ³⁹ A.V. Chubukov, Phys. Rev. B **44**, 392 (1991).
- ⁴⁰ B.I. Halperin and W.M. Saslow, Phys. Rev. B **16**, 2154 (1977).
- ⁴¹ T. Dombre and N. Read, Phys. Rev. B **39**, 6797 (1989).
- ⁴² P. Azaria, B. Delamotte, and T. Jolicoeur, Phys. Rev. Lett. **64**, 3175 (1990).
- ⁴³ A.B. Harris, C. Kallin and A.J. Berlinsky, Phys. Rev B **45**, 2889 (1992); J.T. Chalker, P.S. Holdsworth and E.F. Shender, Phys. Rev. Lett. **68**, 855 (1992); P. Chandra, P. Coleman and I. Ritchey, Phys. Rev. B, to appear; A.V. Chubukov, Phys. Rev. Lett. **69**, 832 (1992); J. von Delft and C.L. Henley, Phys. Rev. Lett. **69**, 3236 (1992); J.N. Reimers, A.J. Berlinsky and A.-C Shi, Phys. Rev. B **43**, 865 (1991); R.R.P. Singh and D. Huse, Phys. Rev. Lett. **68**, 1706 (1992); D.L. Huber and W.Y. Cheong, Phys. Rev. B **47**, 3220 (1993).
- ⁴⁴ S. Sachdev, Phys. Rev. B **45**, 12377 (1992).
- ⁴⁵ S-k. Ma, *Modern Theory of Critical Phenomena*, Benjamin/Cummings, Reading (1976).
- ⁴⁶ J.B. Parkinson, J. Phys. C **2**, 2012 (1969); B.S. Shastry and B. Shraiman, Phys. Rev. Lett. **65**, 1068 (1990); R.R.P. Singh, Comments Cond. Matt. Phys. **15**, 241 (1991).
- ⁴⁷ M.E. Fisher, M.N. Barber, and D. Jasnow, Phys. Rev. A **8**, 1111 (1973).
- ⁴⁸ B.D. Josephson, Phys. Lett. **21**, 608 (1966).
- ⁴⁹ A.H. Castro Neto and E. Fradkin, paper 9301009 on cond-mat@babbage.sissa.it
- ⁵⁰ A.N. Vasil'ev, Yu.M. Pis'mak and Yu.R. Honkonen, Teor. Mat. Fiz. **46**, 157 (1981).
- ⁵¹ C. Holm and W. Janke, preprint; P. Peczak, A.M. Ferrenberg, and D.P. Landau, Phys. Rev. B **43**, 6087 (1991).
- ⁵² In an earlier version of the manuscript we had an incorrect conjecture of the form of the subleading term in the large $x_{1,2}$ expansion. S. Chakravarty pointed out to us, and we determined by explicit computation the present correct form.
- ⁵³ D. Stauffer, M. Ferer, and M. Wortis, Phys. Rev. Lett. **29**, 345 (1972).
- ⁵⁴ P.C. Hohenberg, A. Aharony, B.I. Halperin, and E.D. Siggia, Phys. Rev. B **13**, 2986 (1976); C. Bervillier, *ibid.* **14**, 4964 (1976).

- ⁵⁵ M.P.A. Fisher, G. Grinstein, and S.M. Girvin, Phys. Rev. Lett. **64**, 587 (1990); K. Kim and P.B. Weichmann, Phys. Rev. B **43**, 13583 (1991); M.-C. Cha *et.al.*, Phys. Rev. B **44**, 6883 (1991).
- ⁵⁶ M.N. Barber in *Phase Transitions and Critical Phenomena*, ed. C. Domb and J. Lebowitz, v. 8, pg. 145, Acad. Press (New York).
- ⁵⁷ V. Privman and M.E. Fisher, Phys. Rev. B **30**, 322 (1984).
- ⁵⁸ D.S. Fisher, Phys. Rev. B **39**, 11783 (1989).
- ⁵⁹ M.E. Fisher and P.-G. de Gennes, C.R. Acad. Sci. Ser. B **287**, 207 (1978).
- ⁶⁰ A.B. Zamalodchikov, Pis'ma Zh. Eksp. Teor. Fiz **43**, 565 (1986); [JETP Lett. **43**, 730 (1986)].
- ⁶¹ H.W.J. Blote, J.L. Cardy, and M.P. Nightingale, Phys. Rev. Lett. **56**, 742 (1986); I. Affleck Phys. Rev. Lett. **56**, 746 (1986).
- ⁶² D.P. Arovas and D. Auerbach, Phys. Rev. B **38**, 316 (1988); Phys. Rev. Lett. **61**, 617 (1988).
- ⁶³ B. Rosenstein, B.J. Warr and S.H. Park, Nucl. Phys. B **336**, 435 (1990).
- ⁶⁴ E. Brezin, J. de Physique **43**, 15 (1982); M. Henkel and C. Hoeger, Z. Phys. B **55**, 67 (1984); S. Singh and R.K. Pathria, Phys. Rev. B **31**, 4483 (1985) and references therein.
- ⁶⁵ R.F. Dashen, S-K. Ma and R. Rajaraman, Phys. Rev. D **11**, 1499 (1975).
- ⁶⁶ S. Sachdev, Phys. Lett. B **309**, 285 (1993).
- ⁶⁷ A.M. Polyakov, *Gauge Fields and Strings*, Harwood, New York (1987).
- ⁶⁸ S. Coleman, R. Jackiw and D. Politzer, Phys. Rev. D **10**, 2491 (1974).
- ⁶⁹ I.A. Aref'eva, Ann. Phys. (N.Y.) **117**, 393 (1979).
- ⁷⁰ J.L. Cardy, J. Phys. A. **17**, L385 (1984); R. Shankar and S. Sachdev, unpublished.
- ⁷¹ A.M. Polyakov, Phys. Lett. B **59**, 79 (1975).
- ⁷² P.B. Wiegmann, Pis'ma Zh. Eksp. Teor. Fiz. **41**, 79 (1985) [JETP Lett. **41**, 95 (1985)].
- ⁷³ E. Brezin and J. Zinn-Justin, Phys. Rev. B **14**, 3110 (1976).
- ⁷⁴ A.M. Polyakov and P.B. Wiegmann, Phys. Lett. B **131**, 121 (1983).
- ⁷⁵ A.V. Chubukov, Phys. Rev. B **44**, 12318 (1992).
- ⁷⁶ M.I. Kaganov and A.V. Chubukov, Usp. Fiz. Nauk **153**, 537 (1987) [Sov. Phys. Usp. **30**, 1015 (1987)]; in "Spin Waves and Magnetic Dielectrics" eds. A.S. Borovik-Romanov and S.K. Sinha, Elsevier Science Publ. (1988).
- ⁷⁷ S. Tyc and B.I. Halperin, Phys. Rev. B **42**, 2096 (1990).
- ⁷⁸ B.I. Halperin and P.C. Hohenberg, Phys. Rev. **177**, 952 (1969).
- ⁷⁹ In the recent paper by one of us⁷⁵, it was suggested that the damping may become comparable to the real part of the quasiparticle energy at the spatial scales which parametrically exceed ξ . The more sophisticated analysis presented here shows that it is more likely that 2D antiferromagnet has the same typical spatial scale (correlation length) for both static and dynamic phenomenon, as is predicted by the dynamical scaling hypothesis.
- ⁸⁰ J. Igarashi, Phys. Rev. B **46**, 10763 (1992).
- ⁸¹ R.R.P. Singh, Phys. Rev. B **39**, 9760 (1989); see also R.R.P. Singh and D. Huse, Phys. Rev. B **40**, 7247 (1989).
- ⁸² A. Singh and Z. Tesanovic, Phys. Rev. B **41**, 614 (1990); A. Singh, Z. Tesanovic and J.H. Kim, Phys. Rev. B **44**, 7757 (1991); A. Auerbach and B.E. Larson, Phys. Rev. B **43**, 7800 (1991).
- ⁸³ B.I. Shraiman and E.D. Siggia, Phys. Rev. Lett. **61**, 467 (1988); Phys. Rev. B **42**, 2485

- (1990).
- ⁸⁴ B.I. Shraiman and E.D. Siggia, Phys. Rev. B **46**, 8305 (1992).
- ⁸⁵ A.V. Chubukov and D. Frenkel, Phys. Rev. B **46**, 11884 (1992).
- ⁸⁶ J. Gan, N. Andrey and P. Coleman, J. Phys. Condens. Matter **3**, 3537 (1991).
- ⁸⁷ S. Sachdev, unpublished.
- ⁸⁸ R.R.P. Singh, Phys. Rev. B **39**, 9760 (1989).
- ⁸⁹ A. Millis and H. Monien, Phys. Rev. Lett. **70**, 2810 (1993).
- ⁹⁰ D.C. Johnson, S.K. Sinha, A.J. Jacobson and J.M. Newsam, Physica (Amsterdam), **153-155 C**, 572 (1988).
- ⁹¹ F. Mila and T.M. Rice, Physica C **157**, 561 (1989); S. Shastry Phys. Rev. Lett., **63**, 1288 (1989).
- ⁹² A.J. Millis, H. Monien and D. Pines, Phys. Rev. B **42**, 167 (1990).
- ⁹³ E. Manousakis and R. Salvador, Phys. Rev. B **39**, 575 (1989); E. Manousakis, Phys. Rev. B **45**, 7570, (1992).
- ⁹⁴ E. Manousakis and R. Salvador, Phys. Rev. B **40**, 2205 (1989).
- ⁹⁵ A. Sokol, private communication.
- ⁹⁶ A. Chubukov, S. Sachdev and A. Sokol, Phys. Rev. B, submitted.
- ⁹⁷ M. Makivic and M. Jarrell, Phys. Rev. Lett., **68**, 1770 (1992).
- ⁹⁸ M.P.A. Fisher, P.B. Weichmann, G. Grinstein, and D.S. Fisher, Phys. Rev. B **40**, 546 (1989).
- ⁹⁹ R.N. Bhatt and P.A. Lee, Phys. Rev. Lett. **48**, 344 (1982).
- ¹⁰⁰ I. Affleck and A.W.W. Ludwig, Nucl. Phys. **B360**, 641 (1991).
- ¹⁰¹ K. Binder and A.P. Young, Rev. Mod. Phys. **58**, 801 (1986).
- ¹⁰² G. Murthy and S. Sachdev, Nucl. Phys. **B344**, 557 (1990).
- ¹⁰³ D.S. Fisher, private communication.
- ¹⁰⁴ U. Wolff, Phys. Rev. Lett. **62**, 361 (1989).

FIGURES

FIG. 1. Phase diagram of \mathcal{H} (Eqn. (1.1)) as a function of g and temperature T (after Ref.¹²). The coupling g measures the strength of the quantum fluctuations. It is inversely proportional to S for large spin and its value also depends on the ratios of the J_{ij} . The parameters $x_1 = Nk_B T / (2\pi\rho_s)$, and $x_2 = k_B T / \Delta$ control the scaling properties of the antiferromagnet (here ρ_s is the spin-stiffness of the Néel-ordered ground state, and Δ is the spin 1 gap in the quantum-disordered ground state).

FIG. 2. Properties of the nearly-critical antiferromagnet as a function of the observation wavevector k , or frequency ω in the three different regions of Fig. 1. The appropriate regime is determined by the larger of $\hbar ck / (k_B T)$ or $\hbar\omega / k_B T$. In the renormalized-classical regime, ξ is the actual correlation length, while ξ_J is a Josephson correlation length related to the spin-stiffness by $\hbar c / \xi_J = \rho_s / \Upsilon$, with Υ a universal number. In the quantum disordered region, Δ is the gap for $S = 1$ excitations at $T = 0$. The thermodynamic behavior in the various regions is discussed in the text.

FIG. 3. The scaling function $\text{Im}\Phi_{1s}(\bar{k}, \bar{\omega}, \infty)$ for the staggered susceptibility in the quantum-critical region. The results have been computed in a $1/N$ expansion to order $1/N$ and evaluated for $N = 3$. The shoulder on the peaks is due to a threshold to three spin-wave decay.

FIG. 4. Scaling function $\Xi_1(\bar{k}, \infty)$ for the structure factor in the quantum-critical region.

FIG. 5. Scaling function $F_1(\bar{\omega}, \infty)$ for the imaginary part of the local susceptibility in the quantum-critical region. The oscillations at large $\bar{\omega}$ are due to a finite step-size in the momentum integration.

FIG. 6. Feynman graph for the staggered and uniform susceptibilities to order $1/N$. The solid line represents the n_ℓ field and the dashed line represents the propagator of the λ field (polarization operator), where λ is the Lagrange multiplier imposing the constraint.

FIG. 7. Quantum Monte-Carlo³³ (squares) and our theoretical (line) results for the uniform susceptibility $\bar{\chi}_u = (3J(a\hbar/g\mu_B)^2)\chi_u^{\text{st}}$ of a square lattice spin-1/2 Heisenberg antiferromagnet (a is the lattice spacing). The experimental results for weakly doped La_2CuO_4 are very close to the Monte-Carlo data³¹. There are *no* adjustable parameters in the theoretical result (1.24). Over the range of T plotted, the function $\Omega_1(x_1)$ (recall $x_1 = Nk_B T / (2\pi\rho_s)$) is very close to its large x_1 behavior given in Eqn. (3.35,4.13). We used the theoretical result at $N = 3$. The theoretical and experimental slopes agree remarkably well. The good agreement in the intercept is somewhat surprising as its theoretical value is known only at $N = \infty$.

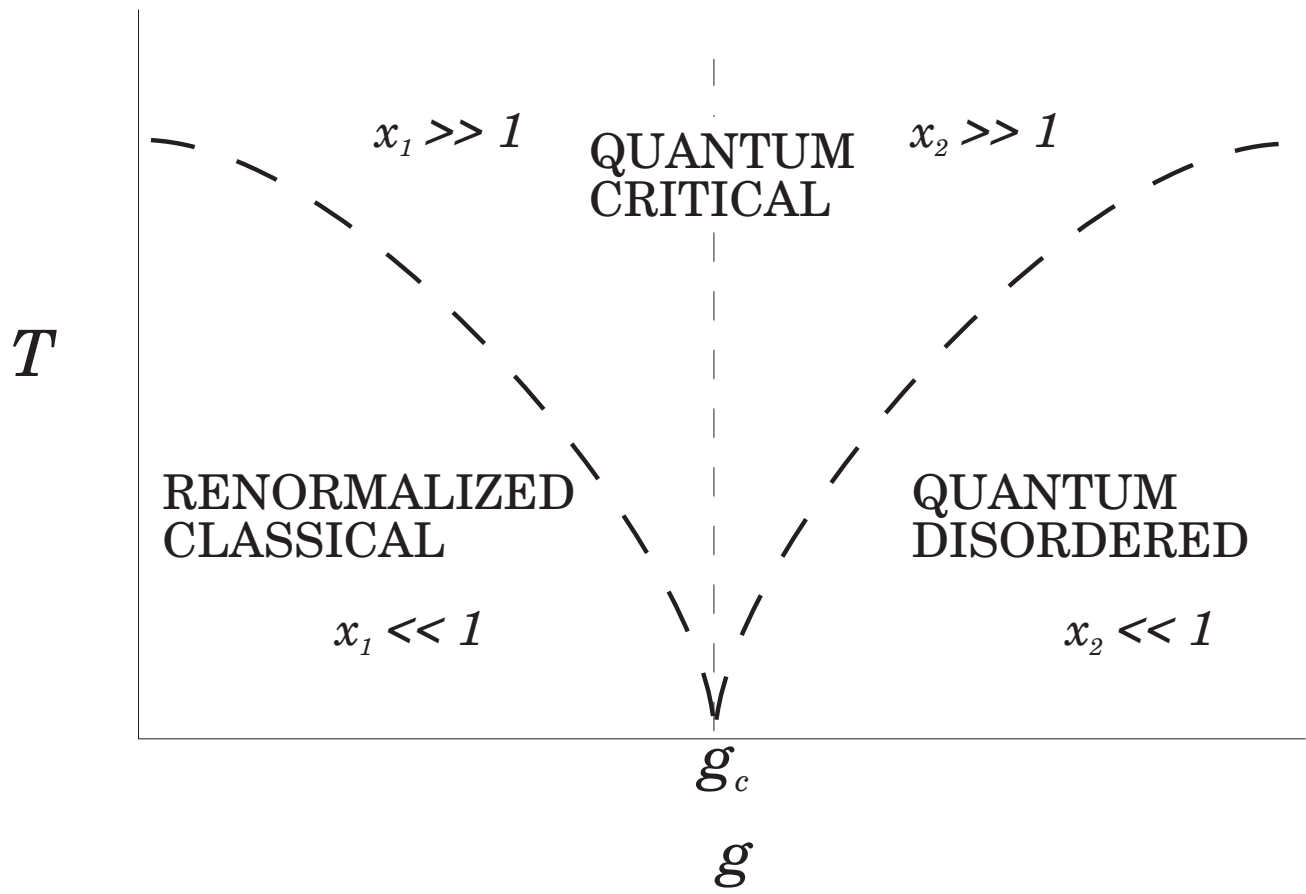
FIG. 8. Theoretical scaling function at $N = \infty$, Eqn. (7.6) (line) and Quantum Monte-Carlo data³³ (squares) for the equal-time structure factor in the $S = 1/2$ Heisenberg antiferromagnet at $k_B T = 0.42J$. The correlation length is taken from the Monte-Carlo data ($\xi \sim 5.7a$). We expect that for most of the values of $k\xi$ plotted, the antiferromagnet is in the quantum-critical regime where $1/N$ corrections to (7.6) are small. The only adjustable parameter in the theoretical curve is the k -independent overall factor \bar{S} in (7.6). The best fit value of \bar{S} was found to be ~ 1.45 times larger than our $N = \infty$ result.

FIG. 9. Schematic of the renormalization group flows of the action S (Eqn. (B2)) of a classical XY model on a cubic lattice. The coupling h_4 is a cubic anisotropy perturbation which is irrelevant at the critical fixed point $T = T_c$, $h_4 = 0$. Its neglect is however dangerous in the low temperature phase because h_4 is relevant at the $T = 0$, $h_4 = 0$ fixed point.

TABLES

TABLE I. Results of the Monte Carlo simulation of the classical statistical-mechanics model (C2) at $K = K_c = 0.6930$. We used a box of $L \times L \times L_\tau$ sites with periodic boundary conditions. The stiffness ρ_τ is defined in (C4). The last column is obtained by a polynomial extrapolation in inverse powers of $1/L$. The three runs had 70000, 70000, 210000 flips per spin respectively. A weighted average of the three runs was used in the extrapolation.

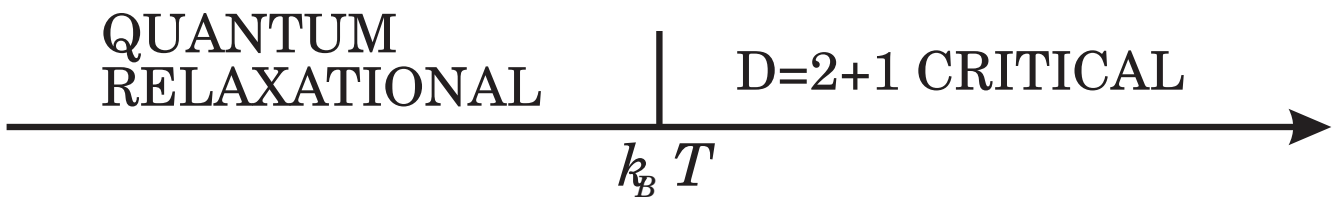
L_τ	L	$L_\tau \rho_\tau$			$\lim_{L \rightarrow \infty} L_\tau \rho_\tau$
		Run 1	Run 2	Run 3	
5	10	0.3983	0.3866	0.3898	0.3257
	15	0.3693	0.3701	0.3663	
	20	0.3596	0.3515	0.3527	
	25	0.3511	0.3574	0.3478	
	30	0.3483	0.3529	0.3511	
7	10	0.4138	0.4087	0.4099	0.3037
	15	0.3718	0.3766	0.3747	
	20	0.3650	0.3625	0.3506	
	25	0.3529	0.3419	0.3442	
	30	0.3424	0.3405	0.3402	
10	15	0.4079	0.4049	0.4020	0.2890
	20	0.3861	0.3743	0.3713	
	25	0.3650	0.3671	0.3511	
	30	0.3548	0.3521	0.3425	



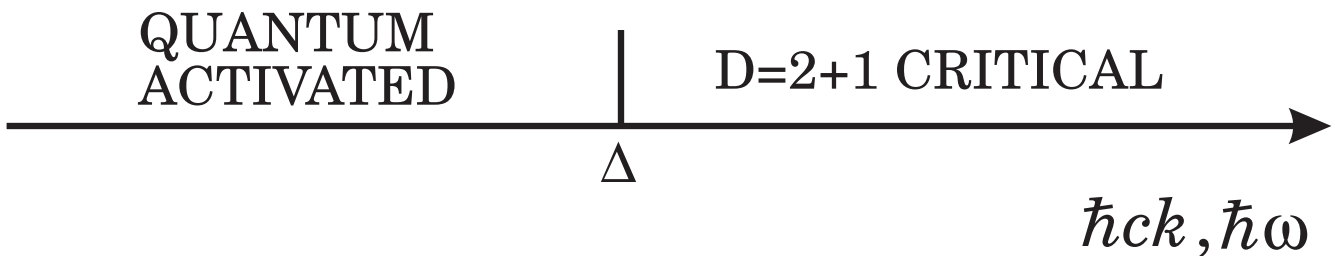
RENORMALIZED CLASSICAL

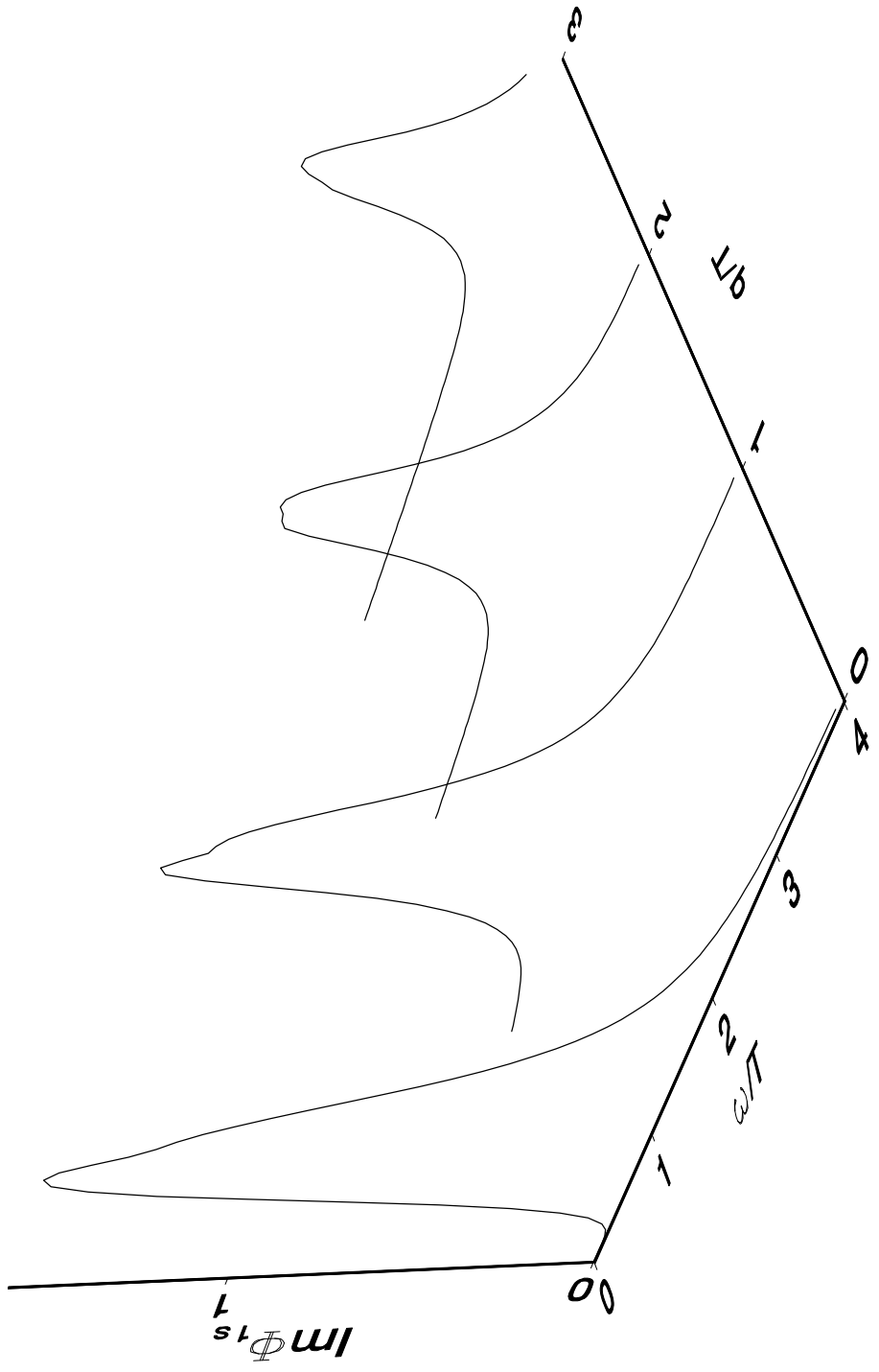


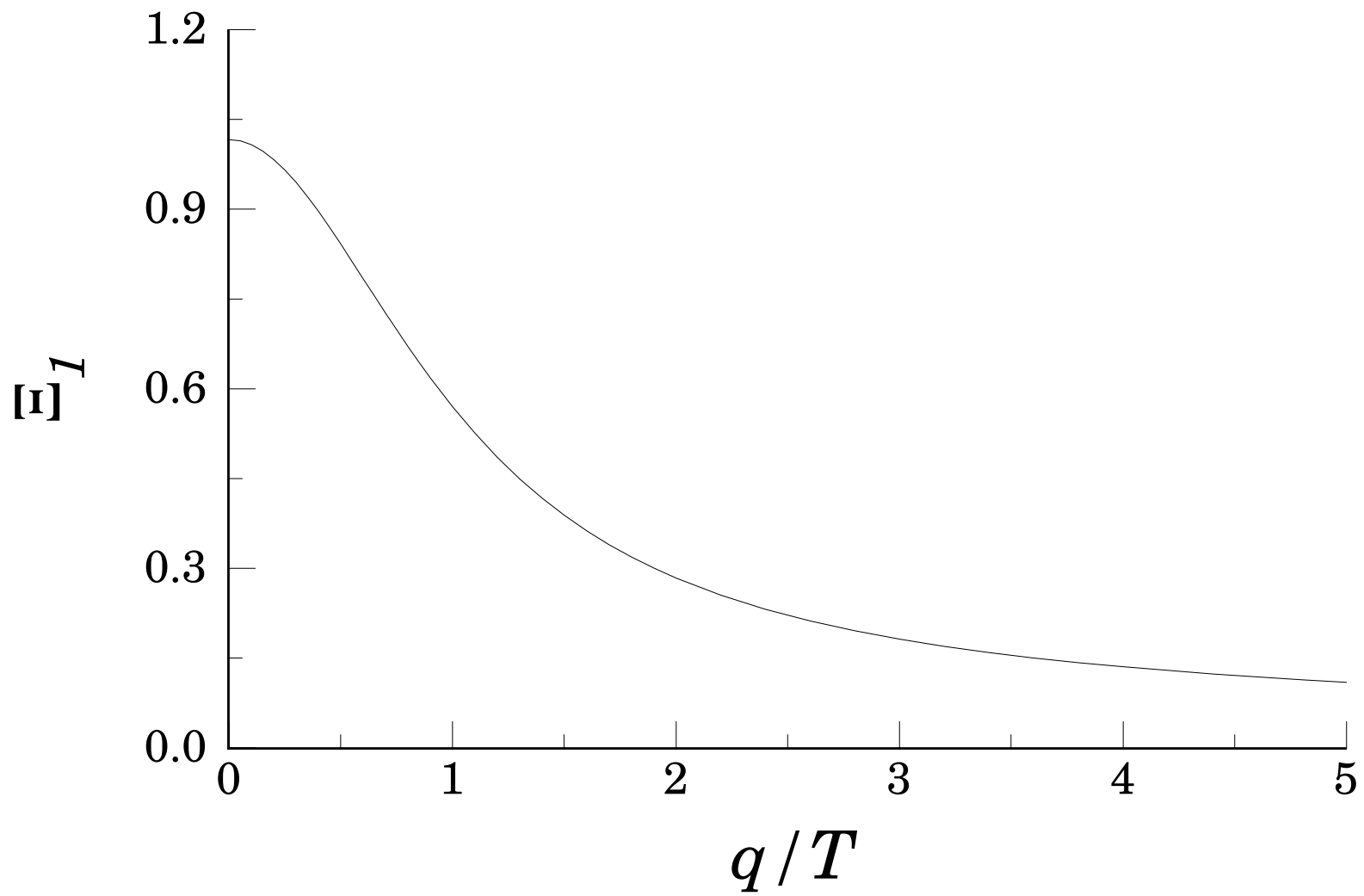
QUANTUM CRITICAL

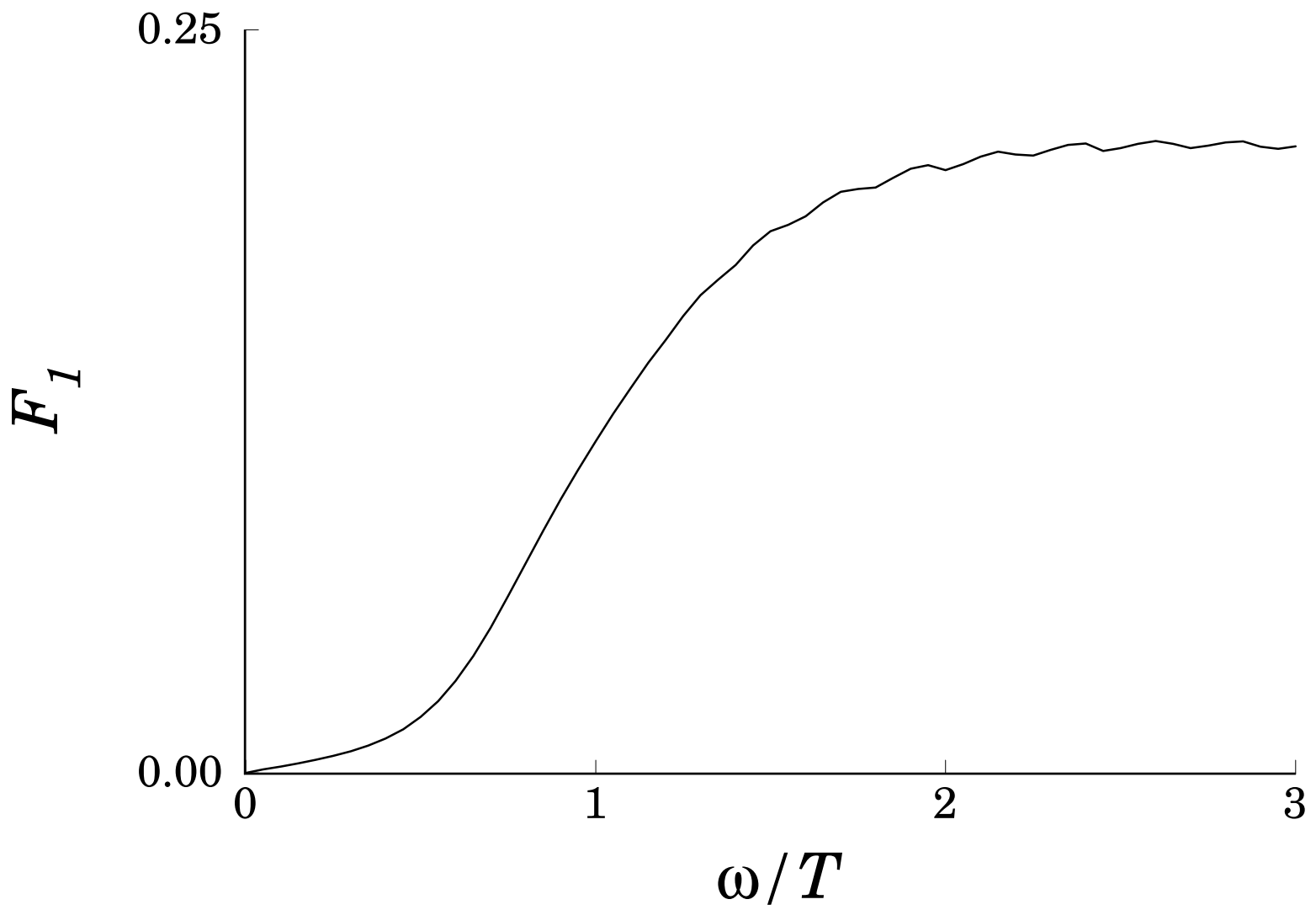


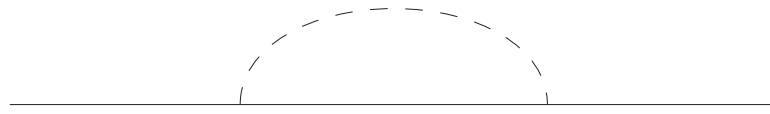
QUANTUM DISORDERED



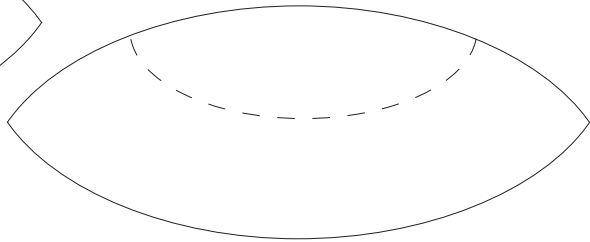
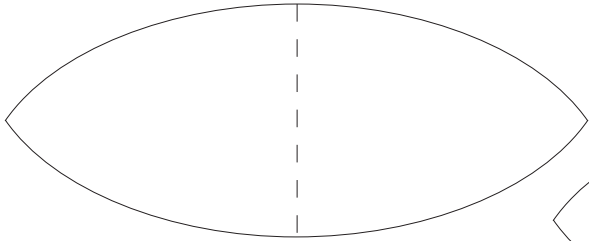
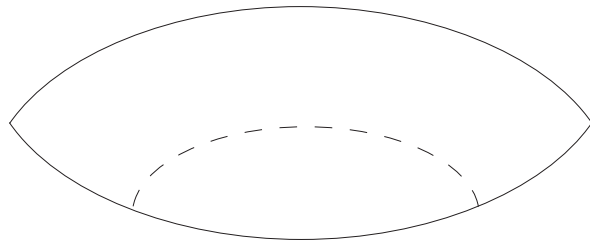
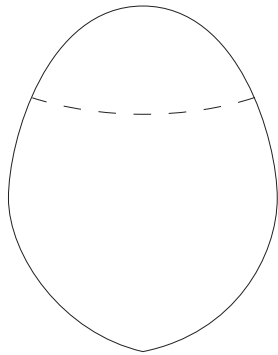








χ_s



χ_u

